Iron Powder as a fuel on Service Vessels

Master Thesis

E. Scherpenhuijsen Rom

Maritime Engineering
3mE
May, 2023

TU Delft

Iron Powder as a fuel on Service Vessels

Master Thesis

by

E. Scherpenhuijsen Rom

to obtain the degree of Master of Science
at the Delft University of Technology,
to be defended publicly on Tuesday May 16, 2023 at 13:45.

Report Number:	MT.22/23.032.M.	
Student number:	4422104	
Project duration:	April 22, 2022 – May 16, 2023	
Thesis committee:	Dr. A. Kana	TU Delft, supervisor
	Dr. P. de Vos,	TU Delft
	Mr. A. Souflis-Rigas,	TU Delft

An electronic version of this thesis is available at http://repository.tudelft.nl/.

TU Delft

Preface

This research process has been at times difficult, stressful but most importantly, interesting. Doing a design feasibility study on a vessel type with limited public information in an in-house research is not something I can recommend to just anyone. With an engineering brain it is difficult to accept that some values will simply be estimates, indications towards a specific recommendation. Throughout this year of research, I have come to accept this fact and the fact that while this research cannot provide an absolute perfect solution, it still provides valuable information and conclusions in relation to this field of research.

This acceptance is largely thanks to my supervisor Austin Kana, who has been a massive help throughout this research process. Thanks to his reassurance and positive reinforcement nudging me in the right directions, I am able to be proud of the research I have done in this report. Peter de Vos has also been invaluable in this research process with his key insights into the marine engineering aspect of this research field. Furthermore, my house-mate's extended programming knowledge helped increase the level of my research and my sister's diligence managed to catch hopefully all of my spelling and grammar mistakes.

This past year of provided me a great interest in the offshore construction sector and especially the construction vessels like the semi-submersible crane vessel. It has also opened my scope for the potentials in sustainability in the maritime sector with new alternatives being constantly developed and being possibly applicable to one of the multitude of different vessel types travelling across the seas.

E. Scherpenhuijsen Rom
Rotterdam, May 2023

Summary

This thesis looks to provide a look into the possibilities of iron powder as a fuel on service vessels. The sustainable characteristics of iron powder can reduce emissions of seagoing vessels and create a potentially fully cyclical energy resource. Iron powder application on vessels is very limited with only a general application and possible short-sea shipping application study done so far. With the objective of sustainability and feasibility in mind, the research objective of this thesis is to 'Analyse and evaluate the feasibility of an iron powder powertrain on a specific type of service vessel with specific focus on the vessel design as well as the powertrain configuration and components.'.

This research process is started with a literature review covering the two areas being combined; iron powder powertrains and service vessels. The characteristics, components and limitations of iron powder are all examined to determine an optimal iron powder powertrain setup. This information is then used to use a two-phase filtering method to determine the most optimal service vessel type for a further feasibility study. The final choice for optimal iron powder setup includes storage in vertical silos, transport with a pneumatic two-phase transport system, combustion in an external combustion engine with filtering done by a combination of cyclone and bag house filters. For energy conversion, the choice is made to use the Mitsubishi UST cycle. The service vessel choice ended up with the semi-submersible crane vessel as the most optimal choice for this particular hybridised iron powder setup.

In order to test the base feasibility of an iron powder setup on a semi-submersible vessel, the hybrid iron powder setup has to be simulated on a semi-submersible crane vessel design. A design method starting with input values of the vessel dimensions and operating profiles was made with the output consisting of a feasibility test and an emissions comparison. To obtain feasibility values, a turbine installation mission of 12 weeks is simulated on four semi-submersible vessel designs. These simulations would deliver a load profile from which a hybrid split can be determined. This hybrid split allows for an estimation of the engine room, bunker and ship element dimensions and weights. These can then be used in a base feasibility study in which the transverse and longitudinal stability are tested against the ship classification rules. The increased mass is also looked at regarding its impact on the vessel's draft. The emissions of the vessels are examined by comparing the hybrid output with the original output.

To evaluate whether the results from this method and its applied case study can be trusted, a validation study is done. This is done using the validation square which is considered the most applicable validation method for a design research.

The results of this research show a significant increase in mass due to the iron powder silos even in a hybrid configuration. This mass increase increases the draft of the larger vessels by 1-2m and the smaller vessels by 6-8m. The stability of the vessels was less impacted as only the smallest case study vessel was deemed infeasible with a hybrid iron powder setup. The emissions comparison showed a significant yearly decrease in both CO_2 and NO_x output from the case study vessels. This leads to the conclusion that especially larger semi-submersible crane vessels appear to be potentially feasible candidates for a hybrid iron powder powertrain setup.

Contents

1

Introduction

Sustainability has been one of the defining subjects over the past few decades. Whether people take it seriously or not, everyone knows about the issues regarding climate change and the impact humanity has had in accelerating it. Countless initiatives and research development costs have gone into trying to reduce our impact on climate change in all sectors of human industry worldwide. This is no different in the maritime industry and this report will attempt to add to a growing list of alternative, sustainable options that can be taken into account when designing sea-going vessels.

1.1. IMO and Climate Change

The maritime impact on climate change is one that cannot be overlooked. The emissions of maritime traffic accounts for 2.9% of global emissions caused by human activities in 2018, ["Reducing emissions from the shipping sector", n.d.]. If current trends continue the impact of the maritime emissions output could increase to around 17% of global human caused emissions by 2050, ["Maritime shipping", n.d.]. The International Maritime Organization (IMO) is attempting to prevent this emissions output growth to continue as well as decrease the current output of greenhouse gases which in 2018 reached 1,076 million tons of CO_2, ["Reducing emissions from the shipping sector", n.d.]. They are doing this by setting targets of emissions reduction in the maritime industry for all sea-going vessels. These targets include the reduction of CO_2 output across international shipping by 40% by 2030 and up to 70% by 2050, ["IMO's work to cut GHG emissions from ships", n.d.]. These output values are compared to the recorded emissions in 2008. Monitoring, reporting and verification of CO_2 emissions has become a norm for all marine vessels due to EU and IMO legislation requiring vessels to track their emissions, ["Monitoring, reporting and verification of CO2 ... - european parliament", n.d.]. In order to ensure these emissions trackers start showing emission reductions, new sustainable energy sources are being developed for maritime application. Some of the front runners of these sustainable maritime energy sources are bio-fuels, hydrogen and wind power. Aside from the most popular alternatives, there are a large variety of other sustainable energy sources being used in different situations aboard a multitude of vessels. One such sustainable energy source that has been gaining more and more attention in recent years are metal fuels.

1.2. Metal Fuels

Metal fuels are a promising sustainable alternative to conventional energy sources as they are dense energy carriers. Metal powders are used to create power through two mechanisms; the wet cycle and the dry cycle, [Bergthorson, 2018]. The wet cycle is considered the indirect energy generation process and the dry cycle is considered the direct energy generation process. The scope of this research is focused on the dry cycle with a particular focus on iron powder. There are a large group of potential metal fuels that can be used as an energy source; Aluminium, silicon, zinc, iron etc. Of these metal fuels, the most commonly occurring in human industry is iron powder and is therefore considered the most popular of the metal fuels, [Bergthorson, 2018]. The main feature attributed to the iron powder power generation process that makes it such a high potential alternative fuel source is the fact that the combustion of this powder results in no CO_2 byproduct, [van Rooij et al., 2019]. This means it can be an

extremely useful method of reducing CO_2 emissions and reaching the IMO's targets. What makes iron powder even more interesting as a fuel source is the possibility of having a fully cyclical sustainable energy generation process. This entails that the byproducts of iron powder combustion (iron oxides) can be fully collected, processed and reduced back into iron powder form for re-combustion. This process of reduction can potentially be done in a sustainable manner using hydrogen meaning that the entire cycle can be done sustainably. This would result in the elimination of further bunker costs as one load of bunker could theoretically be continuously reused as an energy source. The potential of iron powder as a fuel source on vessels is not entirely new as van Rooij et al., 2019 have conducted research in the general application of iron powder on marine vessels. Furthermore, de Kwant, 2021 has built upon this research with a specific focus on the application on short-sea shipping. In an attempt to advance this particular field of research, this report will look into the potential of applying an iron powder powertrain aboard a marine service vessel.

1.3. Research Objective and Sub-questions

This report will start with a look at the state-of-the-art of iron powder energy generation to determine the current most optimal setup to be installed aboard a marine vessel. This will be followed by a study of the marine service vessel types to determine which is best suited for an iron powder powertrain installation. The conclusions from these two studies will result in the creation of an applicable method of testing iron powder feasibility on the chosen service vessel type. This method of testing feasibility will then be applied to a set of case study vessels in an attempt to fulfill the primary research statement.

Analyse and evaluate the feasibility of an iron powder powertrain on a specific type of service vessel with specific focus on the vessel design as well as the powertrain configuration and components.

The primary research objective above is further split into six research sub-questions. The answering of these research questions should result in the fulfillment of the research statement. The research questions are split over two areas of research, the literature review and the individual research. The questions regarding the literature review are as follows.

What is the current state-of-the-art of energy generation using iron powder? What are the most significant physical components?

What types of service vessels are best suited for iron powder powertrain installation? What are key features and operational profiles of these vessels?

What are the key challenges faced by installing an iron powder powertrain on a marine service vessel? What are potential solutions to these challenges?

These questions can be answered through a comprehensive study of the iron powder energy generation system and the marine service vessel fleet. Once these sub-questions are answered, the individual research is started in order to answer the remaining three sub-questions listed below.

How can models and simulations be used to analyse and compare different variations of the iron powder powertrain aboard a service vessel?

What techniques of validation and verification can be used to back up the results from this model?

What can be concluded from these models and simulations of the powertrain and the vessel design regarding iron powder implementation on service vessels?

Once an answer can be provided for each of the research sub-questions, the primary research statement is fulfilled and the goal of the research has been achieved.

2

State-of-the-Art

The state-of-the-art research focuses on the iron powder powertrain and its components. First, the overall advantages and limitations of the iron powder powertrain will be highlighted (2.1). Then, key components of the iron powder powertrain will be discussed along with the challenges of placing these on a ship (2.2). Finally an analysis will be made of the possible output capacity of an iron powder powertrain on a vessel (2.3).

2.1. Iron Powder System Characteristics

Metal powder combustion is one of the more promising sustainable power generating alternatives to conventional sources of power such as fossil fuels. Metal powders are dense energy carriers that can be turned into a power source using two processes [Bergthorson, 2018]. The first of which is known as the wet cycle in which the metal is reacted with water at high temperatures for heat and hydrogen production [Dirven et al., 2018]. The product can be used either in heat engines or in fuel cells. The second process is the dry cycle in which the metals are directly combusted in an external combustion chamber and converted into mechanical energy directly [Dirven et al., 2018]. The dry cycle is a more direct form of energy generation as opposed to the two step process of the wet cycle. This means that the dry cycle will be more compact in practical use than the wet cycle and require less volume. Therefore the use of the dry cycle is far more practical onboard a ship with limited area and volume. This will therefore be the power production process discussed in this report. There are many metal powders that can be combusted to produce energy. On the periodic table, the range of possible elements that can act as electrofuels is limited only by their ability to oxidize in air and a high specific energy. This leaves all elements within groups 1-14 and periods 1-4 shown in figure 2.1 in colour.

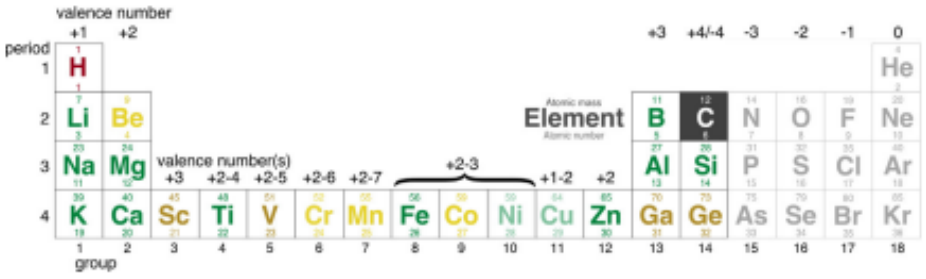

Figure 2.1: Periodic table of elements highlighting the possible electrofuels [Bergthorson, 2018]

Of all of these possible electrofuels, the most interesting metals are listed as aluminium, silicon, zinc and iron [Bergthorson, 2018]. This is due to the filtering out of certain metals whose oxides are toxic (highlighted yellow on figure 2.1) and certain metals whose procurement is deemed too expensive (highlighted gold on figure 2.1). The focus of this report will be on the generation of energy using iron as the metal fuel source in the dry cycle. This process will have its advantages and limitations in

comparison to both fossil fuel energy generation as well as other metal alternatives.

2.1.1. Availability

A key advantage of using iron as a power source is its overall abundance as a resource. Iron makes up around 5% of the earths crust making it the 4th most common element in the crust [Bergthorson, 2018]. This means that there will be enough resource availability for this particular use alongside the conventional uses of iron in construction and other sectors. Other metals that can be considered for electrofuels such as cobalt are far less abundant and more difficult to obtain making them more expensive and less attractive as an alternative fuel. The advantage of the abundance of iron as a metal fuel source is helped even further by the key advantage of recyclability of using iron powder as a fuel source.

2.1.2. Recyclability

As can be done with a number of other metal fuel sources, iron can be fully recycled after the process of energy generation. When iron powder is burned in a combustion chamber, the remaining products are iron oxides. These iron oxides cannot be used again for combustion in the state they are in as they have already been oxidised. Using either coke (a high-carbon distillate of coal) or hydrogen it is possible to reduce the iron oxides back into iron powder making the energy generation process full circle shown in figure 2.2 [Dirven et al., 2018].

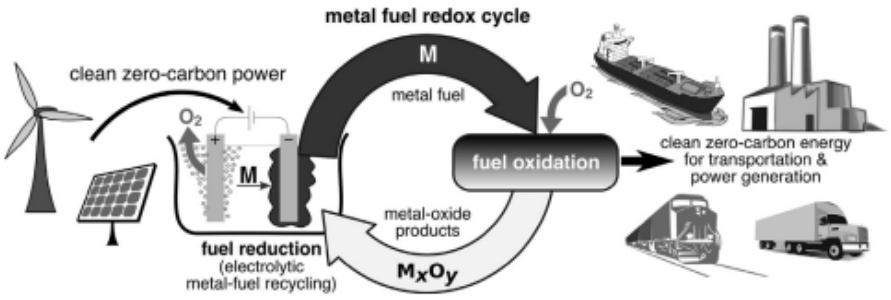

Figure 2.2: Metal reduction cycle applicable for iron [Bergthorson, 2018]

This has the main advantage that generally only one supply of iron powder is required for a specific application as this source can be infinitely reused through the reduction process. This is, of course, not possible with fossil fuels as their combustion products cannot be reduced back into the fuel.

2.1.3. Zero-Emission

The main advantage of using iron as a fuel source over fossil fuels is of course its extremely low emission in combustion. The combustion of iron releases no carbon dioxide as a byproduct and very low levels of nitrous oxide with a maximum of 94 ppm of nitric oxide and 1 ppm of nitrogen oxide measured in a 100kW test setup by TU Eindhoven [van Rooij et al., 2019]. The low level of nitrous oxide byproduct is dependent on both the temperature of the combustion as well as the amount of hydrogen atoms present in combustion. For iron powder the temperature still reaches levels where some nitrous oxide may be released. However the lack of hydrogen atoms in this combustion ensure this level is extremely low, especially when compared to conventional diesel engine combustion [van Rooij et al., 2019]. Furthermore, the entire cycle of iron powder energy generation can be considered zero-emission as well. This is because it is possible to reduce the iron oxides into iron powder using sustainably produced hydrogen.

2.1.4. Safety

Fossil fuels like diesel and gasoline are volatile substances that must be kept in very specific conditions in order to store and transport safely. This is also the case with sustainable fuels such as hydrogen and methanol. Iron powder and iron oxides are not volatile substances and thus bring about much less safety concerns [Seijger, 2020]. Heavy fuel oil, ammonia and methanol are fuel sources that are either considered a health hazard, acutely toxic or both [van Rooij et al., 2019]. Iron powder is not

considered either and does not require a specific temperature or pressure level for safe containment [Seijger, 2020]. This makes the transport and storage of iron powder significantly less complicated than many other fuel sources.

2.1.5. Retrofit and Filtering

The final key advantage of using iron powder is the possibility for use of existing systems rather than requiring new equipment to be built. This is because the flame temperature required for iron powder combustion is roughly the same as that required for hydrocarbon combustion (around 2000 C) [van Rooij et al., 2019]. This flame temperature also remains below the phase change temperature from liquid to gas. This ensures that the oxide particles created through combustion will remain around the same size as the iron powder, an order of several tens of microns [Huang et al., 2013]. Filtering then becomes much easier as existing filtering systems need only be slightly altered to be applied for iron oxide collection. The collection of these oxides is one of the key steps that makes iron powder a fully sustainable fuel source. Other metals can combust into the gaseous phase making filtering and oxide collection much more difficult as the particles will be in sub-micron order of size.

2.1.6. Energy Density

A good measure of comparison with other energy sources is its energy density which gives a good indication of how much fuel is needed for a certain amount of power delivered. This energy density can be split into a volumetric energy density and a gravimetric energy density. Considering the iron is in powdered form it can be estimated that around 50% more volume will be required to store the powder as opposed to the iron in solid form [van Rooij et al., 2019]. This results in a volumetric energy density estimate of around 0.04 kWh/L for a test setup of 50MW [van Rooij et al., 2019]. This is close to the volumetric energy density of a 36MW diesel engine which comes in at 0.03 kWh/L [van Rooij et al., 2019]. The gravimetric energy density is mainly impacted by the high mass of iron as a material. Furthermore, after combustion the oxides will end up a factor 1.4x heavier than the iron powder [van Rooij et al., 2019]. This results in a gravimetric energy density of 0.07 kWh/kg for the 50MW test setup. This is once again quite similar to the 0.04 kWh/kg energy density found for a 36MW diesel engine.

2.1.7. Abrasivity

Both iron and iron powder are hard and abrasive substances. Iron powder has a hardness level of 4 MOHS and an average particle size of 45 microns [van Rooij et al., 2019]. The iron oxides have a hardness level of 5-6 MOHS, meaning these will likely be even more abrasive than the iron powder [van Rooij et al., 2019]. This is a concern for the maintenance of the storage, transport and combustion systems that the powder travels through. While the powdered form does decrease abrasiveness of the iron, more research is required to determine to what extent this abrasiveness is decreased.

2.1.8. Moisture Sensitivity

Iron powder reacts negatively when it comes into contact with moisture. The iron powder particles may start to clump making transport more difficult. Even more importantly, contact with moisture may cause the particles to oxidise early [Huang et al., 2013]. This is especially undesirable as this oxidisation process needs to occur in the combustion chamber for maximum heat extraction. A low moisture level also results in a lower nitrous oxide byproduct [van Rooij et al., 2019]. This means that iron powder needs to stay out of contact with water. This becomes especially difficult on a ship.

2.1.9. Efficiency

A key issue requiring more innovation and research is in improving the efficiency of energy generation through iron powder combustion [de Kwant, 2021]. The energy generation is done through an external combustion engine as the combustion process is not quick enough for an internal combustion engine [de Kwant, 2021]. The external combustion engine has far higher thermal losses than an internal combustion engine. The heat energy created through combustion is then converted to mechanical energy through a steam turbine whose total system efficiency is also significantly lower than that of a standard diesel engine. Newer steam turbines with higher efficiencies are in development and are discussed in section 2.2.4. These are still, however, in the early stages.

2.2. Key Components Iron Powder Powertrain

The iron powder powertrain consists of multiple systems in order to complete the entire cycle of power generation. A large array of infrastructure, systems and equipment are required both on land and onboard to complete the process. Figure 2.3 shows all the components required.

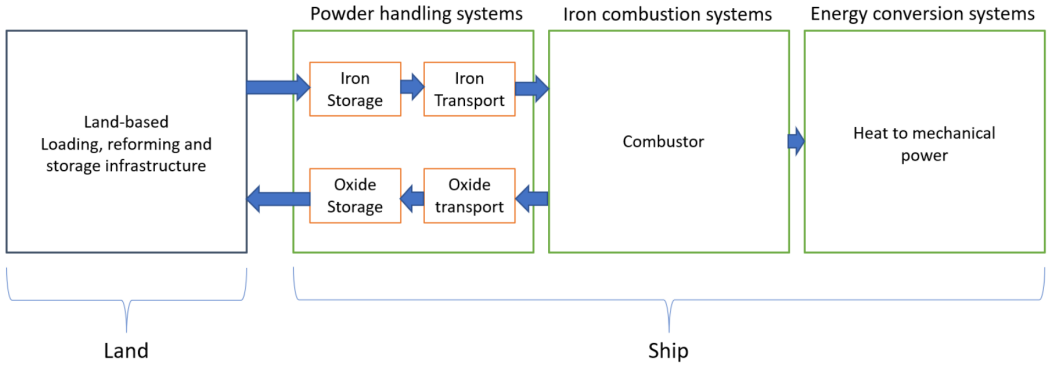

Figure 2.3: An overview of the components in the iron powder powertrain [de Kwant, 2021]

The land based components are mainly the storage areas as well as regeneration plants. These are of less importance for the ship processes and will therefore not be further looked into in this report. The components onboard the ship can be split into four different systems: storage, transport, combustion and energy conversion systems. These systems will be further explored taking a look at the current state-of-the-art, as well as some ideas that are still in development or testing phase. These systems will also be analysed in context of the challenges that arise with placement onboard a ship.

2.2.1. Storage

The storage of iron powder is fundamentally different to the storage of conventional liquid fuels such as marine diesel oil (MDO) and heavy fuel oil (HFO). Whereas liquid fuels are stored in tanks at a around 40 degrees Celsius, iron powder cannot be stored in tanks and does not necessarily require a specific minimum temperature level [Seijger, 2020]. As with all other bulk goods, iron powder is best stored in silos [van Rooij et al., 2019]. The powdered form of the iron powder results in a higher volume requirement as well as a high mass level as was discussed in subsection 2.1.6.

There are two types of silos that can be used for iron powder storage, a horizontal or vertical silo shown in figures 2.4a and 2.4b respectively [van Rooij et al., 2019]. An advantage of using horizontal silos is the potential for a lower center of gravity. Due to the large amount and therefore high mass of iron powder required for substantial energy production, the storage compartments become a key system to consider when determining the center of gravity of the vessel in relation to its overall stability. A horizontal silo is more comparable to the shape of a tank allowing for much lower placement to ensure a low center of gravity for the vessel. A key disadvantage of the horizontal silo however is its lower discharge level in comparison with the vertical silo [“The Difference Between Horizontal and Vertical Silos”, 2019]. The vertical silo can discharge its bulk content through the hopper system mainly through gravitational forces and flow design. A horizontal silo requires a special mechanical extraction system, a ”walking floor”, to ensure full discharge of the bulk material within [“The Difference Between Horizontal and Vertical Silos”, 2019]. These horizontal silo systems are constantly being developed and improved and may soon be the preferred storage unit. However, at this current moment the vertical silo is more reliable despite its higher center of gravity.

(a) Typical Horizontal Silo [“Horizontal silos EUROSILO”, n.d.]

(b) Typical Vertical Silo [“Horizontal silos EUROSILO”, n.d.]

The design of the vertical silo must take into account the material characteristics of the iron powder as well as the dynamic motions of the ship during transit. For storage, the most important material characteristics are the theoretical mass density, bulk-mass density, average particle size and hardness. These values are needed for both the iron powder as well as the iron oxide powder as both will need to be stored in these silos. Table 2.1 shows the important material characteristics for both the iron powder and the oxides respectively.

	Iron Powder	Iron Oxide (Hematite)	Unit
Theoretical Mass Density	7.874	5.26	t/m^3
Bulk-Mass Density	2.45	3.5	t/m^3
Average Particle Size	45	45	μm
Hardness	4	5-6	MOHS

Table 2.1: Material Characteristics Iron Powder and Iron Oxide [van Rooij et al., 2019]

The bulk-mass density determines how much volume the silos will need to store a certain mass amount of iron powder. More volume will be needed to store the iron oxides than the iron powder by a factor of around 1.4. The mass and volume will, of course, be determined by how much power is required for a specific vessel to operate between refueling. The size of the particles determines the extent to which cohesion and adhesion properties may impact the flow. The shape of the particles also plays a large role in this, however, the particle shape differs per particle and is therefore difficult to measure [de Kwant, 2021]. Silo design for iron powder particles will be based upon the angle of internal friction and the friction angle [van Rooij et al., 2019]. These determine the level of flow and the efficiency of discharge of the silo, and must be specifically adapted to the bulk material being stored. Hardness and abrasion levels will need to be tested to ensure the structural integrity of the silo. The silo must also be fully closed to prevent sea moisture from contaminating the iron powder particles. This also fixes the problem of premature oxidisation as well as potential explosive dangers. As of yet it is unsure as to what temperature the silo design will be able to operate at. The iron oxide particles that return to the silo after combustion are heated to much higher temperatures than the iron particles to be combusted. The ”bottom ash”, to be further discussed in subsection 2.2.3 are especially hot and further research will determine whether cooling systems may be required for these oxides before they enter the storage silo again.

The setup for the vertical silos is a problem of space optimisation. This is especially important on a ship where the volume available is much more limited than on land. Two designs, shown in figures 2.5a and 2.5b, exist currently for how to set up the vertical silos for storage of both the iron powder and the iron oxides [de Kwant, 2021]. While there is no danger concern regarding the mixing of iron powder and iron oxide, the particles must be separated to ensure optimal combustion efficiency. This can be done through the creation of a horizontal barrier in the silo to separate the outgoing iron powder at the bottom from the incoming iron oxide above. This mechanism will require an extra power source and will likely create a problem when the silos are loaded with bulk [van Rooij et al., 2019]. The loading of a vertical silo can only be done at the top and discharge can only be done at the bottom, a barrier in between the two causes difficulties. Therefore, a more practical alternative has been designed in which

more volume will be taken up by an extra vertical silo for iron oxide storage. While both designs have certain flaws and advantages, the feasibility of designing an extra vertical silo instead of a riskier splitting mechanism that disrupts loading and unloading of iron oxide makes the extra silo storage system more appropriate. Further research into a splitting mechanism that does not interfere with refueling may change the design of the vertical silo setup in the future.

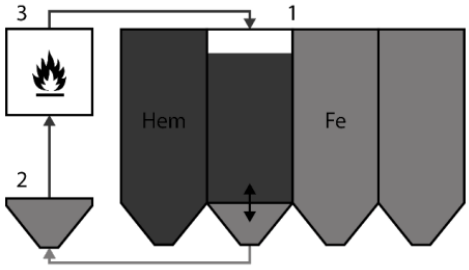

(a) Silo setup with mechanical barrier between iron powder and iron oxide [de Kwant, 2021]

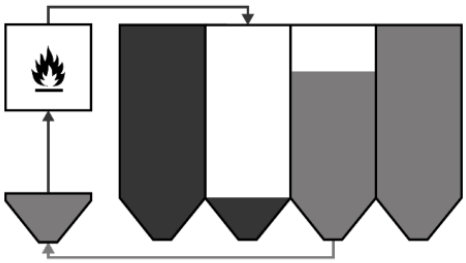

(b) Silo setup with extra silo for iron oxide storage [de Kwant, 2021]

2.2.2. Transport

Transport of bulk material can be done through many different systems, each with certain characteristics that provide both advantages and limitations. Two types of transport are considered feasible for iron powder transport, direct carrying transport systems and airflow transport systems. Here, the drag conveyor and the pneumatic two-phase conveyor transport systems will be considered. The transport systems in the powertrain will include transport from the storage silo to the dispersal system, from the dispersal system to the combustion chamber and from the combustion chamber back into the storage silo. The first two stages of the transport path are for the transport of iron powder and the last stage is for the transport of iron oxides back into the silo. The main point of concern regarding the transport of iron powder and iron oxides is dealing with the hardness and abrasiveness. The selected feasible transport systems all have the highest degree of resistance against abrasive materials.

Drag Conveyor

The drag conveyor, pictured in figure 2.6, functions like the name suggests in that it 'drags' the bulk material through the transport chute through a chain of 'flights' (paddles) [Cavallo, n.d.]. This type of conveyor transport is much less sensitive to the effects of abrasion than for example a typical belt conveyor. The drag conveyor is also adept at providing a homogeneous flow of bulk which is especially important in the transport from the dispersal system to the combustion chamber. The flow rate will likely need to be lowered in order to ensure no abrasive damage is done to the transport system. The rate of fill of this system is quite high leading to a higher efficiency and higher possible flow rates when compared to other bulk transport systems like the bucket conveyor. These systems are, however, quite expensive in both acquisition and upkeep [van Rooij et al., 2019].

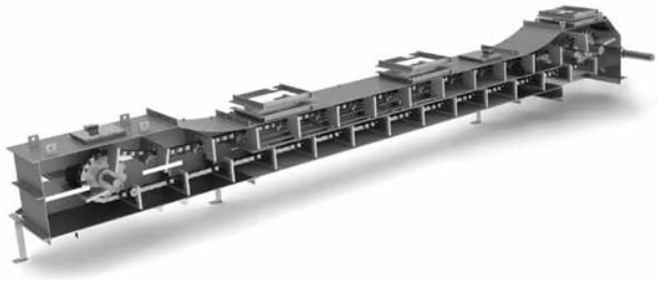

Figure 2.6: Drag Conveyor ["Drag Conveyor Professionals", n.d.]

Pneumatic Two-Phase Transport

Pneumatic two-phase transport, pictured in figure 2.7, functions completely differently to drag conveyors in the fact that it transports the bulk material through an air stream rather than direct contact [“Pneumatic conveying: Process Technology”, n.d.]. This air stream is created inside a tubular enclosed piping by a pump or high power fan to push the bulk materials through the piping. This system is able to provide transport with sharp turns in any direction. Its high transport speed in the air stream makes it possible to minimise the size of the transport tubes whilst maintaining the minimum level of flow required. Similar to the drag conveyor, this flow level may need to be reduced to ensure minimal damage due to abrasiveness of the iron powder and oxide powder. The pneumatic two-phase transport system is also able to provide a homogeneous flow rate for transport from the dispersal system to the combustion chamber [van Rooij et al., 2019]. This system has already been used for zinc transport whose properties are highly comparable to iron powder. The main concern with this system is the high amount of power required to operate in comparison to most other bulk transport systems.

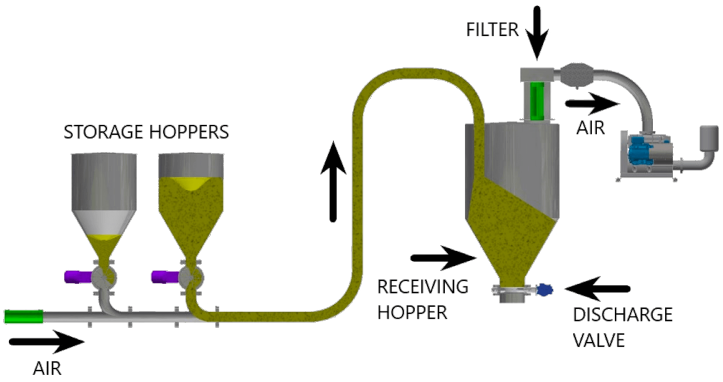

Figure 2.7: Pneumatic Two-Phase Transport [“Dilute phase pneumatic conveying”, n.d.]

2.2.3. Combustion & Filtering

The process of iron powder combustion is done in an external combustion chamber. This is due to the fact that the combustion process for iron powder is much longer than is possible in an internal combustion chamber [van Rooij et al., 2019]. This is coupled with the possibility of clogging of the iron powder particles in an internal combustion engine [van Rooij et al., 2019]. The chemical process of iron combustion is shown in equation 2.1 with the left side of the equation being the iron powder and oxygen and the right side of the equation being iron oxide and heat [Bergthorson, 2018].

$$xFe + yO_2 \rightarrow Fe_xO_{y*2} + heat \tag{2.1}$$

There are two main types of oxides that can result from iron powder combustion, namely Magnetite and Hematite and in very small amounts Wüstite [Bergthorson, 2018]. Magnetite and Wüstite are produced when incomplete oxidation occurs. Through full optimisation of the combustion process it is possible to ensure that only hematite particles are produced from combustion. This process of hematite production through iron powder combustion is displayed in equation 2.2.

$$2Fe + 1.5O_2 \rightarrow Fe_2O_3 + 825.5J/mol \tag{2.2}$$

These hematite particles exist in two categories after combustion, as a ’fly ash’ or a ’bottom ash’ [de Kwant, 2021]. The fly ash travel with the heated exhaust gas mixture and the bottom ash fall to the bottom of the combustion chamber. The collection of bottom ash is relatively simple and can be incorporated into the boiler design. Bottom ash will contain a significant portion of the heat energy produced in combustion, the key to improving the overall efficiency of the powertrain lies in the collection of this heat in these bottom ash. The most common method of heat extraction from bottom ash is a so called ’wet bottom ash handling’ system [de Kwant, 2021]. This system uses a large amount of floor space and is therefore sub-optimal for use aboard a ship. Another system of ’dry bottom ash handling’ is in development requiring further research to determine its potential aboard a ship [Ricci et al., 2018]. Fly ash collection is possible through a variety of methods. These particles are generally smaller than the

bottom ash and therefore more complicated when it comes to collection.

The three systems currently being used to collect fly ash are the rotational particle separator, the bag filter and the cyclone filter [van Rooij et al., 2019]. Cyclone filters are simple systems that require low maintenance. Similar to the rotational particle separator filter, the particles are filtered through a rotational, centripetal motion. These systems are generally followed by a bag house filter whose particle size limit is smaller than that of the cyclone and rotational particle separator. Here, the flow of exhaust gas is passed through a special filtering cloth which collects the remaining particles in the size range of a few nanometers. These three collection systems are shown in figures 2.8a, 2.8b and 2.8c.

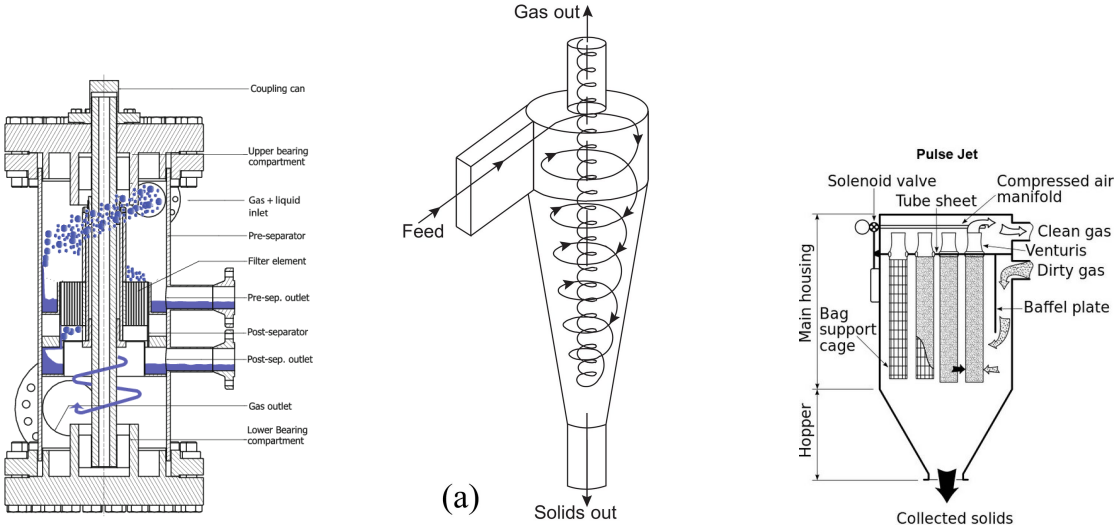

(a) Schematic overview of rotational particle separator [Brouwers and Van Kemenade, 2012] (b) Schematic overview of cyclone filter [Nakhaei et al., 2020] (c) Schematic overview of bag house filter ["Air Pollution Control Methodologies", n.d.]

Collection of the oxides is a key factor in ensuring that iron powder as a fuel source remains both sustainable and completely cyclical. According to European regulations, an iron powder system with an efficiency of around 38% should have an oxide collection rate of 99.999% [van Rooij et al., 2019].

In testing, the assumption is made that the combustion process is fully optimised and that the only oxide produced is hematite. With this assumption, the heat energy produced in combustion is estimated to be around 5.2 MJ per kilogram of hematite formed [van Rooij et al., 2019]. This works out to around 7.4 MJ of heat per kilogram of iron powder being combusted [van Rooij et al., 2019]. To minimise the heat 'lost' to the hematite, the mixture of air and iron powder can be altered. An increase in amount of air in the mixture will result in a lower percentage of combustion heat ending up in the hematite [van Rooij et al., 2019]. The increase in amount of air in the mixture is done through an exhaust gas re-circulation system.

2.2.4. Energy Conversion

The heat energy created from the iron powder combustion is converted to mechanical power through a thermodynamic cycle. There are several systems available for this cycle, each with certain advantages and disadvantages. The Stirling cycle, Brayton cycle, externally fired gas turbine cycle, Rankine cycle, supercritical steam cycle, supercritical carbon dioxide cycle and combined Brayton-Rankine cycle are possible thermodynamic cycles available for heat energy conversion into mechanical power [van Rooij et al., 2019]. Two cycles that are quite popular on an industrial scale as well as on ships are the Brayton cycle and combined Brayton-Rankine cycle [van Rooij et al., 2019]. These systems, however, are unable to burn iron powder internally. The Stirling cycle and externally fired gas turbine cycle are largely unable to reach their theoretical potential making these processes too risky to use in their current state [van Rooij et al., 2019]. This leaves the traditional Rankine, the upgraded ultra steam cycle (UST), the supercritical steam and carbon dioxide cycles as potential heat energy converters. These systems will be further explored to determine which system is most efficient and feasible. Here the focus will be on practical efficiency rather than theoretical efficiency as there is no telling how much development is

needed for certain cycles to be able to reach their theoretical efficiency. The feasibility will be determined through how common the practical use of these particular cycles is in current energy conversion systems.

Supercritical Steam Cycle & Supercritical CO_2 Cycle

The supercritical steam cycle and CO_2 cycle are able to reach a peak theoretical efficiency of around 60% [van Rooij et al., 2019]. This estimation is based off of what the efficiency the cycle can reach through feasible temperature levels and the physical limitations of the cycle itself. Supercritical steam cycles operate similar to a sub-critical steam cycle, however with a much higher pressure and temperature level in order to increase power and efficiency of the cycle as is shown in the T-s diagram in figure 2.9a. Currently the supercritical steam cycle operates at 250 bar and 600 degrees Celsius however, with further improvements and technical developments these temperatures can reach over 700 degrees [Nomoto, 2022]. There is, however, a certain limit to the steam temperature increase where beyond this point the costs of innovation will not be returned in high enough efficiency [Nomoto, 2022]. Current research is focused on finding this optimal point where the cycle efficiency is at its highest without diminishing returns. One of the main points of development for the supercritical steam cycle especially is the development of stronger and more durable materials that make up the components of the supercritical steam cycle as the high pressures and temperatures have a fatigue effect on lesser materials causing lower efficiency and more maintenance [Besarati and Goswami, 2017]. A recent estimation of the supercritical steam cycle puts the total cycle efficiency at 47%. This is however based on a plant design of several gigawatts which, when scaled down to ship output size, will likely lead to an efficiency of around 40% on a vessel design [van Rooij et al., 2019].

The supercritical CO_2 cycle setup has the potential to be a factor 10x smaller compared to a standard steam cycle making it a very interesting option especially for use onboard a ship where the space is more constrained [Yoonhan et al., 2015]. What makes the supercritical CO_2 cycle a potentially high efficiency cycle is its higher turbine inlet temperature [Seijger, 2020]. This high thermal efficiency is highly dependent on the cycle's ability to recuperate its high outlet temperatures [Yoonhan et al., 2015]. The development of supercritical CO_2 cycles is primarily focused on conversion of nuclear power however, studies have determined that other sources of heat energy such as iron powder combustion can also be connected to these systems. The supercritical CO_2 cycle is depicted in figure 2.9b as a T-s diagram. A recent estimation of the supercritical CO_2 cycle puts the efficiency of the total cycle at 49% [van Rooij et al., 2019].

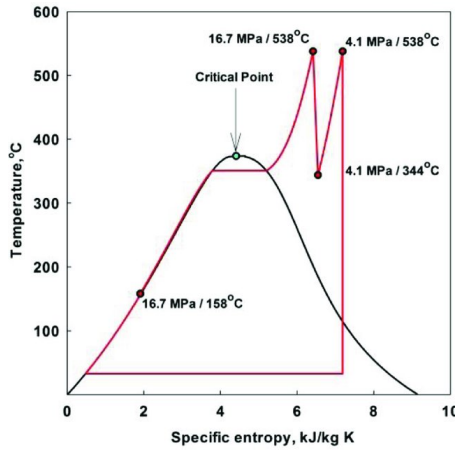

(a) A diagram comparing the sub and supercritical steam cycles, [Balakrishnan and Balakrishnan, 2017]

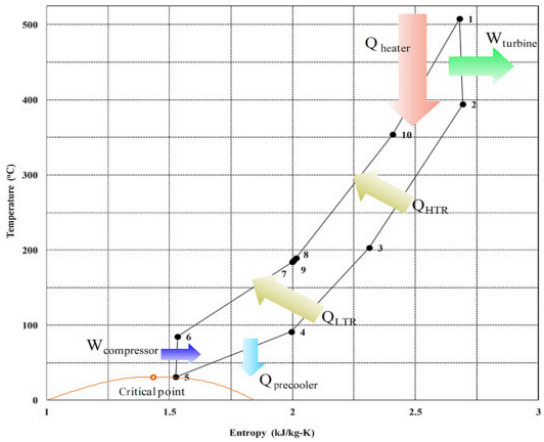

(b) A diagram depicting the supercritical CO_2 thermal cycle, [Yoonhan et al., 2015]

Rankine Steam Cycle & UST Cycle

The most feasible in terms of its commercial use at this stage of technological development is the Rankine steam cycle [de Kwant, 2021]. This cycle is easiest described using the four key stages pic-

tured in figure 2.10a. Through use of a pump, boiler, turbine and condenser, the heat energy taken from the iron powder combustion can be transferred into mechanical energy [Dincer and Zamfirescu, 2018]. Simply put, the pump ensures a steady flow of both heated water and steam throughout the system. The boiler changes the state of the water to steam which is passed through the turbine to generate a mechanical torque. This steam is then condensed and run through the pump to be recycled through the steam cycle again. This process is shown in a T-s diagram in figure 2.10b. This cycle does have a lower theoretical and practical efficiency than the two supercritical configurations at 30% total cycle efficiency [van Rooij et al., 2019]. Table 2.2 shows some of the key thermodynamic properties of the working fluid as it passes through each stage of the Rankine cycle.

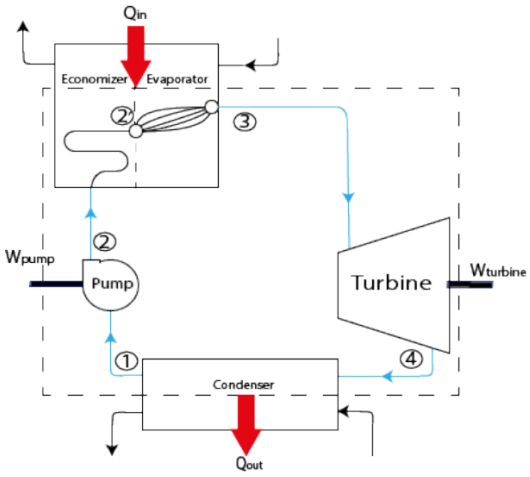

(a) Schematic overview of Rankine steam cycle, [Seijger, 2020]

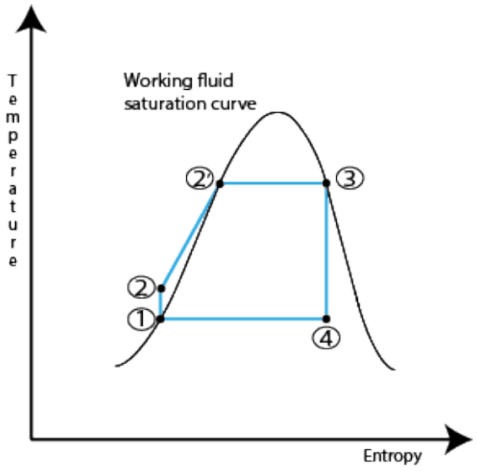

(b) T-s diagram of Rankine steam cycle, [Seijger, 2020]

Stage	Temperature [$C°$]	Pressure [bar]	Specific enthalpy [kJ/kg]	Specific entropy [$kJ/(kgC°)$]
1	99.61	1	1.303	417.4
2	99.97	29	1.305	421.1
3	232.0	29	6.199	2803
4	99.61	1	6.632	2404

Table 2.2: The properties of the working fluid through each stage of the Rankine cycle.

Mitsubishi has produced a new ultra steam turbine (UST) design, pictured in figure 2.11a, that acts as a reheated Rankine steam cycle [de Kwant, 2021]. This design utilises state-of-the-art reheat-regenerative systems to increase the efficiency of the total system [“Product Detail Information”, n.d.]. Thanks to other high end technologies, the UST is also more reliable and safe and durable giving it a far longer life expectancy [“Product Detail Information”, n.d.]. The three turbines in the UST cycle are linked to the reheating systems as they are passed through the turbines after each stage of reheating. It is this process of reheating and extracting through the turbine that minimises the heat and turbine losses [“Product Detail Information”, n.d.]. This results in an estimated efficiency increase of around 15% compared to standard steam cycles [“Product Detail Information”, n.d.]. Table 2.3 shows some of the key thermodynamic properties of the working fluid as it passes through each stage of the UST cycle.

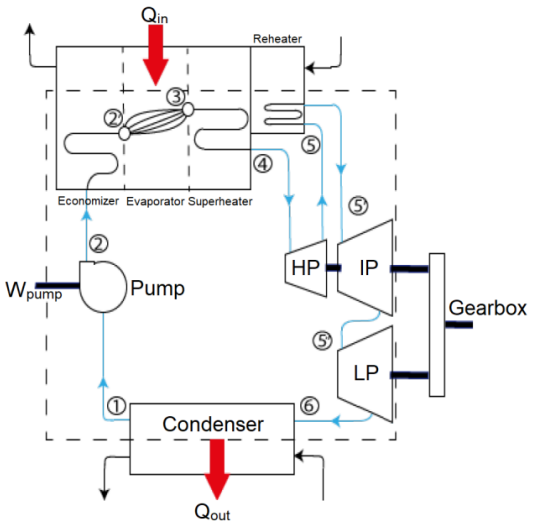

(a) Schematic of Mitsubishi's UST plant, [de Kwant, 2021]

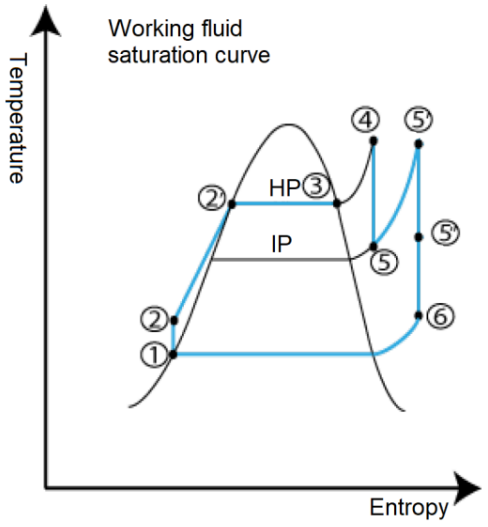

(b) T-s diagram of Mitsubishi's UST plant, [de Kwant, 2021]

Stage	Temperature [$C°$]	Pressure [bar]	Specific enthalpy [kJ/kg]	Specific entropy [$kJ/(kgC°)$]
1	47	0.106	196.8	0.655
2	47.95	100	209.4	0.673
3	311	100	2726	5.616
4	560	100	3527	6.789
5	467.1	40	3370	6.992
5'	560	40	3583	7.263
5"	305.3	7	3071	7.319
6	47	0.106	2585	8.124

Table 2.3: Key thermodynamic properties of working fluid passing through the UST cycle

2.3. Iron Powder Powertrain Key Limiters

There are certain points of concern that dictate the iron powder powertrain's output capability. These key limiters are the volume and mass concerns that come with iron powder storage systems, the part load and dynamic load issues that come with energy conversion and potential filtration issues concerning the heat collection from oxides in the combustion system. These issues are all discussed with respect to their impact on a maritime application. Finally, a comparison is made of the iron powder powertrain's optimal power output for each configuration.

2.3.1. Volume and Mass

Regardless of what combustion process, storage system, transport system or energy conversion system is used, it is clear that there will be a high volume and mass requirement for the iron powder powertrain. From vertical storage silos to filtering systems to the boiler system and turbine the total volume taken up by the entire powertrain becomes significant with regards to ship stability. This requires a deep dive into the possibilities for different configurations of this system keeping in mind the high energy cost for pneumatic two-phase transport between these systems. Previous research into the configuration of the iron powder powertrain have concluded with a placement of the storage silos toward the bow of the ship while keeping the combustion, filtration and conversion systems at the aft of the ship [de Kwant, 2021]. This is done in order to minimise the impact on the trim of the vessel. The vertical silos need to be placed as low as possible in the ship in order to maintain a low center of gravity. This configuration is subject to change depending on the vessel's own dimensions as well as its operational profile.

2.3.2. Part Load and Dynamic Load Issues

One of the main drawbacks of using a steam cycle for energy conversion is the low capability for part load conditions as well as dynamic loading. When the ship is in part load condition, the power requirement is lower than the design point of the power generation and conversion system. At this point the system is no longer working at optimum efficiency as this is only the case at the design point. This is the case with most power units however the drop in efficiency for a steam cycle can be quite stark as displayed in figure 2.12. Here the thermal efficiency η_i is seen to decrease significantly as the power output of the cycle is decreased in a test setup [Karakurt and Gunes, 2016].

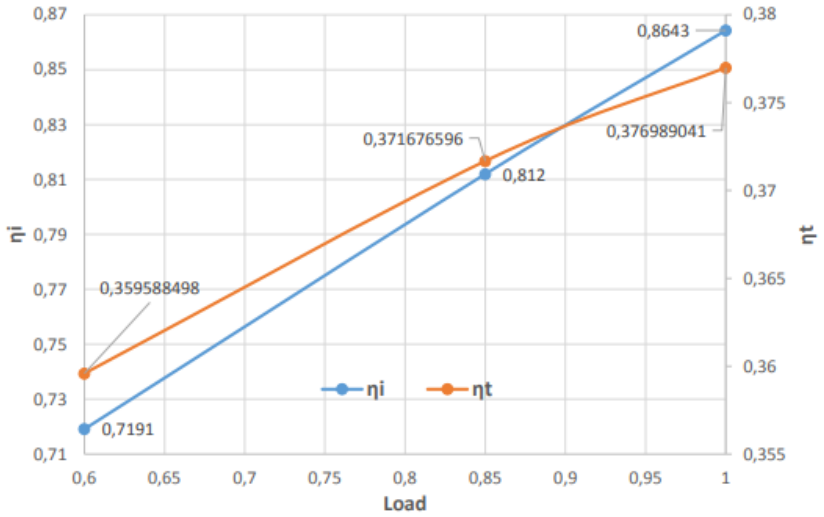

Figure 2.12: Diagram depicting thermal efficiency loss at partial loading of test setup [Karakurt and Gunes, 2016]

One of the most prominent solutions to the part load concern pertaining specifically to transit is the use of a controllable pitch propeller [van Rooij et al., 2019]. This propeller is able to change the angle of the blades in order to deliver a different propulsive power at the same power output. This allows the ship to travel at different speeds without changing the steam cycle from its nominal power output.

Another issue regarding the steam cycles is the lack of dynamic load capability. This is especially important on a ship and even more so on a service vessel. Dynamic loading is required in transit when the sea state is less than optimal but also in auxiliary power as certain systems only require a power source in bursts. A prime example of a dynamic loading situation on a service vessel is the use of a crane. A crane will require a high level of power but only over a short time space causing a significant load variation over a relatively short space of time. These load variations can be seen in section 3.2. Two solutions to the dynamic loading issues on vessels currently exist in the maritime sector. One is the use of an electric motor connected to the power generation system and the other is the use of multiple types of power generations systems for different propulsive and auxiliary load requirements.

Firstly, the power generation system can be connected to an electrical motor as displayed in figure 2.13b. This is similar to the use of diesel-electric propulsion systems in many current ship designs. This setup will likely increase the installation costs by around 10-15% [Doorduin et al., 2016]. The electric motor is far better equipped to deal with dynamic loading. Through the use of frequency converters, the RPM of the motor can be adjusted to change the mechanical power output [Doorduin et al., 2016]. This improves the manoeuvrability of the ship as well as running costs while keeping the entire powertrain fully sustainable.

Secondly, a hybrid configuration can be used to make up for the load variations [van Rooij et al., 2019]. Hybrid systems are already very common aboard ships with an example setup displayed in figure 2.13a. Hybrid configurations allow for a combining of different power sources to ensure the power requirements of all systems can be met at all times. The main power source can be used for propulsive power and the secondary power source can be used for additional loads such as hotel, equipment and

crane loads. Hybrid setups are possible with just about any power source, however in order to keep the setup fully sustainable, the use of batteries is most optimal. Similar to electric motors, batteries are able to discharge large amounts of energy over short periods of time [Linstad et al., 2017]. This setup would also increase installation costs as well as increase the mass of the setup significantly depending on how much power the batteries need to store. These batteries can, however, be reused as it is possible for them to be recharged by the iron powder powertrain after discharge. Another alternative to hybridise the iron powder powertrain with is fuel cells as these also are sustainable power sources with fast discharge capability [Klebanoff et al., 2020]. Once again, the increased setup costs and increased safety hazards make this a less attractive option [Klebanoff et al., 2020].

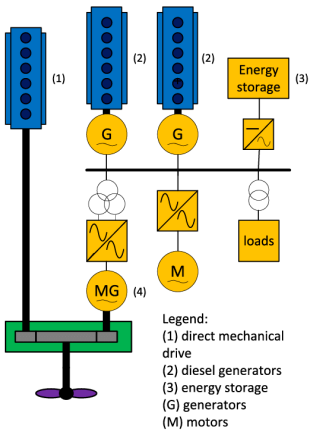

(a) Diagram of a hybrid propulsion setup [Geertsma et al., 2017]

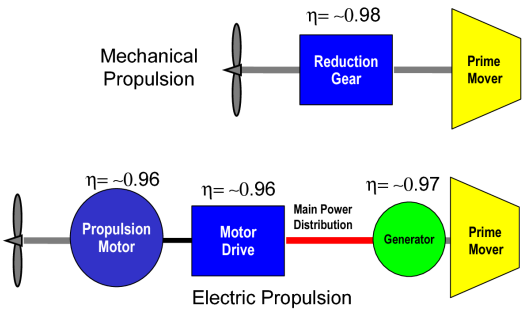

(b) Diagram of an electric propulsion setup [McCoy, 2002]

2.3.3. Heat Collection of Oxides

The boiler is one of if not the most crucial system component as it combines the combustion of the iron powder with the heat conversion of the steam cycle. The entire iron powder powertrain setup depends highly on the state and capacity of the boiler to transfer this heat energy. The efficiency of the boiler is highly dependent on the amount of bottom ash and its temperature [Ricci et al., 2018]. If there is a lot of bottom ash and its temperature is high then that accounts for a significant portion of the heat energy that will not continue with the heated gas mixture and the fly ash to be converted into mechanical energy [van Rooij et al., 2019]. The impact of the amount of bottom ash and its temperature can have an impact of up to 15% thermal efficiency of the boiler as is depicted in figure 2.14 [van Rooij et al., 2019].

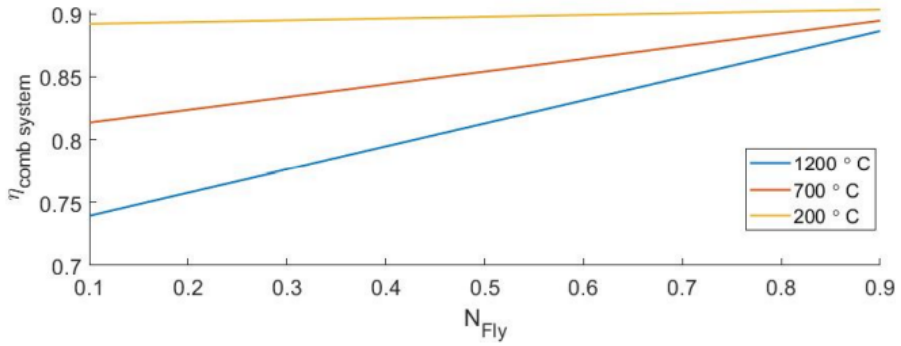

Figure 2.14: Graph depicting the potential loss in boiler efficiency at varying fly to bottom ash mixtures and temperatures [van Rooij et al., 2019]

Heat must be collected from the bottom ash to ensure that the total system efficiency remains high enough. If it is not collected then this potentially substantial amount of heat is lost to the environment significantly decreasing the total efficiency of the system. This heat energy from the bottom ash can be

used to preheat the combustion air up to 700C depending on both the temperature of the oxides and the ratio of fall to fly ash [van Rooij et al., 2019]. As mentioned earlier, the commonly used 'wet bottom ash handling' systems cannot be used for iron powder systems aboard a ship due to the involvement of water and the large area requirement [Ricci et al., 2018]. The 'dry bottom ash handling' systems are currently in development and can provide an ever improving way to collect heat from bottom ash.

Where the wet bottom ash handling systems use water to cool the bottom ash, the dry bottom ash handling system pictured in figure 2.15 uses cooled air [Ricci et al., 2018]. This airflow is used to both cool the bottom ash as well as heat up the air in a heat exchanging manner. After the air is heated it enters the boiler again, this time at a higher temperature. This heat extraction from the bottom ash and its use as preheating of the air mixture in the boiler increases the boiler efficiency van Rooij et al., 2019. This is due to the increased oxidising atmosphere created by preheated air in the boiler further reducing the chance of unburned iron powder particles after combustion [van Rooij et al., 2019]. Most dry bottom ash systems include a crusher system that crushes the oxide particle to a smaller size, however, this is not needed for iron powder as the average size of the oxide is already small enough [de Kwant, 2021]. This means that the precrusher in figure 2.15 designed for coal bottom ash can be left out in an iron powder design allowing the cooled oxides to be directly transported to the storage silo.

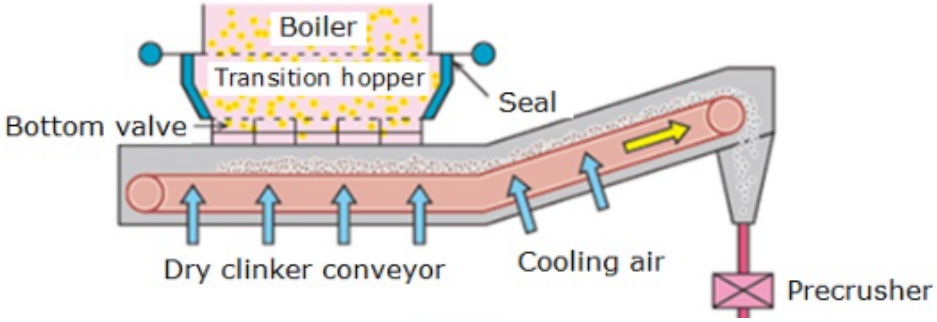

Figure 2.15: Schematic overview of a dry bottom ash handling system ["Kawasaki Receives Order from Kobe Steel for Two Coal Plant Ash Handling Systems", 2016]

2.3.4. Specific Energy and Energy Density

One of the main indicators of the power output capability of the iron powder powertrain is its specific energy and energy density. These values are of course dependent on the efficiency of the system used to combust and convert its heat energy to power. Iron powder is assumed to have a heat of combustion of around 7.4 MJ/kg [van Rooij et al., 2019]. Assuming the combustion, transport and storage are at optimal efficiency, the variation in specific energy and energy density is due to the different available thermodynamic cycles. The specific energy and energy density are displayed in table 2.4 for the simple high pressure Rankine cycle, UST cycle, supercritical steam cycle and supercritical carbon dioxide cycle. Due to lack of system information, the specific energy and energy density of both the UST cycle and the supercritical carbon dioxide cycle was made in an estimation based off of data such as the inlet pressure and temperature [van Rooij et al., 2019].

	Specific Energy [kWh/kg]	Energy Density [kWh/l]
High Pressure Rankine Cycle	0.434	1.52
Mitsubishi UST Cycle	0.472	1.65
Supercritical Steam Cycle	0.674	2.36
Supercritical Carbon Dioxide Cycle	0.702	2.46

Table 2.4: Table showing the specific energy and energy density of the iron powder in the case of these four thermodynamic cycles [van Rooij et al., 2019]

The difference between the supercritical and (Upgraded) Rankine cycles is made very clear in this table. A reduction of around 30-40% of the required mass and volume of bunker is substantial and

highlights the importance of further development of these supercritical cycles. These values can be used in section 4.3 to determine what storage volume is required for bunkering as well as the mass. While the supercritical cycles appear to be the most obvious choice for iron powder energy conversion it is also important to recognize the feasibility of these systems. Both supercritical systems are still largely in development and therefore untested in marine environments. The UST cycle is a proven and commonly used system which makes maintenance much easier. Therefore, despite its lower specific energy and energy density, the UST cycle will be used as the energy conversion system while keeping an eye out for the further development of the supercritical cycles.

2.4. Conclusion

The results of this investigation into iron powder powertrains has yielded a good understanding of what the state-of-the-art of energy generation using iron powder is and what areas can be improved most in future research. It is clear that there are many different components of importance throughout the entire powertrain with many still in development that can increase the efficiency of this energy generation type. It is clear that this form of metal combustion has the potential to be fully sustainable due to its availability, recyclability, safety and zero-emission characteristics. These are coupled with certain challenges that require more development and research, mainly the thermal efficiency and mass/volume requirements.

With regards to ship design and specifically the general arrangement of the vessel it is the storage of the iron powder together with the transportation that requires new ideas and approaches to the powertrain setup aboard a vessel. This due to the high volume and mass requirements that come with iron powder use. The current preferred method of storage is a vertical silo which has a significant impact on ship stability. The current method of particle transport aboard a vessel is the pneumatic two-phase transport which may end up connecting over large sections of the ship depending on component placement.

Regarding the combustion and energy conversion the state-of-the-art systems are split between the following key components: the combustion chamber, filtering/particle collection systems and the energy conversion system. The combustion chamber is an external combustion chamber due to the iron powder simply not being able to combust optimally in an internal combustion chamber. This does create a higher level of temperature losses compared to combustion done in an internal combustion chamber. Filtering and particle collection systems are necessary to ensure the process is fully sustainable as the oxides released in combustion must be collected for regeneration back into iron powder. Full collection of iron oxides is believed to be possible through a cyclone filter in combination with a bag house filter. The energy conversion system is one undergoing serious development with resources being poured into the creation of new more efficient thermodynamic cycles such as the supercritical steam cycle or the supercritical CO_2 cycle. The current state-of-the-art concerning the energy conversion from combustion heat to mechanical power is the reheated Rankine cycle known as the ”Ultra Steam Turbine” by Mitsubishi. This system has the the highest efficiency of the currently commercially available thermodynamic cycles that are assumed to be compatible with iron powder combustion.

The current iron powder powertrain configuration has several challenges that concern installation aboard a vessel. The volume and mass specifications of iron powder limit vessels of certain sizes to a lower range than a diesel powered configuration. This means that ship type, size and operational profile will be important in the installation of an iron powder powertrain. The poor part-load and dynamic load characteristics of steam cycles will likely have and impact on the operation of the vessel with electric conversion and hybrid propulsion configurations available to solve this issue. The collection of the ”more difficult to filter” fly ash will need further research with dry bottom ash handling systems being in development.

With the current state-of-the-art components of the iron powder power generation there are certain configurations of iron powder powertrains feasible on vessels. In section 3, the most optimal service vessel for the iron powder powertrain will be selected through a two-step filter.

3

Service Vessels

The term service vessel encompasses a large variety of ship types with varying sizes and functions. A broad list of service vessels is put through a two-phase down selection starting with the wide range of service vessels and ending with one, most optimal service vessel type. First, a list of different types of service vessels will be made and their feasibility for an iron powder powertrain determined based upon size and range (3.1). A select few vessel types that have passed first filter will then be further analysed based upon their operational modes and missions (3.2). These operational profiles will be used to make an estimation load variation over the course of a mission and of the total output requirements along with their initial iron powder volume and mass requirements (3.3).

3.1. Types of Service Vessels and their Functions

The term service vessel is one that can be understood to contain a large assortment of various types of ships. Some consider only propulsive support vessels to be service vessels while others consider a wider range of vessels to fit within the service vessel ship type. In this research the range of service vessels to be looked at will encompass the specific transport, support, construction and specialty vessels that can be considered service vessels. Service vessels are often identified by their more complex and mission specific functions that set them apart from the common transport vessels. Many of these service vessels are used for construction or maintenance tasks on offshore projects such as offshore wind farms. Others have specific functionalities to perform certain operations at sea such as dredging, research and pipe-laying. These vessels come in various sizes with varying functionality and propulsive and auxiliary requirements. Table 3.1 shows a list of the most common service vessels used within the four categories of transport, support, construction and specialty vessels.

Transport Vessels	Support Vessels
- Walk to Work Vessel - Platform Support Vessel - Heavy Lifting Cargo Vessel - Daughter Craft/Crew Transfer Vessel	- Tugboat - Anchor Handling Tug Supplier
Construction Vessels	**Specialty Vessels**
- Offshore Subsea Construction Vessel - Semi-submersible Vessel - Jack-up Vessel	- Pipe-laying Vessel - Research Vessel - Dredger

Table 3.1: Table of commonly used service vessels

These are the types of service vessels that are becoming more and more common in the global fleet and will certainly require more sustainable sources of power in the near future. The following subsections will cover all of the service vessel types listed and provide a general analysis regarding the

main dimensions of these vessels as well as speed, range and functions aboard to determine which vessels are fit for iron powder powertrain installation. The two most important specifications are the size of the vessel and the range of the vessel. It is important that the vessel is large enough to house an iron powder powertrain system without this system having to change the ship's main dimensions or stability. The range of the vessels is important because ships that travel longer distances will subsequently require larger volumes and masses of iron powder once again increasing the effect on the main layout of the vessel and its stability. Vessels that fit the size and range constraints for iron powder powertrain installation will be considered for further investigation in section 3.2 looking into their operational profiles.

By taking a look at each of the mentioned service vessel types further detailed in appendix A, a number of vessels are eliminated based on their size, range and functionality. A few of the remaining vessels are considered highly similar in terms of size, range and functionality such as the platform supply vessel and the walk-to-work vessel. Of these highly similar groups of vessels, the one with the most available information to work with is chosen leaving only five different vessel types remaining for the second filter; the platform supply vessel, the jack-up vessel, the semi-submersible transport vessel, semi-submersible crane vessel and the research vessel. These five vessels are then further analysed in the second filter focusing on the operating profile and load profile.

3.2. Operational Profiles

On basis of the short analyses of the different service vessel types and their size, functions and capacities a shortlist of the four most promising service vessel types has been made. This selection was largely made based upon the limited data made available for the operational profiles of service vessel types. Only service vessel types with sufficient information regarding operational profiles were considered for further analysis. Sufficient distinction between the operating profiles of these four vessels was another important factor as this would allow for a clearer comparison between the chosen vessels. The four service vessel types that best fit these requirements are the standard platform support vessel, the jack-up vessel, semi-submersible vessel types and the research vessel. In order to aid in a further down selection, a more comprehensive operational profile will be taken into account regarding the possibilities for an iron powder powertrain. These operational profiles will be used in order to come to a load variation estimation and a total power output requirement off of which the iron powder powertrain will be based. Using these operational profiles, load profiles and power requirements the final selection will be made to determine which service vessel is most optimal for iron powder powertrain use.

3.2.1. Operational Profiles

Platform Support Vessel

The platform support vessel (PSV), as mentioned in section 3.1, is designed specifically for offshore platforms. It carries personnel and supplies from the shore to the platform in order to provide either inspection, maintenance or repair of offshore structures [Bronkhorst, 2021]. This means that the ship is equipped with hotel facilities for the passengers and crew as well as extensive storage holds for equipment [Satpathi et al., 2017]. As most PSV's are built for similar operations it is best to take one example of an existing PSV and analyse its operations and onboard systems to determine its operational profile and different power requirements. The Platform Supply Vessel 4000 CD is a design by Damen and its main function is offshore supply ["The complete Platform Supply Vessel", n.d.].

Figure 3.1: A 3D rendering of the PSV 4000 CD [“The complete Platform Supply Vessel”, n.d.]

During the course of a particular mission, the PSV will be in varying operational modes from transit to dynamic positioning to standby to port operations [Guegan et al., 2020]. The annual operational profile for a platform support vessel (or offshore support vessel) is displayed in figure 3.2 pitting the average power demand against the annual hours of a particular operational mode.

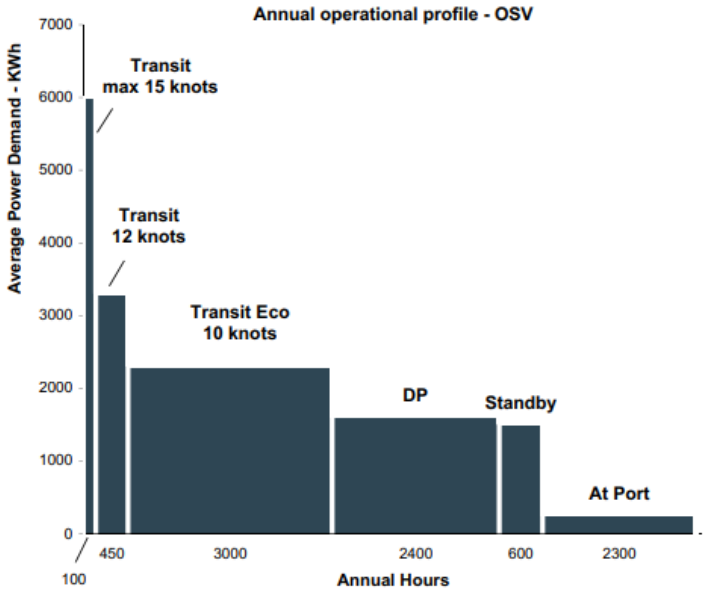

Figure 3.2: Overview of annual operational profile of platform/offshore support vessels. [Linstad et al., 2017]

Here it is clear that transit takes up the most time annually with 3550 hours of the total 8850 hours. Dynamic positioning and port operation are relatively even at 2400 hours and 2300 hours respectively with only 600 hours spent in standby annually [Linstad et al., 2017]. With the knowledge that not every mission is similar and that environmental circumstances may cause variation of these percentages, it is possible to take these percentages of operational modes and use them as a basis for the operational profile of a single mission. Figure 3.3 shows this percentage distribution of time spent in these operational modes.This distribution of operational modes over time is the basis for which a load estimation will be done. This will give further insight into the workings of a platform supply vessel and what the requirements from an iron powder powertrain would entail.

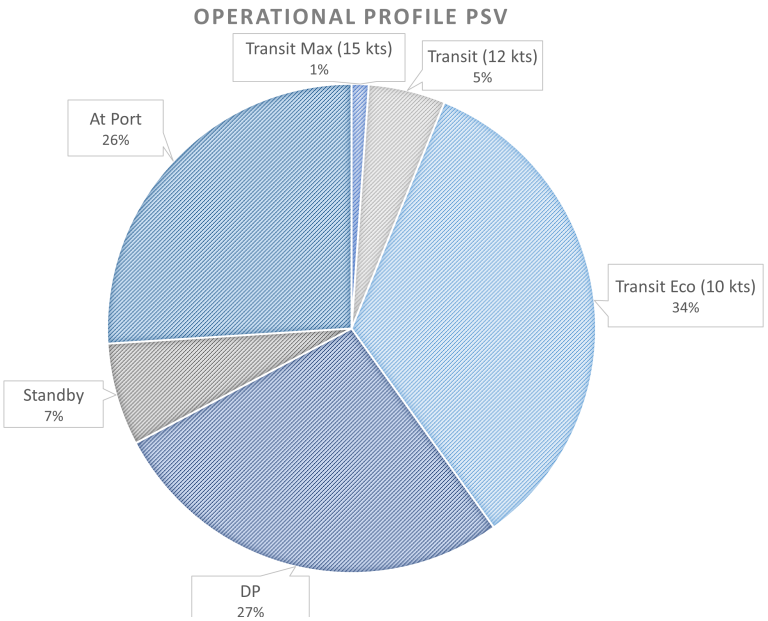

Figure 3.3: Percentage distribution operational modes of PSV. [Linstad et al., 2017]

Jack-up Vessel

Jack-up vessels are much larger vessels compared to platform support vessels as these vessels are built for installation of offshore structures as well as heavy maintenance. These vessels are equipped with much larger cranes as well as four pillars on which the jack-up vessel can lift itself out of the water. Similar to the platform supply vessel, a specific model of jack-up vessel will be used for further analysis of its operational profile. The 'Vole au vent' (figure 3.4) is an offshore jack-up installation vessel designed by 'Jan de Nul' built in 2013 ["Vole au vent: Offshore Jack-Up installation vessel", n.d.].

Figure 3.4: Image of the 'Vole au vent' lifting itself out of the water ["Vole au vent: Offshore Jack-Up installation vessel", n.d.]

Jack-ups can perform multiple mission types with the most common being either drilling or installation. The mission duration for drilling can reach up to the 30 day endurance stated for the 'Vole au vent'. T. Lerchenmueller claims that installation performed by Jack-ups is done for only a few days

in between reloading and possible refueling [Personal Communication, 2022]. With focus on installation, specifically that of wind turbines, the operational modes of the Jack-up vessel include: loading at port, transit, jack-up, installation, heavy maintenance and jack-down [Stempinski et al., 2014]. These operational modes all require different levels of power and propulsion levels. A main difference to the PSV operational profile is that the thrusters are not constantly being used for either propulsion or dynamic positioning due to the jack-up process. T. Lerchenmueller claims that when loading at port and when installing a wind turbine, the jack-up vessel is standing on its pillars out of the water [Personal Communication, 2022]. A table of time spent in a particular operational mode during a single jack-up installation mission [Stempinski et al., 2014] has been used to create the percentage distribution of operational modes of a jack-up vessel in figure 3.5.

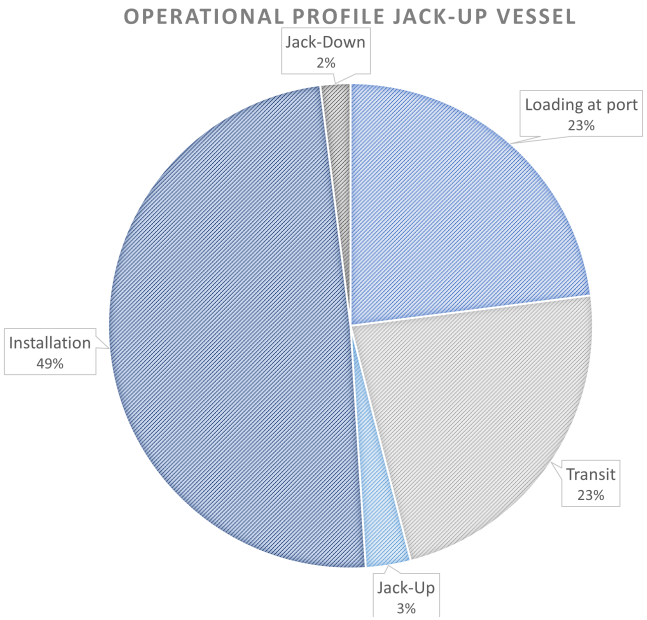

Figure 3.5: Percentage distribution operational modes of Jack-Up

This operational profile is based upon one particular mission and is therefore subject to change. This can be due to weather conditions causing delays or due to difference in installation or maintenance mission and its time cost. Another factor is the transit distance as some offshore structures require longer transit times than others. Due to lack of available information regarding the operations of jack-up vessels and in the interest of providing a simple estimation of operations and load variations aboard a jack-up, the operational profile in figure 3.5 will be used as the main reference for the load variation estimation.

Semi-submersible Vessel

Semi-submersible vessels can vary largely in shape depending on its main function being either transport or installation. The semi-submersible crane vessels as pictured in 3.6b does not have the hullform of a conventional seagoing vessel and is designed in a catamaran style. The transport focused semi-submersibles as pictured in 3.6a have a more conventional hullform and are monohull. The key feature of these vessels is their ability of the semi-submersible vessel to partially sink its hull into the water. The operational profile of a semi-submersible can vary from drilling to simply transport and installation of large offshore structures.

(a) The 'Swan' semi-submersible transport vessel [HeavyLiftPFI, 2021]

(b) The 'Thialf' semi-submersible crane vessel ["Thialf HMC Equipment", n.d.]

For transport semi-submersibles the main modes of operation are; Loading, Transit, Discharge, Mobilisation and Idle [Banen, 2015]. Loading, Discharge and Idle can be further subdivided into sub-operational modes listed in table 3.2a. For semi-submersible crane vessels the main modes of operation are; Idle & Repair, Transit, Working [Hagen, 2021]. The Idle & Repair mode is then further divided into sub-operational modes listed in 3.2b.

Operational mode	Sub-mode
Loading	Prepare Vessel
	Loading
Transit	Transit
Discharge	Discharge
	Reinstate Vessel
Mobilisation	Mobilisation
Idle	Repair & Maintenance
	Bunkering
	Off-hire
	Idle contract

(a) All operational modes for a semi-submersible on a transport and installation mission [Banen, 2015]

Operational mode	Sub-mode
Idle & Repair	Loading
	Unloading
	Repair
	Idle at Sea
Transit	Sailing
Working	Installation

(b) All operational modes for a semi-submersible on a transport and installation mission [Hagen, 2021]

The average percentage of time spent in any of these operational modes over the course of a year is displayed in figures 3.7a and 3.7b.

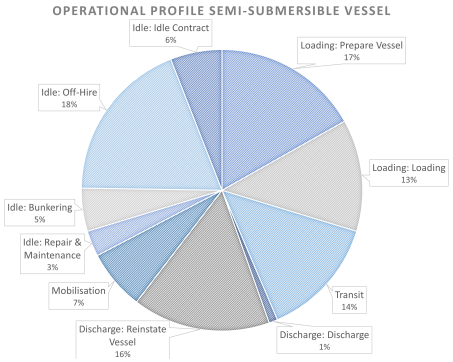

(a) Percentage distribution operational modes of transport semi-submersible vessel, [Banen, 2015]

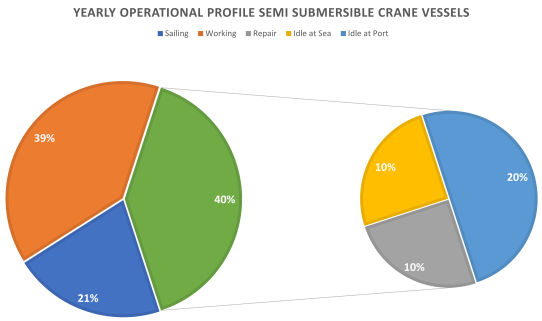

(b) Percentage distribution operational modes of Semi-submersible crane vessel. [Hagen, 2021]

These figures show that for both vessel types a large portion of time is spent in idle mode and relatively low amount of time spent in transit mode. These time distributions will be used to generate simplified load profiles in order to better understand the variation of loads required for each vessel type.

Research Vessel Operational Profile

Research vessels are generally the least complex operationally as they are designed only for scientific research at sea. The auxiliary load is directed towards hotel and equipment load aboard a vessel such as acoustic systems, hydrophones, onboard laboratories etc [Gualeni et al., 2019]. Most research vessels also include an onboard crane for deployment of autonomous underwater vehicles (AUVs). There are many classes of research vessel and many designs with different operating profiles depending on the climate in which they operate. A reference ship based on the typical design of a research vessel by the Fincantieri shipbuilding company will be taken as a main source for further analysis [Papanikolaou, 2021]. A rendering of this reference research vessel is displayed in figure 3.8a. As the research vessel is the least complex operationally it stands to reason that the operating modes for the research vessel are limited [Gualeni et al., 2019]. The main operating modes concern the ship speed as low speeds correlate with research gathering in mission areas and high speeds correlate with transit from the coast to the mission area. This reference vessel is assumed to operate 165 days in a year with the other 200 days assumed to be in harbour or in dry dock. The operational modes can be split into 16 days of transit at 0-5 knots (entering/exiting harbour), 58 days of transit at 6-8 knots (research operation), 8 days of transit at 9-11 knots (speed transient phase), 58 days at 12-14 knots (design speed) and finally 25 days at maximum speed of 15-17 knots [Gualeni et al., 2019]. Figure 3.8b shows the percentage distribution of times spent in these operational modes.This operational profile will be used as the basis for a load variation estimation over the course of a research vessel mission in section 3.3.

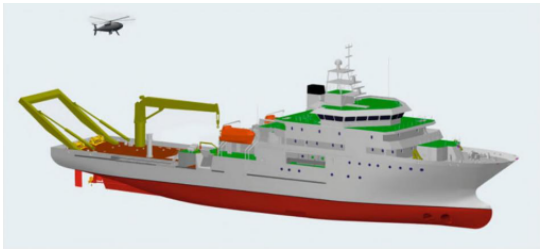

(a) A 3D render of the reference research vessel [Papanikolaou, 2021]

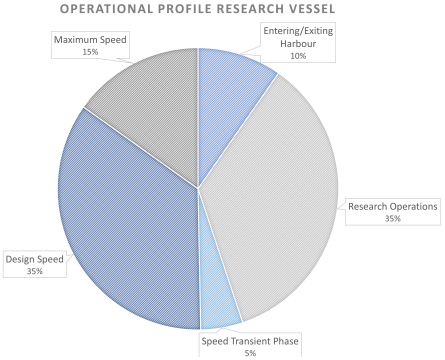

(b) Percentage distribution operational modes of the research vessel [Gualeni et al., 2019]

3.2.2. Load Profiles

Platform Supply Vessel Loads

The operational profile given in figure 3.3 can be scaled down to the duration of a single mission. Depending on weather conditions as well as distance from shore to an offshore structure to port a typical PSV mission can take from a couple of days to up to a week from port to port. This mission duration coincides with other service vessels performing similar tasks such as the walk 2 work vessel. For ease of calculation we will assume a mission duration of a week from port to port. The variation in load depending on the operational mode can be very simply estimated and visualised for the PSV 4000 CD using data from similar offshore support vessels [Guegan et al., 2020]. We assume that hotel loads are relatively constant for the 20 crew and 6 passengers with the variations small enough to be left out of total load variation. The transit loads are estimated to be between 2450kW for economical transit (10-11 kts) and 3000kW for faster transit (13-14 kts) [Guegan et al., 2020]. Harbour operating loads are estimated to be around 300kW as only certain secondary loads are active at that time. The dynamic positioning loads over weather conditions and sea state with a minimum of around 2250kW for calmer weather (Beaufort scale 3) and around 3550kW for harsher weather (Beaufort scale 7). Similar to dynamic positioning loads, the standby loads also depend on weather conditions with a minimum of 1800kW for Beaufort 3 and 2800kW for Beaufort 7 [Guegan et al., 2020].

Jack-Up Vessel Loads

The operational profile in figure 3.5 is an average distribution over a single installation mission. T. Lerchenmueller claims that a single mission of wind turbine installation will range from 3-5 days [Personal Communication, 2022]. In this time, around 3-5 wind turbines can be installed [Personal Communication, 2022]. This depends on both the distance to installation location as well as capacity of the jack-up vessel. The power loading information concerning Jack-ups is highly secretive and not available for public access. Therefore it is not possible to get exact values for the power requirement of each operational mode. The variation of these power levels can however be shown over the course of a mission in a load profile.

T. Lerchenmueller claims that the peak power level required for most standard Jack-Up vessels is between the values of 15-20MW [Personal Communication, 2022]. This power level is mainly required for the combination of Jacking up and jacking down with dynamic positioning. Dynamic positioning is required mostly for the jack-up and jack-down operational modes and occasionally during transit depending on weather conditions [van Nood, 2019]. As with other vessels the power level required for dynamic positioning is very similar to that required for transit.

Semi-Submersible Loads

Taking the operational profile in figure 3.7a and disregarding the off-hire and idle contract time gives a good general distribution of time spent in various operational modes over the course of a transport and installation mission. This will not be entirely accurate to any specific mission as these vary depending on external factors. However, this can be used to gain a better insight into the load profile of both a transport semi-submersible vessel as well as a semi-submersible crane vessel.

The load profile is determine from an estimation of the percentage of total available power required for each operational mode/sub-mode. These are combined with the percentage time distributions of these modes over the course of a mission to give an overview of a typical load profile. Mission duration for semi-submersible transport missions depend mostly on the transport distance. Assuming the transport of an offshore structure from a location nearby it is likely that the transport time will be no more than a few hours up to a day. We assume a total transport time of 20 hours for this load profile making the total mission duration a around 4 days. This assumption impacts the total power requirement calculation and can alter for any specific transport mission.

Research Vessel Loads

The operational profile displayed in figure 3.8b is once again scaled down to the duration of a single mission. The brake power levels differ per operational mode as well as the auxiliary power levels. The brake power levels used for propulsion vary from 83kW while manoeuvring at port to 3617kW at maximum speed. The percentage load on the diesel generator sets also varies from 71% at port manoeuvring to 41% at maximum speed [Gualeni et al., 2019]. Using these values, a load profile estimation can be made for the course of one research mission for both the transit power as well as auxiliary power. With a given range of 3000 nautical miles and a design speed of 13 knots, one can determine the maximum duration of a mission to be around 9.5 days [Gualeni et al., 2019]. Assuming margins for sea state and other external factors we assume a mission on this vessel will last around a week. For simplicity, we assume that the operational profile over the course of a year given in figure 3.8b can be used for the operational profile over the course of one mission.

Load Profiles

Figures 3.9a, 3.9b, 3.10a, 3.10b and 3.11 are the estimated load profiles of each of the vessel types over the course of a typical mission. These load profiles will provide a visual overview of the dynamic loads and the expected frequency of peak loads over the course of a mission.

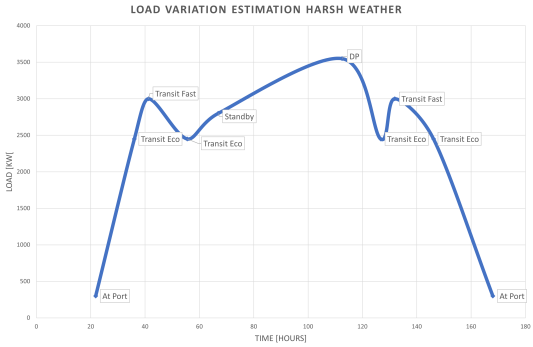

(a) Load profile estimation of the Platform Supply Vessel

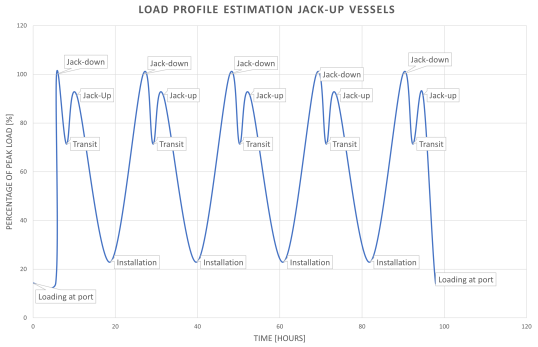

(b) Load profile estimation of the Jack-Up Vessel

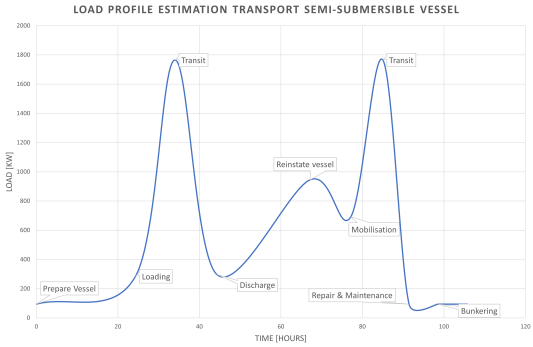

(a) Load profile estimation of the transport semi-submersible vessel

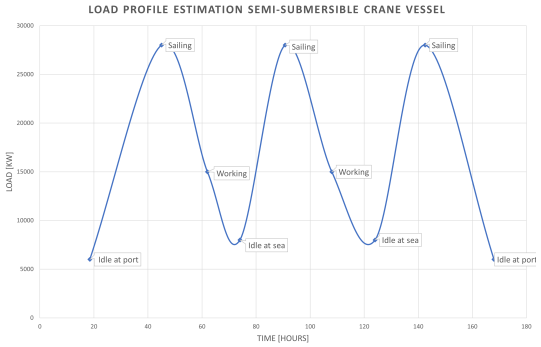

(b) Load profile estimation of the semi-submersible crane vessel

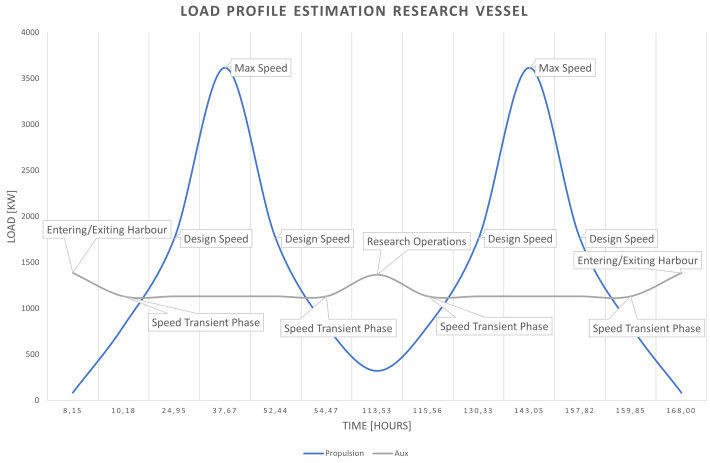

Figure 3.11: Load profile estimation of the Research Vessel

While they are of course extremely rough estimates, these load profiles all show a high degree of load variation over the course of a mission. The idle operating modes are generally accompanied by a low load requirement while sailing and other operations will require high loads. This makes it clear that all of these vessels would not be optimal for the iron powder powertrain in a non-hybrid form. However, some of these load profiles show a high base load requirement which can serve as a good basis for a hybrid energy supply. For purposes of a basic volume and weight estimation of iron powder storage in comparison to ship size and weight, the assumption is made that the full power requirement would be delivered by iron powder in the power requirement calculations in 3.3.

3.3. Power Output Requirements

This load variation not only gives a good depiction of the variation in load but can also be used to estimate the total power load as both power and time are given. To calculate the total power load over the entire mission the sum is taken of the products of the power (P) needed for a particular operational mode and time (t) spent in that operational mode. This is visualised in equation 3.1.

$$\sum_{n=1}^{6} P_n t_n = P_{total}, [n = OperationalMode] \tag{3.1}$$

Platform Supply Vessel

For PSV, this calculation equates to a total power requirement of 153MWh in harsher conditions over the course of a 1 week mission. Using the energy density estimation of iron powder in the UST steam turbine given in table 2.4 the total iron powder tonnage required for a single mission can be estimated. This equates to around 400 tonnes for harsher conditions required for a week long operation. 400 tonnes is equal to almost 10% of the PSV 4000's 4100t deadweight. This is a significant mass requirement which also makes placement of the storage silo's an issue due to the relatively limited extra volume for silos. Using the known density of iron (7800 kg/m^3) as well as the knowledge that iron particles will require 50% more volume than solid iron, the total volume needed becomes around 76m^3 in harsher conditions. If a PSV were to be fully iron powder fueled it would require a complete redesign of the ship's general arrangement in order to ensure the all iron powder systems are installed without significant impact on ship stability. A hybrid setup as mentioned in section 2.3 would decrease the amount of iron powder required as well as allow for redundancy and better dynamic load performance.

Jack-Up

These high dynamic loads over short spaces of time are not ideal for the iron powder powertrain which is much better served as a constant base load. Here also, a hybrid configuration can be installed for excess power loads. The jack-up procedure combined with the mass requirements that come with iron powder powertrains cause the biggest issue. T. Lerchenmueller claims that the power capacity of the jack-up system is limited to a certain mass level which includes the mass of the jack-up, systems aboard as well as the wind turbine components to be installed [Personal Communication, 2022]. A fuel with a lower density such as MFO, methanol or LNG are much more optimal for these operations as they will not result in an even larger mass for the jack-up system to lift. The estimated tonnage of iron required, likely to be higher than the 800 tonnes required for a PSV, make it infeasible for the jack-up system to lift this level of bunker. With around 80% of the mission time spend on pillars it becomes clear that an iron powder powertrain is not suitable for a jack-up vessel due to its mass and dynamic loading limitations [Personal Communication, 2022].

Semi-Submersible Crane Vessel

Using a measured load profile for an existing semi-submersible drilling vessel in figure 3.12, a more accurate view of the total power requirement can be determined than estimating for the 'Swan' or the 'Sleipnir'. Total combined power output required based upon the average propulsion and auxiliary load profiles is nearer 1052MWh and a storage requirement of 2229t of iron powder in a volume of 428m^3 [Ghimire et al., 2022]. This is an incredible difference to the power requirements estimated for the 'Swan' showing how different the requirements can be depending on the operational profile and size of the vessel. It is worth noting that the use of a hybrid configuration for the drilling semi-submersible will reduce the storage requirement by a significant margin. If the iron powder were only used as a steady auxiliary power source only a total power of 600MWh would need to be supplied over the 120 hours of operation [Ghimire et al., 2022]. This would result in a storage requirement of 1271t and 244m^3 of iron powder.

Research Vessel

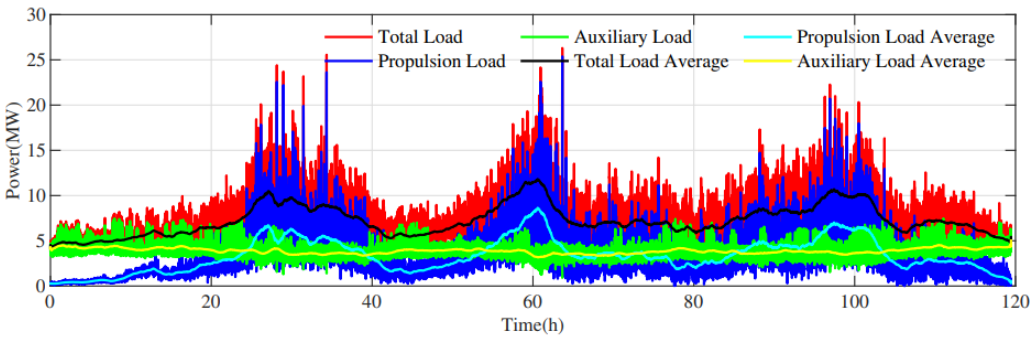

Figure 3.12: Load profile semi-submersible drilling vessel, [Ghimire et al., 2022]

The total power calculation for a one week mission on a research vessel is once again done using equation 3.1. Here the n value in this case becomes 5 as there are 5 separate operational modes on the research vessel. The total power requirement for the research vessel comes out to around $222MWh$ propulsive power and $208MWh$ auxiliary power for a one week mission. Using the same energy density as for the previous calculations the total iron powder tonnage is equal to 912 tonnes. This is equal to around 25% of the 3600t deadweight which is even more than was the case for the PSV. The volume requirement is estimated to be around $175m^3$. This means that even more than for the PSV, an entire redesign of the research vessel would be needed for proper implementation of the iron powder setup. This, however, is not the case for a hybrid setup as was already the case for this research vessel. If the iron powder powertrain were used only for hotel load or only transit power delivery, the required iron powder tonnage would halve. This would make a potential redesign much more feasible. A fitting hybrid setup would also ensure more redundancy and better dynamic loading performance.

3.4. Conclusion

Through a two-step filtering system, certain service vessels were concluded to be unsuited for iron powder implementation based upon certain characteristics. The first step of the filtering was mainly based upon the size and range of the vessels to ensure the bunker mass and volume did not become impossible to carry aboard the vessel. Through this filter certain service vessel types such as the daughter craft (crew transfer vessel) and tugboat were declared unsuitable. From this filter, only four vessel types would remain. A look at the types of operations and functions of these vessels would determine to what extent an iron powder installation could impact the total power consumption of the vessel.

Of the remaining feasible vessels, a select few were chosen for further analysis of their operational profiles. This was based largely on their functions, size and the information that was made available about these vessel types. The vessel types selected for further analysis were the platform support vessel, the jack-up vessel, semi-submersible vessel and the research vessel. The platform support vessel is comparable to many other types of transport and support vessels such as the walk to work vessel or anchor handling tug supplier in both size and operation. The jack-up vessel is comparable to the semi-submersible vessel and other construction vessels in size but differs fundamentally in operation. The research vessel was considered operationally different from the rest of the service vessel types due to its mainly transit focused operations. Choosing these four vessel types allowed for a wider range of operational profiles to be investigated for different vessel sizes.

For these four vessel types existing data was used to generate an operational profile and a load profile estimation. This information was then used to determine what the total power requirement for this type of vessel which was converted to a mass and volume estimation for the amount of iron powder bunker required for a single mission. The final bunker mass estimations for all four vessel types are listed in table 3.3. Note that the estimation for the Jack-up vessel was not done due to the fact that operational modes ”Jack-up” and ”Jack-down” could likely not be performed with the iron powder

bunker required making this vessel entirely unsuitable.

	Maximum Bunker Mass [t]	Maximum Bunker Volume [m^3]
Platform Supply Vessel	650	102
Jack-up Vessel	N/A	N/A
Semi-submersible Vessel	2229	428
Research Vessel	912	175

Table 3.3: List of all of the maximum bunker mass and volume requirements per vessel type

The main concern with platform supply vessels and research vessels is the relatively small capacity for extra volume and mass. These vessels are largely under 100m in length with largely varying loads over the course of a mission. Another issue is the densely packed state of the hulls of these smaller supply vessels, with minimal room on deck and below deck, placement of the silos will prove difficult. The tonnage of these vessels compared to the tonnage of the required iron powder bunker would likely require a significant redesign of the vessels. A hybrid configuration would likely make this redesign easier. Despite this, the mass and volume issues would likely be too complicated to resolve without serious concessions in hull shape and stability.

With the Jack-up being unable to perform its primary function while carrying the significant iron powder bunker required to perform it, it becomes clear that the semi-submersible is the most optimal of this particular list of service vessels. While the load requirements of the transport semi-submersible vessel will likely be lower than that of the semi-submersible crane vessel. The overall size of the semi-submersible crane vessel and its hullform make it far more ideal for iron powder powertrain implementation. The large pillars connecting its pontoons to the deckbox are ideal for silo placement. The general size of these semi-submersible crane vessels ranging from 130m up to 210m will likely decrease the total impact of the iron powder powertrain on the design of the vessel with regards to volume and mass constraints. As with the other vessels, the load profiles have shown a potential for a hybrid installation which will ensure the power requirement of the vessel is satisfied while still decreasing the GHG emission.

4

Methods

In order to test the feasibility of a hybridised iron powder setup on a semi-submersible crane vessel, information is required regarding both the characteristics of the semi-submersible vessels as well as the systems to be placed aboard. The main inputs are the main dimensions and operating profiles of a selection of SSCVs. These are used to generate load profiles from which the hybrid split can be determined. With this hybrid split the weight estimations can be made and used to test for stability and feasibility. Finally, an emissions comparison can be made to asses the environmental impact of the hybrid setup. This process is visualised in the diagram shown in figure 4.1.

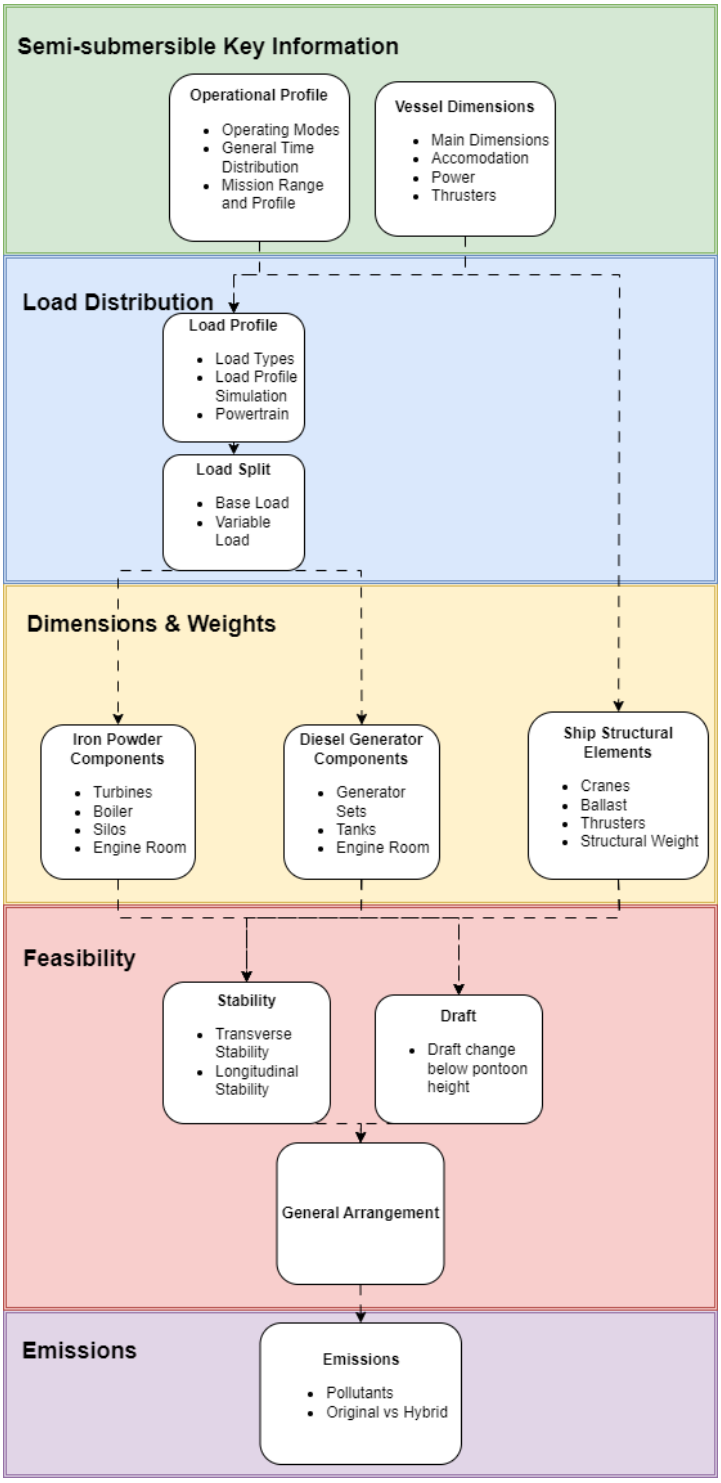

Figure 4.1: Methodology diagram showing steps undertaken to determine base feasibility

4.1. Semi-submersible Key Information

4.1.1. Vessel Dimensions

To ensure the feasibility tests results are as much a reflection of reality as possible, existing vessel information is needed. In this case, a market study is done of the existing worldwide fleet of semi-submersible crane vessels. From this study, a set of four semi-submersible vessel designs, each with differing main dimensions, power outputs and crane capacities will be used to form a case study. Four vessels is deemed enough to be a representation of the semi-submersible crane vessel fleet. This

is because this particular vessel type is generally quite limited with a total fleet estimated to be in the between 10 and 20. The information from these vessels will be crucial in determining load distributions, weight estimations and stability calculations. The information on the four chosen vessels can be found in section 5.1.

4.1.2. Operational Profile

Determining the operational profile of semi-submersible crane vessels means looking at the operating modes of the vessel, the distribution of time spent in a particular operating mode and using this information to create a realistic mission profile with an accurate range.

Operating Modes

The operational profile of a semi-submersible crane vessel can be viewed over two time-spans, over the space of a year and over the space of one mission. The standard semi-submersible crane vessel has three operating modes; idle and repair, sailing and working mode [Hagen, 2021]. The idle and repair mode is assumed to be split between three sub modes; repair, idle at port and idle at sea. These modes are listed below with a short description of the functions performed.

- *Idle & Repair*: Any time spent either not in working or sailing mode. Can be for repair in port, loading and unloading in port or waiting at sea.
  - *Repair*: Time spent at port in repair be it in dry dock or otherwise.
  - *Idle at Port*: Time spent at port performing loading, unloading or bunkering operations.
  - *Idle at Sea*: Time spent outside sailing or working mode at sea due to unforeseen events such as weather conditions or issues aboard the vessel.
- *Sailing*: Time spent travelling from one location to another, either from port to working area and vice versa or from one working area to another.
- *Working*: Time spent performing the main objective of the mission; either installing, modifying or decommissioning offshore structures.

General Time Distribution

The distribution of time spent in each operating mode over the course of a year is displayed in figure 4.2.

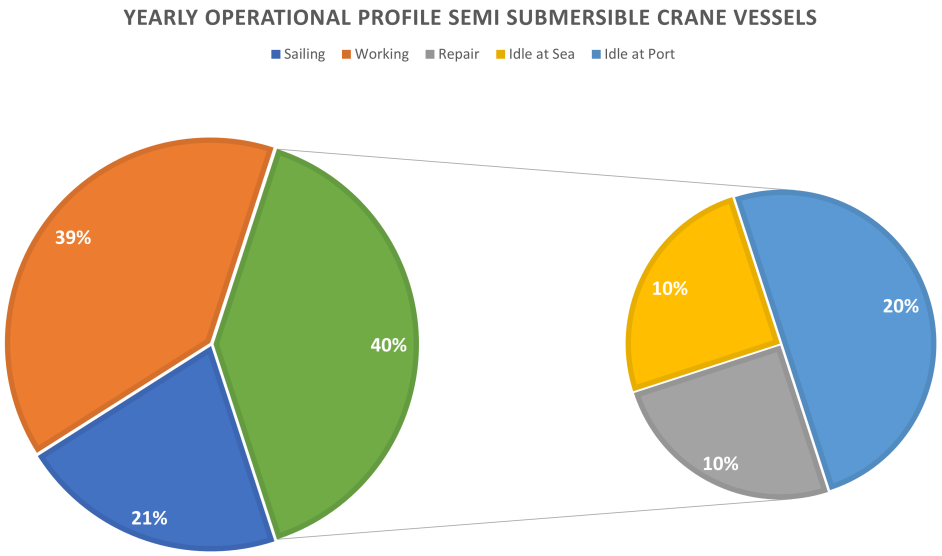

Figure 4.2: A pie chart showing the percentage time distribution of the operating modes of semi-submersible crane vessels over the course of a year, [Hagen, 2021]

The yearly operating profile provides a good indication for the operating profile on a mission. It is assumed that the distributions of time spent in various modes can be loosely transferred from the yearly operating profile to the mission operating profile. This is mission operational profile will exclude the time spent in repair and keep the same same ratio of time spent in an operating mode of the remaining modes as shown in figure 4.3. A semi-submersible crane vessel mission can be described using a long and short cycle. In this case the 'long cycle' consists of the time spent loading, bunkering and unloading at port coupled with the time taken to sail from port to the working area. The 'short cycle' then consists of all the time spent in the working area, this includes the time spent installing the offshore structures as well as potential idle times at sea and sailing time between offshore construction locations. This cycle is visualised in figure 4.4.

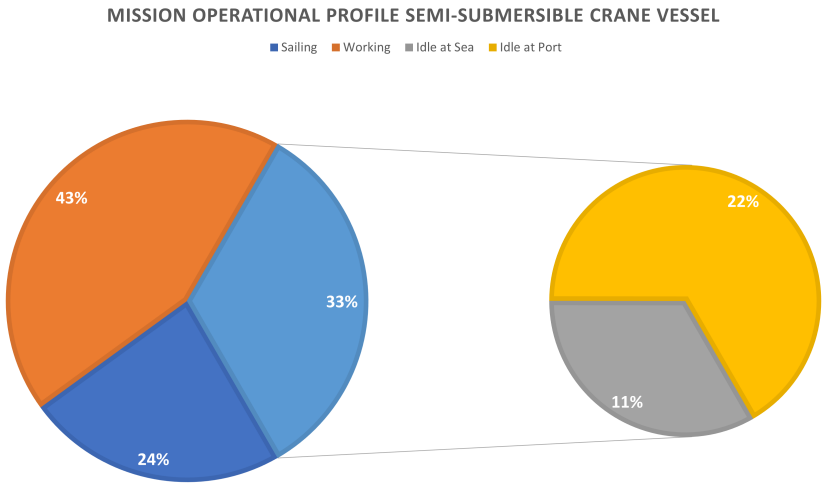

Figure 4.3: A pie chart showing the percentage time distribution of the operating modes of semi-submersible crane vessels over the course of a mission

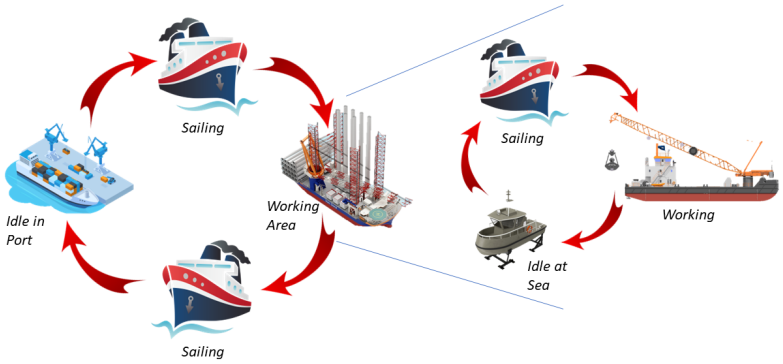

Figure 4.4: Diagram visualising the short and long cycles performed by a semi-submersible vessel over the course of a mission.

Depending on the mission type and duration the order and amount of times the short cycle is repeated can vary. The operational mode "idle at sea" is highly influenced by external forces and can therefore occur at any time during the short cycle and even in rare occasions during the long cycle. This general layout of the operating profile over the course of a mission is however accurate enough to use as a base for a load profile creation in section 4.2.

Mission Range and Profile

Before a load profile can be generated, key information regarding the mission and the loads must be determined. The start and finish of a mission must be clear as well as the distances sailed and time spent in working mode. The power levels required per operating mode must also be determined for each vessel.

Mission Range

The mission duration for semi-submersible vessels can vary greatly ranging from 7 weeks up to 15+. According to I. van Winsen (personal communication, March 10 2023) the time between bunkering is estimated to be around 7-12 weeks. This thesis assumes that loading and unloading operations occur during bunkering. These bunkering and loading/unloading operations are often performed several miles outside the main port as the size and draft of the semi-submersible vessel makes it difficult to maneuver safely within port. This bunkering and loading/unloading procedure is therefore seen as part of the mission time in the long cycle. The total mission time for the load profiles of these vessels is therefore assumed to be 12 weeks, the maximum time between bunkering operations.

Mission Profile

The missions for semi-submersible vessels vary significantly based upon what structures need to be installed, changed or decommissioned. The sheer variety in operations makes it near impossible to simply take an average of all mission types and create a generic load profile. Therefore the choice was made to focus on one specific mission type that is becoming increasingly common with installation vessels; Wind turbine and mono-pile installation. This mission type also fits well with the theme of sustainability. In the case of this mission type the mission profile is depicted in figure 4.5.

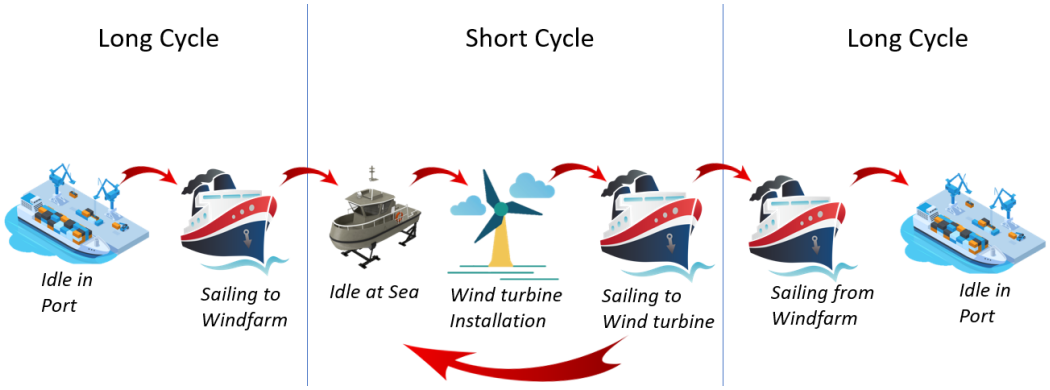

Figure 4.5: Wind turbine installation mission profile

Here the long cycle consists of loading/unloading and bunkering operations alongside sailing to the wind farm and back. The short cycle then occurs at the wind farm with installation of the wind turbine, idle at sea due to external factors and sailing between the wind turbines. The selected mission time of 12 weeks determines how many short cycles can be performed. This mission type can be easily altered in the model as the key inputs are distances travelled from port to wind farm, from wind turbine to wind turbine and average time spent in working mode. For this particular mission, a maximal distance of 100 nautical miles was chosen for the distance between port and wind farm to simulate and extreme case where the nearest port is located far from the wind farm, [Diaz and Guedes Soares, 2020]. The distance between wind turbines was estimated to be around 1 nautical mile based off of Nijssen et al., 2016. The average time spent in working condition was based on wind farm installation data Lacal-Arántegui et al., 2018 stating an average of 32 hours spent installing a wind turbine.

4.2. Load Distribution

The load profile is created using the operating profile generated in section 4.1. The load profile is then simulated 10000 times and the averages are taken to provide as accurate as possible a view of a semi-submersibles power demand over the course of a mission (4.2.1). This information is then used to create a load split between the base and variable load which will be covered by the iron powder and diesel generator sets respectively (4.2.2).

4.2.1. Load Profile

The load profile determination starts with an understanding of the load types and how these power demands can be estimated and extrapolated from existing information. With this information a load profile simulation can be made to generate a time vs power graph. Finally, according to the results of the load profile simulations, the existing powertrain can be adapted to a hybrid powertrain.

Load Types

There are three main load types to be considered on a semi-submersible crane vessel. These three load types encompass all the consumers of the vessel over the course of a mission:

1. **Hotel Load:** A constant load providing power to hotel systems aboard the vessel. These include the lighting, heating, HVAC systems and other small consumers aboard. Aimed towards providing a base level of comfort for crew aboard.
2. **Thruster Load:** A constant load while in sailing condition and variable load in working condition. All power used for thrusters either in transit or dynamic positioning. Thruster load is maximal in sailing mode and minimal in idle mode.
3. **Crane Load:** A variable load delivered to the cranes mounted on the deck. Cranes require high peak loads over irregular time windows depending on weight of cargo hoisted. These peak loads occur over very short time frames; the initial slewing motion requires a high peak load before it drops to a base load.

The load per operating profile is determined based upon the data available for one semi-submersible crane vessel, to be used as a reference. The power level required for each operating mode is available for this vessel but not for the rest of the vessels. Due to most hotel systems being aimed at crew comfort or are systems used by the crew it is most likely that the hotel load can be scaled according to the crew capacity of the vessel. Using this reference vessel as a base, half of the factor difference in crew capacity is used as the difference in hotel load. This is because apart from the extra crew quarters, many areas such as the mess hall will not require as significant an increase in hotel load to accommodate for more crew. The thruster load of a vessel is mainly dependent on the installed thruster power. This is available for all vessels and can therefore be scaled to the same level as for the reference vessel. This can be assumed because of the tier III dynamic positioning requirements applicable to all four vessels meaning each vessel will require a similar level of redundancy. The thruster loads in dynamic positioning mode will be determined by a maximum thruster load and a base thruster load. Finally, the crane load is scaled based on the total powertrain of the vessel as the hotel load and thruster load have already been determined. This means that the remaining load for each operating mode is covered by the cranes. The variable crane loads are determined by a maximum crane load and a base crane load.

Load Profile Simulation

These loads per operating mode are the basis on which the load profile will be determined. Each operating mode is simulated for the previously determined mission type for the determined mission length. As the operating mode of the simulation varies over the mission, so does the power requirement of the vessel. This gives an indication of the total power requirement needed for each vessel as well as where the hybrid split should be made. Firstly, a load profile containing the three main consumers is created to show the variation of the power requirement over the course of a mission as well as where the peak loads occur. These are then summed up to create an estimation of the total power requirement of the

vessel.

It is important to note that these load profiles are generated from assumptions made for the load requirement of each consumer. While the simulation of a relatively constant load such as the hotel load is quite simple, the simulation of a varying load is more complex and results in a wider range of results with each simulation. This is mainly the case for the thruster and crane load when the vessel is in working mode. With the base and peak load estimations made, the probability of the load requirement being any value between the base and peak load must be determined. This was done based on the existing crane energy demand data available for the semi-submersible crane vessel 'Sleipnir', shown in figure 4.6.

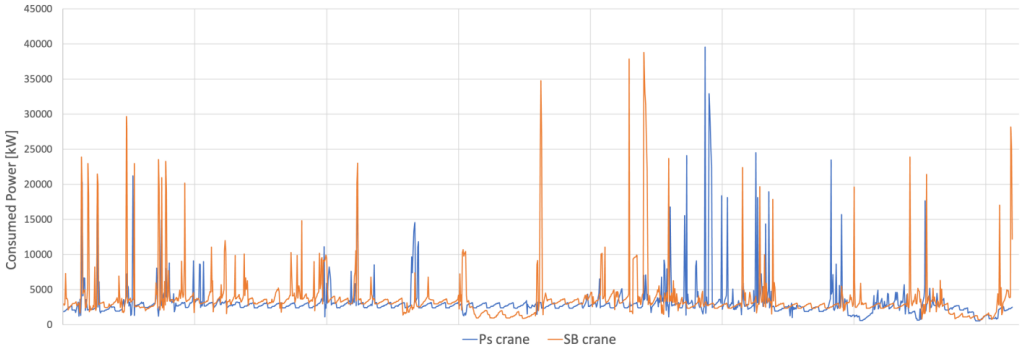

Figure 4.6: The energy demand of the Sleipnir's cranes during one day in working mode, [Hagen, 2021]

This frequency of peak power demand over one day for each crane was extrapolated for an entire operation in working mode. By calculating the amount of times certain power demands were reached over the course of a day, a probability of a certain power demand could be generated and applied to each vessel. While this does not perfectly reflect the reality of the power demand for each vessel, it does give sufficient and reliable indication of the distribution of power demand for both the cranes and the thrusters. The thrusters in working mode are set to dynamic positioning mode and these more often than not work in tandem with the crane operations. When the crane undergoes a large movement it requires a large amount of power for lifting but also for the dynamic positioning in order to stabilise the vessel. This coupling of the thruster and crane in working mode allows this distribution of power demand to be used not only for the crane loads but also the thruster loads.

The use of probability in determining when the peak load is reached results in a wider range of results (up to 50MW range between base and peak load) from multiple load profile simulations compared to when looking only at the constant loads with a far smaller range of power requirement (only 1-2MW range). The load profile simulations were run 10000 times in order to provide a range of results. This is deemed enough times as difference in absolute value of the average output value calculated from 100,000 simulations and above becomes marginal and insignificant. From these results, the average total power consumption is used as the basis for the powertrain design. From this average total power consumption, the percentile range of the total output by each hybrid component is determined. The exact shape of the load profiles are not as important for further calculations, these are displayed to show when and where the main consumers are reaching peak loads as well as to determine where the base load ends and the variable load starts.

Powertrain
Unlike other conventional vessel types such as the container or tanker ship, the semi-submersible crane vessel does not have a direct drive from mechanical energy generator to propeller. Mechanical energy is directly converted to electrical energy and supplied throughout the vessel at differing voltages depending on the consumer. Higher voltages are used for larger consumers such as thrusters and cranes while smaller consumers like the hotel loads are supplied at lower voltages. The powertrain of the hybrid configuration is based largely on the existing powertrain configuration described below.

Existing Powertrain

The existing powertrain differs slightly over each vessel in terms of total output, however the general layout is similar. The power generation systems are split into multiple engine rooms (3-4 depending on output level and vessel size), [Lyu, 2016]. Each engine room is equipped with multiple power generation sets and is completely isolated from another engine room. These engine rooms are connected through switchboards that distribute the generated power to all consumers. This layout is chosen in order to satisfy the redundancy requirements that come with tier III dynamic positioning systems. This layout is visualised in figure 4.7 depicting the engine rooms of the semi-submersible crane vessel, the 'Sleipnir'.

Each engine room can be uncoupled from the network in case of a failure and the remaining engine rooms would be able to provide up to the peak load required of the vessel. These power generation systems are coupled to the consumers using the switchboards and the electrical grid on the vessel. A full depiction of a typical powertrain from power generation to power consumption is given in figure 4.8 depicting the full powertrain of the semi-submersible crane vessel 'Thialf' (3 engine rooms). In this schematic the red, blue and yellow components describe the generator sets in their respective engine rooms while the green components are the main power consumers such as the cranes and thrusters. This general layout of the powertrain systems will be used in the hybrid setup.

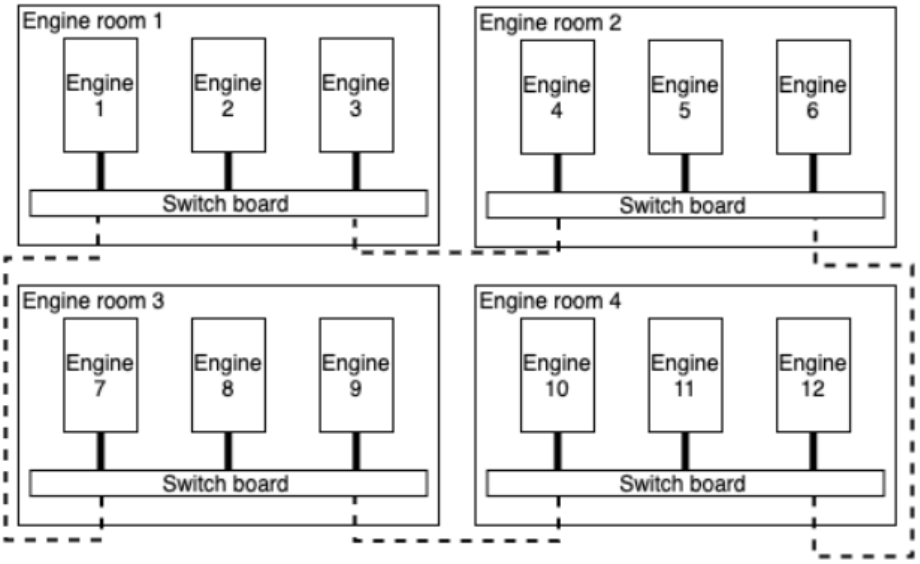

Figure 4.7: Engine room layout of the 'Sleipnir', [Hagen, 2021]

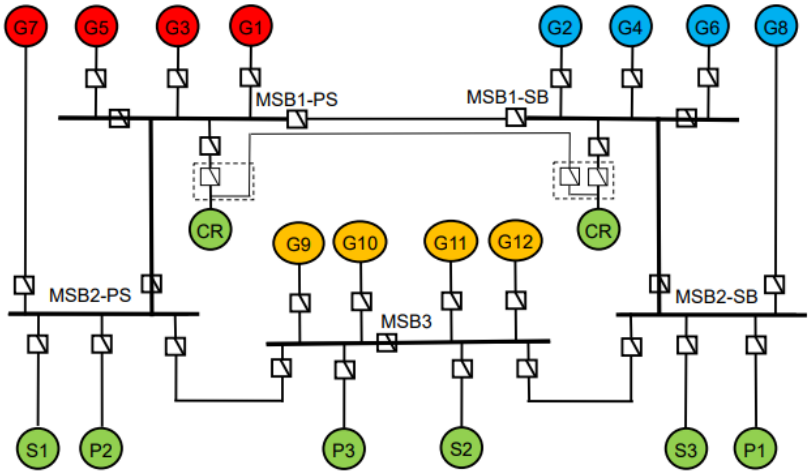

Figure 4.8: Powertrain schematic for the 'Thialf', [Lyu, 2016]

Hybrid Powertrain

Keeping in mind that the power levels will differ significantly per vessel, an outline is made of the general layout of the hybrid powertrain. The main difference between the original powertrain and the hybrid powertrain is the addition of an extra engine room with an iron powder setup. Each vessel will consist of four engine rooms. Three of these engine rooms will be similar to the original engine rooms in that they will be equipped with diesel generator sets to provide the variable load required for the vessel. The iron powder engine room will be equipped with two boilers and turbine sets to provide redundancy. The rated power of each setup will be equal to the base load determined from the load profile. The rated power of the remaining diesel generator sets in the other three engine rooms will be determined based on the redundancy requirements used for the original powertrain design. Two of the remaining three engine rooms must be capable of providing the peak load requirement minus the output of the iron powder setup. The layout of this hybridised powertrain is modelled in figure 4.9.

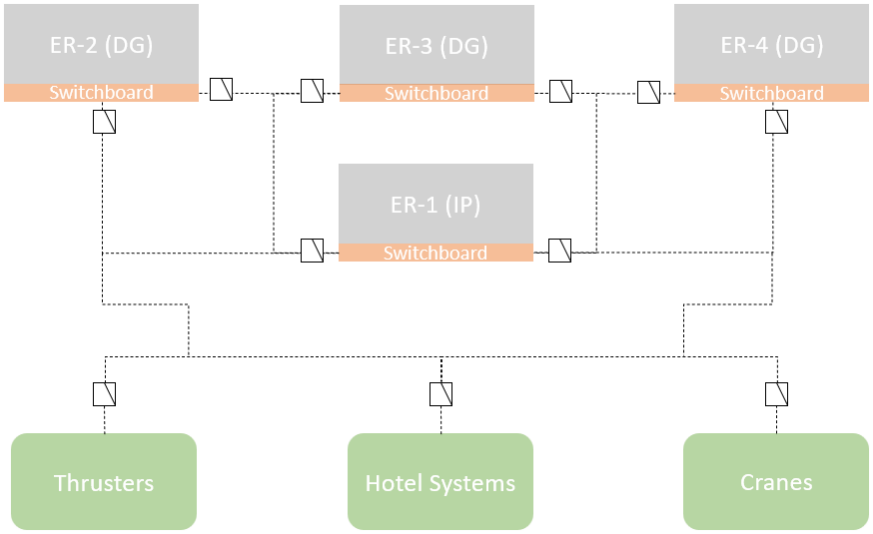

Figure 4.9: Simplified diagram of hybrid powertrain

This powertrain setup, coupled with a load profile for each vessel can be used to determine the hybrid split and allow for an estimation of component dimensions and weights in section 4.3.

4.2.2. Load Split

The load profile simulations will be able to show a distinction between a base load and a variable load for each vessel. This is done by analysing the power versus time graph generated by simulating a particular mission in which the vessel undergoes multiple operating mode changes with varying consumer power demand.

Base Load

The base load is the constant power required over basically the entire mission duration. This is mainly comprised of the hotel load as this is required for the crew aboard the vessel no matter what mode the vessel is operating in. This can be easily identified in the power vs time graph as it is essentially equal to the lowest total power demand of the vessel over the course of the mission. This means that if this base load is constantly met, only the power demand above this value is no longer constant.

Variable Load

The variable load covers the dynamically changing power demand. This is likely to come from the crane and thruster operations in working mode as these power distributions are often irregular with high load peaks. This portion of the load profile is the most difficult to estimate due to the highly irregular nature of the loads. This is why the load profile simulation is done 10000 times and the range of results is taken into consideration when analysing the hybrid split. For the variable load to be used in dimensioning and further steps, an average value is taken to represent the variable load in order to the total time cost especially in the creation of general arrangements while keeping the results as realistic as possible.

4.3. Dimensions and Weights

The dimensioning and weight estimation is split into three main categories. First, the estimation of the iron powder components (4.3.1) is done including everything in the engine room as well as the silos and filters. Next, the diesel generator sets are estimated as well as the bunker tanks (4.3.2). Finally, the main elements (4.3.3) of the ship are estimated including the cranes, lightship weight, thrusters and ballast. These estimations will then be used later in the creation of a general arrangement and stability calculations in section 4.4.

4.3.1. Iron Powder Components

The iron powder components to be estimated are the steam turbines, boiler, filters and silos. These dimensions will vary per vessel as they are dependent on the base load required for each vessel as well as the overall kWh needed over the course of a mission. The method of dimensioning and weight estimation is based largely on the methods used by de Kwant, 2021 for a similar iron powder setup.

Steam Turbines

The UST series by Mitsubishi consists of a set of three turbines, a high pressure turbine, intermediate pressure turbine and a low pressure turbine as stated in section 2.2.4. Each turbine will be dimensioned according to its rotor size. The main objective in the turbine sizing is to keep the turbine efficiency as high as possible. This means that the turbine must be operating at a specific flow coefficient (ϕ) and stage loading coefficient (ψ). As can be seen in figures 4.10a and 4.10b, there is an optimal total-to-total turbine efficiency (η_{tt}) that can be reached when the flow coefficient and stage loading coefficient reach certain levels at particular fluid deflection angle (ϵ).

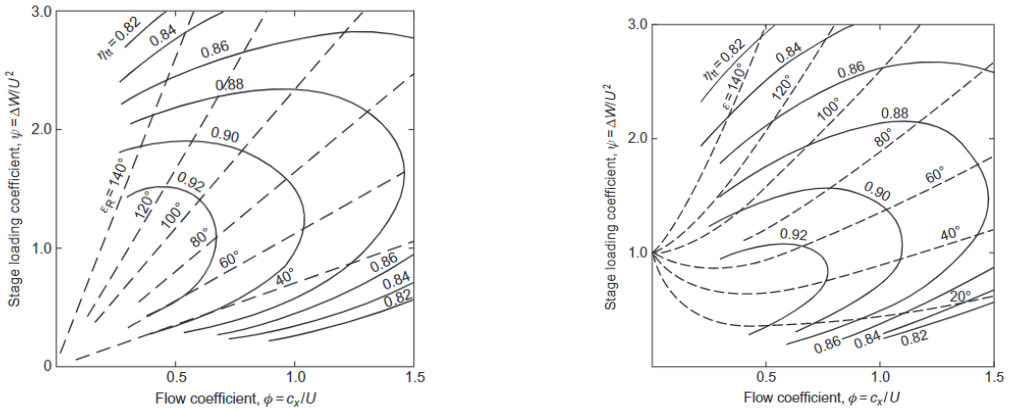

(a) Relation between ϕ, ψ, η_{tt} and ϵ for an impulse stage, Dixon and Hall, 2014

(b) Relation between ϕ, ψ, η_{tt} and ϵ for a reaction stage, Dixon and Hall, 2014

From these relations, it can be determined that the efficiency of the turbine will be optimal at a flow coefficient of 0.5 and a stage loading coefficient of 1. The formulas for these two parameters are stated in equations 4.1 and 4.2, [Dixon and Hall, 2014].

$$\phi = \frac{c_x}{U} = \frac{\dot{m}}{A_{mean} * \rho * U} \tag{4.1}$$

$$\psi = \frac{\Delta W}{U^2} = \frac{W}{n_{stages} * \dot{m} * U^2} \tag{4.2}$$

In equation 4.1 the variable c_x represents the axial speed of the working fluid through the turbine and U represents the mean blade speed. The variable c_x can be redefined using the mass flow of the working fluid ($\dot{m}$), the mean cross-sectional area of the annulus between stages (A_{mean}) and the the density of the working fluid (ρ). In equation 4.2 the variable ΔW represents represents the specific work output per stage. This specific work output per stage can be redefined as the specific output of the whole turbine (W) divided by the number of stages in the turbine (n_{stages}). The turbine power W, mass flow of the working fluid $\dot{m}$ and inlet/outlet conditions of the working fluid can be determine from the base loads determined for each vessel and the UST cycle data points in table 2.3 respectively. Using these data points and the attempting to maximise turbine efficiency, the maximum and minimum diameter of the turbine can be estimated along with the number of stages. This allows for an estimation of the volume and mass of the turbine to be made. The exact process followed for turbine dimensioning is outlined in appendix B.

Boiler

The boiler is designed based off of two key components, the combustion chamber and the heat exchanger. This is where the heat of the iron powder combustion is extracted and converted to the working fluid. Boilers designed specifically for iron powder combustion are not yet commercially available as the combustion process is still being researched. The design of the boiler will therefore be based off of the some general prerequisites of existing boilers paired with what is known of the requirements of iron powder combustion. This is largely based off of the design choices made for the MP-100 iron powder fuelled boiler by team SOLID. A schematic of the general boiler design can be found in figure 4.11.

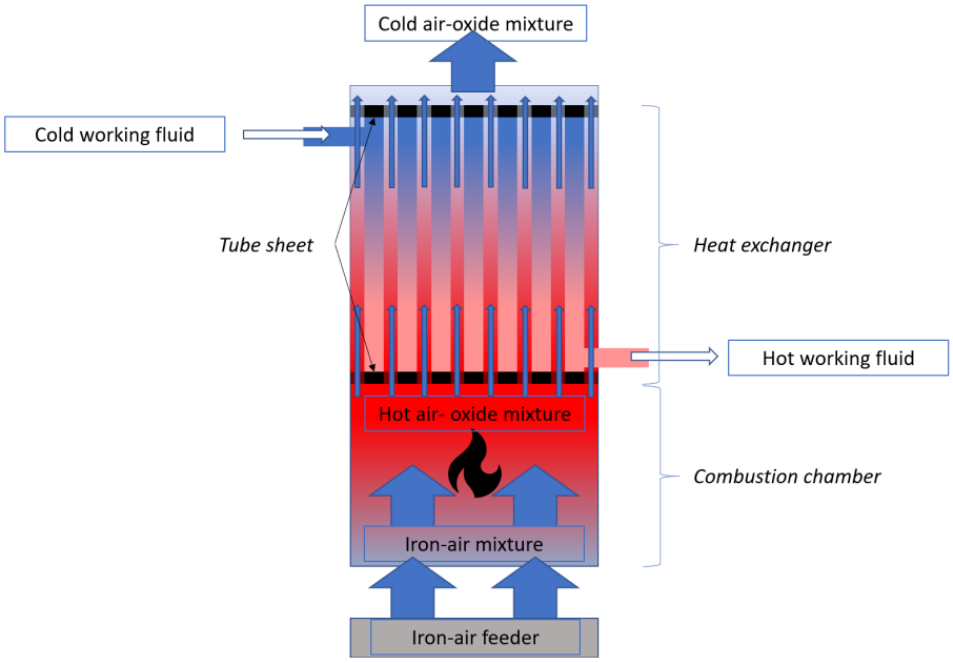

Figure 4.11: Boiler schematic split between combustion chamber and heat exchanger

To ensure a minimum flow rate of the air-fuel mixture is maintained, it is generally best to keep to an elongated vertical tube design. This is done to prevent slagging issues that can occur in horizontally designed boilers. The combustion process leads to a mixture of iron oxide particles and oxygen-poor air travelling through the heat exchanger at 1600K, Seijger, 2020. The significant heat stored in the iron oxide particles and difficulties in filtering at such high temperatures means that the filtering of iron oxide particles will be done after they are passed through the heat exchanger. To minimise the potential abrasive damage that can be caused by the iron oxide particles, a shell and tube heat exchanger design is chosen. Plate heat exchangers, while requiring less volume than shell and tube heat exchangers, are less suitable for this application due to the high pressures. A certain minimum airflow level must be maintained in the heat exchanger as well to ensure the iron oxide particles will travel with the airflow. As the heated airflow mixture is sent through the heat exchanger one way, the working fluid is pumped through the other side of the tubes of the heat exchanger. In order to maintain a minimum airflow level without extreme pump power requirements, the boiler will be as long and thin as possible. The full outline of the boiler design as taken from de Kwant, 2021 is found in appendix C.

Filters

The filters used to extract the iron oxide particles from the airflow after they have been sent through the heat exchanger are a combination of two commonly used filtration systems; the cyclone filter and the bag house filter. The airflow passes through the cyclone filter first to filter out the predominantly large oxide particles from the airflow. The remaining finer particles are then filtered out using the bag house filter.

The design of cyclone filter is done following the steps in Nakhaei et al., 2020. In this case the steps to design a standard 'conventional (3)' cyclone are followed. The ratio between height, diameter and other important dimensions are given for this standard cyclone design as shown in figures 4.12a and 4.12b. All that is needed is the diameter of the cyclone. The diameter of the cyclone is chosen to be as large as possible to reduce the pressure drop as well as increase filter efficiency. As was the case with the boiler, the dimensions of the cyclone filter are far less constrained than on other vessels allowing for a larger diameter. The critical factor is the increased pressure drop over a cyclone filter as power requirement increased. This would determine both the diameter and the amount of cyclone filters required for each iron powder setup. The weight of the cyclone filter(s) would be determined based on a regression analysis of existing cyclone filters. Figure 4.13 shows a comparison of cyclone diameter

and weight based on existing products from “CK Cyclone Collectors”, n.d.

	Cyclone Type					
	High Efficiency		Conventional		High Throughput	
	(1)	(2)	(3)	(4)	(5)	(6)
Body Diameter, D/D	1.0	1.0	1.0	1.0	1.0	1.0
Height of Inlet, H/D	0.5	0.44	0.5	0.5	0.75	0.8
Width of Inlet, W/D	0.2	0.21	0.25	0.25	0.375	0.35
Diameter of Gas Exit, D_e/D	0.5	0.4	0.5	0.5	0.75	0.75
Length of Vortex Finder, S/D	0.5	0.5	0.625	0.6	0.875	0.85
Length of Body, L_b/D	1.5	1.4	2.0	1.75	1.5	1.7
Length of Cone, L_c/D	2.5	2.5	2.0	2.0	2.5	2.0
Diameter of Dust Outlet, D_d/D	0.375	0.4	0.25	0.4	0.375	0.4

(a) Table with the ratios for the design of standard cyclones, Bashir, 2015

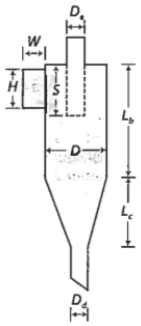

(b) Visual depiction of the dimensions of standard cyclones, Bashir, 2015

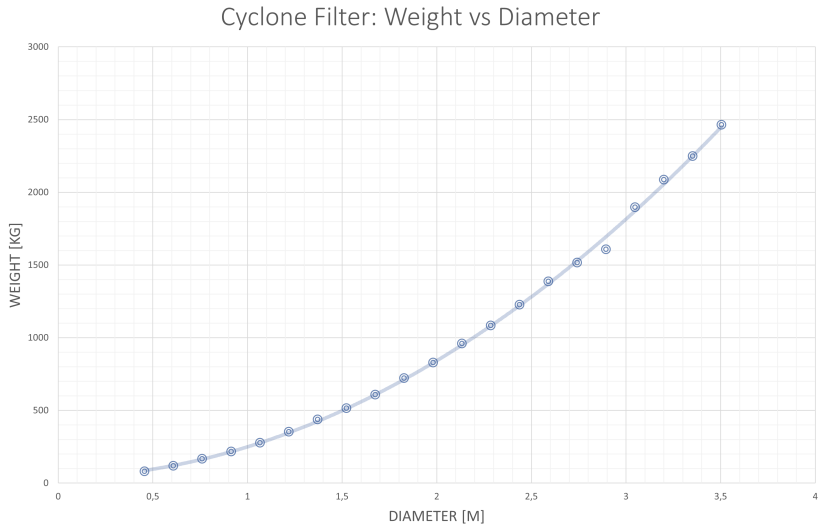

Figure 4.13: Relation between cyclone filter diameter and weight, [“CK Cyclone Collectors”, n.d.]

The bag house filter is designed using the design method outlined in Turner et al., 1987. It is designed as a cube formed filter. The choice is made for a pulse-jet filter to minimize volume taken up. The key factor in determining the bag house filter size is the required square meter area of the filtering bags. This area is dependent on the speed at which the air is travelling through the bags. The minimal cross-sectional area of the filter can be determined based on the maximum filtering velocity, maximum can velocity and the volumetric flow rate of the air mixture. The maximum filtering velocity is 1.1 meters per minute for a pulse-jet bag house filter. The maximum can velocity, velocity of the gas in the space between the bags, is limited at 1.8 meters per second. The volumetric flow rate of the air mixture is known from the boiler design.

Further design constraints are the minimal spacing of 0.1 meters between bags. The bags themselves have a diameter of around 0.15m, typical for bag house filter designs. These constraints allow for the length of the bags to be determined based off of the minimum bag area required. The pressure drop is determined for this bag house design using the method by Cooper and Alley, 2011 to ensure it is not too high. Finally, the weight of the bag house is determined, similarly to the cyclone filter, by a regression analysis of existing bag house filters. Figures 4.14a and 4.14b show the relation between the mass flow rate of the exhaust and the weight and volume respectively.

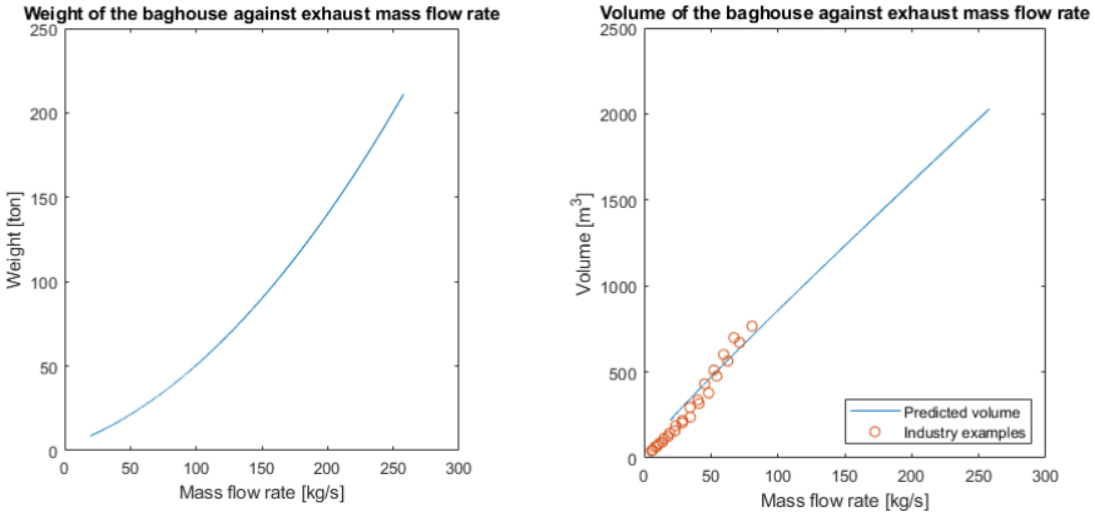

(a) Relation between weight and exhaust mass flow of existing bag house filters, de Kwant, 2021

(b) Relation between volume and exhaust mass flow of existing bag house filters, de Kwant, 2021

Silos

The design of the bunker silos is relatively simple. As discussed in chapter 2 section 2.2.1, the silos will be designed vertically and placed in the pillars of the semi-submersible vessel. The silos are designed in cylindrical form with a total height of around 90% of the height of the pillars. This can be decreased later if the stability calculations conclude that the center of gravity of the silos is too high. Following calculations done according to Schulze et al., 2008, the maximum hopper angle can be determined based on the internal friction angle and the wall friction angle of the bulk material. Using data from Mohajeri et al., 2020 and Lanzerstorfer and Hinterberger, 2017 regarding the angles required for iron powder and iron oxide, the maximum hopper angle is calculated to be 28 degrees. The design of silos according to Schulze et al., 2008 states that the ratio between diameter and length of the silo must be around 5.5 for slender design. As the bulk material can shift relatively easily within the silo it is best to have slender silos in order to minimize the horizontal shift of the center of gravity. The diameter and height of the silos can therefore be determine for each vessel depending on their pillar height. The amount of silos is based on the total kWh to be produced by the iron powder setup taken from the load profile created in section 4.2.1 including a standard fuel margin of 1.2. In order to accommodate iron oxide deposits as stated in chapter 2 section 2.2.1, 4 extra empty silos are added for iron oxide deposit. Four are chosen in order to maintain a balance in both transverse and longitudinal direction of the vessel and prevent a shift in weight of the bunker. The silos are placed as close to the center line of the vessel as possible within the pillars to minimize to increased moment created by the weight of the silos.

4.3.2. Diesel Generator Components

The diesel generator components are far simpler to estimate as these are far more common and readily available for commercial use. This is also the case for the bunker tanks for the marine diesel fuel as the tanks have far more flexibility for placement compared to the silos for iron powder storage.

Generator Sets

The choice was made to choose between the combined generator sets available in the Wärtsilä product sheets for different power ratings, [“Wärtsilä generating sets - Tailored to optimize performance”, n.d.]. The power rating of the generator sets are based on the total output required for the three engine rooms and divided over the amount generator sets per engine room.

Bunker Tanks

The marine diesel fuel bunker tanks are sized based upon the estimated kWh needed for variable load. Due to a these generator sets operating mostly at low efficiency points as well as providing peak loads at various times, the standard fuel margin of 1.2 is increased to 1.5. They will be placed in the pillars of the semi-submersible crane vessels alongside the iron powder silos. The placement will be as low in the pillars as possible to lower the center of gravity of the vessel. The temperature of the tanks is to be kept at around 40 degrees Celsius. Similar to the iron powder silos, the cross-sectional area of the tanks is also limited depending on how far the center of gravity is allowed to shift in horizontal direction.

4.3.3. Ship Main Elements

The ship main elements consist of the remaining weights on the vessel required for an accurate stability calculations. These include the cranes, the ballast, thrusters and the structural weight of the vessel. These elements are estimated separately despite the lightweight of all four vessels being given due to their varying placement aboard the vessel, these weights and their centers of gravity are required for a more accurate stability evaluation.

Cranes

The cranes of the vessel are the key functional elements of semi-submersible crane vessels, [Hagen, 2021]. Most semi-submersible vessels have two large cranes equipped for high tonnage. Some are equipped with two large tub cranes and others are equipped with two large mast cranes. The dimensions of the cranes and weight estimation is done through available technical specifications of the vessels as well as perspective views of the vessels that allowed for a 3D Rhino modelling to be done of each vessel.

The tub cranes consist of multiple different elements; the tub structure, the house structure, the winch structure, the boom and the luffing frame [Huisman, 2018]. The dimensions of each component were estimated and a standard plate thickness of 30mm was applied to the structures based on information in van Daalen, 2015. All elements were assumed to be made of steel so the product of the volume and density of the structures was summed to create the total weight of the crane. The weight of the boom and luffing were estimated separately as these weights were given for the 'Sleipnir'. These weights are scaled for other semi-submersible crane vessel designs based on the height and length of their boom and luffing respectively. A side profile of a tub crane is shown in figure 4.15 with each compartment identified. The two mast cranes have two main components, the mast and the boom, ["Product Brochure: Cranes", n.d.]. The geometry of the boom and crane is easier to replicate in Rhino than that of the tub crane. The volume of the cranes is taken from the Rhino model and the same thickness and steel density are used to estimate the weight of the crane. Figure 4.16 shows an isolated view of a mast crane similar to those used on semi-submersible crane vessels.

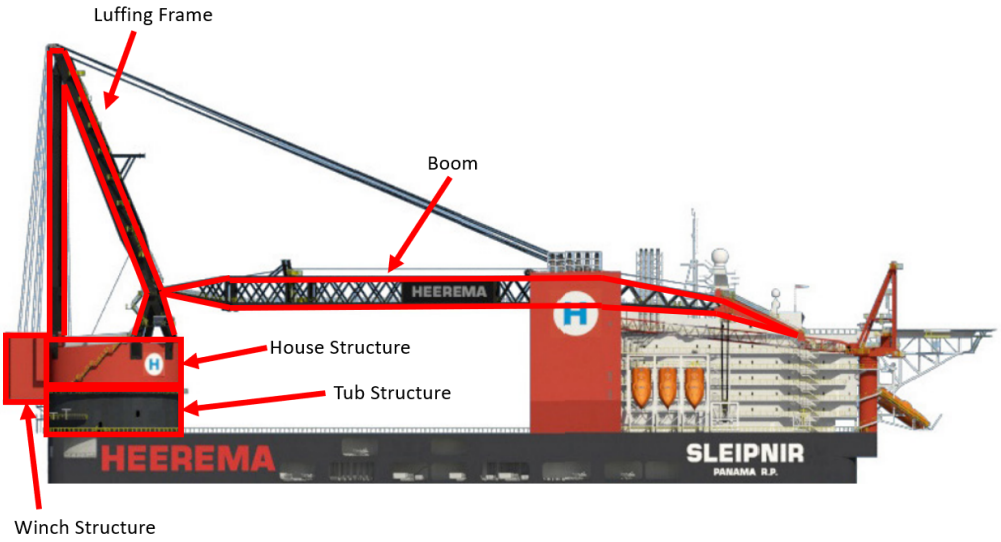

Figure 4.15: Side profile view of tub crane highlighting main elements, [*Sustainability Report*, 2021]

Figure 4.16: Isolated view of mast crane, [“Product Brochure: Cranes”, n.d.]

Ballast

The ballast water of semi-submersible crane vessels is stored mostly in the pontoons and partly in the pillars. This was determined through talks with experts at Heerema Engineering Solutions (HES) as well as general arrangements made available for the semi-submersible platform vessel ’Safe Boreas’ [“Safe Boreas”, n.d.]. The geometry and function of this semi-submersible platform vessel are assumed to be highly similar to that of the semi-submersible crane vessels being evaluated. The pontoons of the vessels also contain space for the thrusters, pumps and freshwater tanks as displayed in the blueprint of a pontoon in figure 4.17.

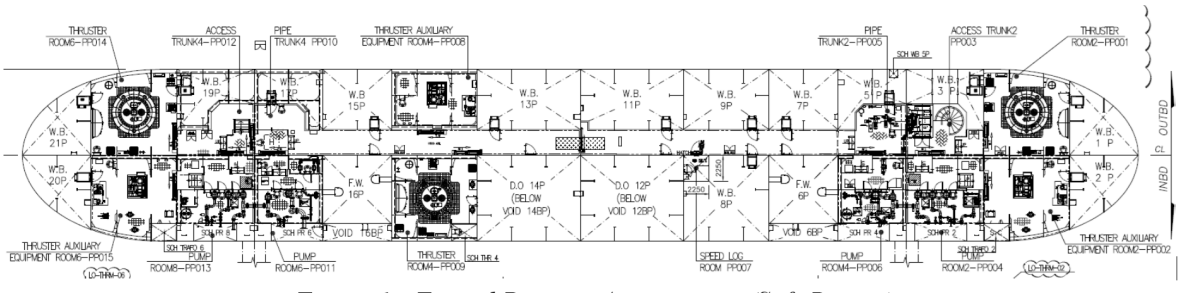

Figure 4.17: A general arrangement of 'Safe Boreas's pontoon, [MacGregor et al., 2019]

Based on this layout, the ratio of total surface area of the pontoon dedicated towards ballast storage over the total pontoon surface area was used to estimate the amount of ballast capacity in the pontoons. The total required ballast capacity for each vessel is dependent on the displacement difference between the transit draft and the maximal draft of each vessel. This determines how much ballast needs to be placed in the pillars for each vessel. The displacement calculations are once again made using the available dimensions of each vessel and the Rhino model created of each vessel.

Thrusters

All of the four vessels investigated are propelled by azimuth thrusters due to the dynamic positioning requirements. The rated power of the thrusters is given for each vessel. Using the product sheets of "L-Drive Azimuthing Thrusters Bottom Mounted", n.d., the rated power can be linked to a weight of an azimuth thruster system. This multiplied by the amount of thrusters per vessel gives the total weight of the thrusters.

Structural Weight

Finally the structural weight of the vessels are determined. This structural weight of the vessel includes the lightweight of the pontoons, pillars, main deck structure, superstructures and deck houses. These are simply calculated by taking the lightweight of each vessel and subtracting the weight of the thrusters, cranes and engine rooms.

4.4. Feasibility

Using the information from the dimensioning and weight calculations in section 4.3, some base stability calculations can be made to determine both the feasibility of a hybrid setup on a semi-submersible crane vessel as well as how this would look like. Due to a lack of information regarding the motions of these types of vessels as well as the exact internal layout of the vessels only the intact stability will be evaluated. This intact stability evaluation will comprise of a transverse meta-centre height check and a longitudinal balancing check (4.4.2). Furthermore, a look at the impact of the hybrid setup on the draft of the vessel is further looked into (4.4.1).

4.4.1. Draft

The draft of a semi-submersible vessel is used as a variable that can increase a vessels stability in working condition. The draft is lowest in sailing condition to minimise the underwater surface area and therefore resistance of the vessel. The draft is highest when performing heavy crane operations as the increased draft ensures a lower ship response to wave loading. The draft is essentially altered through creation of extra deadweight through pumping ballast water into the pontoons and occasionally pillars of the vessel. This increase in vessel weight increases the draft of the vessel. The amount of tonnage required to change the draft of a vessel by a certain amount can be simply determined using equations 4.3 and 4.4, [Rawson and Tupper, 2001a].

$$\Delta W_x = \frac{A_{wl} * x}{\rho_{sw}} \tag{4.3}$$

$$\Delta T = \frac{\Delta W}{\Delta W_x} \tag{4.4}$$

In equation 4.3, ΔW_x represents the tonnes required for a distance x change in draft. A_{wl} represents the water plane area of the vessel and ρ_{sw} represents the density of seawater. In equation 4.4, ΔT represents the total change in draft while ΔW represents the change in weight. This calculation can also be used to determine the estimated impact on the vessels draft due to the extra weight needed for the iron powder hybrid installation. The change in weight is assumed to be almost entirely due to the weight of the bunkers. The weight of carrying only marine diesel fuel as bunker is compared to the weight of carrying both marine diesel fuel alongside iron powder to estimate the change in weight. Applying these weight changes to equation 4.4 for each vessel shows the estimated increase in draft due to the increased weight of the iron powder setup. This value is especially important for the transit draft condition as this cannot be compensated by simply pumping less ballast as is the case for the vessel's maximum draft. This increase in draft will certainly increase the underwater surface area which in turn will increase the resistance of the vessel changing its transit speed. This is an issue that may require a redesign of the vessel geometry to account for the added weight. If the draft at transit level increases to above the height of the pontoons, the issue is deemed serious and requiring significant redesign considerations. If the draft at transit level increases but not above the height of the pontoons, it is considered an issue requiring lass significant and far-reaching redesign considerations.

4.4.2. Stability

The stability of the vessel will certainly be influenced by the placement of the hybrid powertrain components. This is the case in both transverse and longitudinal direction.

Transverse stability

The transverse stability of semi-submersible vessels is generally quite high to accommodate for large moments caused by crane operations. Although the vessel motions due to wave loading are significantly reduced at maximum draft, the metacentre height (GM) is significantly reduced. Therefore the assumption is made that if the GM is acceptable at maximum draft in fully loaded condition, the GM will be acceptable for all other drafts and conditions as well. According to classification rules for heavy lift vessels in *Part 5: Ship Types, Chapter 10: Vessels for special operations*, 2021, the 'GM at equilibrium shall not be less than 0.3 m'. Further criteria include that the 'positive range of the GZ curve shall be minimum 15° in conjunction with a height of not less than 0.1 m within this range'. Finally, the 'maximum righting arm shall occur at an angle of heel not less than 7°'. In order to determine whether this vessel fulfills this criteria, the GM is determined as well as the GZ-curve for the first 15 degrees. This is done using equations 4.5, 4.6, 4.7 and 4.8, ["Barge Stability Guidelines", 2006].

$$GM = KB + BM - KG \tag{4.5}$$

$$BM = \frac{I}{V} \tag{4.6}$$

$$I = \sum_{i=1}^{N_b} \frac{L_{wl,i} * B_{wl,i}^3}{12} + L_{wl,i} * B_{wl,i} * d_{arm,i}^2 \tag{4.7}$$

$$KG = \frac{\sum_{i=1}^{N} KG_i * W_i}{\sum_{i=1}^{N} W_i} \tag{4.8}$$

In equation 4.5 the GM represents the metacentre height of the vessel, KB represents the distance from the keel to the center of buoyancy, BM represents the distance from the buoyancy point to the metacentre and KG represents the distance from the keel to the center of gravity of the vessel.

The centres of gravity of each internal component used to determine the total centre of gravity of the

vessel has been determined either through general arrangements of existing semi-submersible vessels or technical insight provided by experts at HES. The engine room, bunker and ballast locations are determined to be the same as the engine rooms and bunker locations seen on the 'Safe Boreas', a semi-submersible platform vessel with a highly similar configuration to the semi-submersible crane vessels ["Safe Boreas", n.d.]. The placement of these internal components was further confirmed by experts working at HES. Figure 4.18 shows the general arrangement of the bottom deck of the deckbox of the 'Safe Boreas' with the engine rooms placed at this level. Figure 4.17 used to help determine the ballast volume also provides an accurate estimate of its centre of gravity. Cross-sections of the pillars of the 'Safe Boreas' and discussions with experts at HES resulted in the conclusion that the silos and MDO tanks are placed in the pillars.

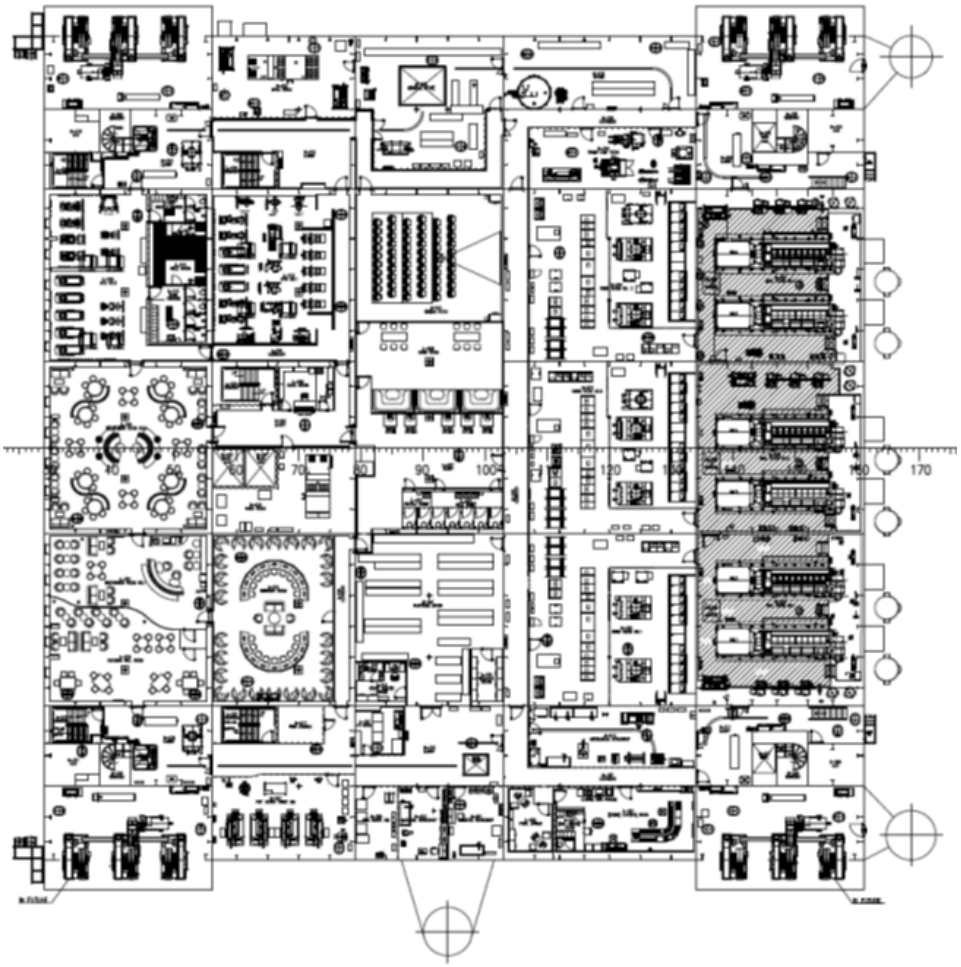

Figure 4.18: General Arrangement of lower deck of 'Safe Boreas's deckbox, [MacGregor et al., 2019]

In equation 4.6, the I represents the moment inertia of the waterline surface at a particular draft and the V represents the volume displaced by the vessel at that draft. Equation 4.7 shows how the moment inertia can be calculated for a multi-hulled vessel where N_b represents the number of bodies (in the case of all four vessels $N_b = 2$), L_{wl} represents the total length of the hull at the waterline, B_{wl} represents the total breadth of the hull at the waterline and d_{arm} represents the distance between the centreline of the hull and the centreline of the entire vessel.In equation 4.8, the center of gravity of the vessel is determined based on the centers of gravity of all components estimated in section 4.3. With the GM, the GZ-curve can be estimated to an acceptable degree of accuracy for the first 15 degrees using equation 4.9.

$$GZ = GM * sin\theta \tag{4.9}$$

Here the θ represents the angle of roll that the vessel undergoes. These GM and GZ calculations are done for all four vessels and the results compared to the requirements in *Part 5: Ship Types, Chapter 10: Vessels for special operations*, 2021.

Longitudinal stability

The longitudinal stability is largely dictated by the distribution of ballast across the length of the vessel. This allows the trim of the vessel to be managed in different circumstances and drafts. The general arrangement of the vessel dictates to what degree the ship will trim and to what extent this trim must be controlled. The trimming moment of the vessel determines how much the vessel will trim and this is calculated simply using equation 4.10, [Biran and López-Pulido, 2014].

$$M_{trim} = \Delta * (LCG - LCB) \tag{4.10}$$

In equation 4.10, the M_{trim} represents the trimming moment, Δ represents the displacement of the vessel, LCG represents the longitudinal centre of gravity and LCB represents the longitudinal center of buoyancy. The trimming moment must be kept as low as possible even to minimise the need for ballast shifting. In order to minimise the trimming moment, the longitudinal center of gravity and longitudinal center of buoyancy must be as close as possible. The longitudinal center of buoyancy cannot be altered unless the geometry of the vessel changes. The longitudinal center of gravity can be altered by changing the longitudinal center of gravity of the components of the vessel such as the engine rooms, bunker tanks, ballast tanks and iron powder silos. Equation 4.11 is used to calculate the longitudinal center of gravity of the ship and the centers of gravity of the components are varied until the resulting center of gravity of the vessel is within a meter of the longitudinal center of buoyancy.

$$LCG = \frac{\sum_{i=1}^{N} LCG_i * W_i}{\sum_{i=1}^{N} W_i} \tag{4.11}$$

4.4.3. General Arrangement

This placement of the various components to fulfill transverse and longitudinal stability creates a general arrangement of the vessel. The components are placed within the bounds of the geometry of the vessel at various heights along the length of the vessel. The placement will of course be symmetrical along the breadth of the vessel as is the case with almost all seagoing vessels. This general arrangement will be displayed in the 3D Rhinoceros model made for each vessel with side and top views of each level shown as well.

4.5. Emissions

The key advantage of iron powder as a power source is its significantly lower greenhouse gas emission in comparison the the marine diesel fuels being used. It is assumed that the installation of an iron powder hybrid setup will likely incur technical concerns regarding the vessel design. The emissions decrease is weighed against these concerns in order to determine whether the degree of feasibility of installing an iron powder hybrid setup on a particular vessel is worth the effort and cost. Firstly, the pollutants to be considered are determined as well as their output for each power source (4.5.1) and then the original powertrain is compared to the hybrid powertrain (4.5.2) to determine the level of emissions reduction.

4.5.1. Pollutants

The combustion of marine diesel fuel results in a large variety of different greenhouse gas emissions beyond simply carbon dioxide and nitrous oxides, [Ma et al., 2023]. The only emission output values known for iron powder combustion are the carbon dioxide and nitrous oxide values. Combustion of iron powder results in 0 ppm emission of carbon dioxide and up to 94 ppm emission of nitrous oxide

according to the limited full-scale tests done by team SOLID [van Rooij et al., 2019]. These values convert to 0 grams of carbon dioxide per gram of iron powder and 0.08382 grams of nitrous oxide per gram of iron powder using a conversion method by ["EMEP/EEA air pollutant emission inventory guidebook 2019 - Update Dec. 2021", 2021]. This is compared to an emissions output of 3.206 grams of carbon dioxide per gram of marine diesel fuel and a best case scenario of 2 grams of nitrous oxide per kWh power generated using marine diesel fuel (assuming tier III emissions regulations are adhered to) ["EMEP/EEA air pollutant emission inventory guidebook 2019 - Update Dec. 2021", 2021].

4.5.2. Original vs Hybrid

The load profile created in section 4.2.1 gives the total kWh required for an entire mission as well as the split between the iron powder setup and the diesel generator setup. The required bunker mass calculated in section 4.3 along with this total kWh required can be used with the emissions values to estimate the total emission of carbon dioxide and nitrous oxide for an entire 12 week mission. Equations 4.12, 4.13, 4.14 and show the calculation of the ratio of total emissions of carbon dioxide and nitrous oxide for both the iron powder and diesel generator setup over the total kWh of power produced.

$$W_{CO2,IP} = \frac{0 * W_{bunker,IP}}{P_{total}} \tag{4.12}$$

$$W_{NOx,IP} = \frac{0.08382 * W_{bunker,IP}}{P_{total}} \tag{4.13}$$

$$W_{CO2,MDF} = \frac{3.206 * W_{bunker,MDF}}{P_{total}} \tag{4.14}$$

The NO_x output of the marine diesel fuel can be easily converted from g/kWh to kg/kWh. This ratio will be used to compare the hybrid powertrain setup with the original powertrain setup. The original emissions output of the vessels will be simulated by having the marine diesel fuel provide the full power delivery as opposed to the hybrid.

5

Case Study

For this case study, a set of four semi-submersible vessel (SSCV) designs was chosen to be a representation of the SSCV fleet. This set of four SSCV designs was based on a market study with a particular focus on the Sleipnir (5.1a), Thialf (5.1b), Balder (5.1c) and Gretha (5.1d). Each vessel design has a slightly different geometry, size and crane capacity. These four vessel designs are considered sufficient to as a representation of the SSCV global fleet as the total global fleet is quite limited with a maximum of 20 operational vessels worldwide. The differing geometry and capacity allows for a clearer comparison between the vessels when evaluating the reasons for technical feasibility.

(a) Sleipnir (Heerema), [“Sleipnir HMC Equipment”, n.d.]

(b) Thialf (Heerema), [“Thialf HMC Equipment”, n.d.]

(c) Balder (Heerema), [“Thialf HMC Equipment”, n.d.]

(d) Gretha (O.O.S. International), [“Semi Submersible Accomodation / Crane Vessel: O.O.S. Gretha”, n.d.]

5.1. Semi-Submersibles Key Information

The key information of the four chosen vessels are split over the vessel dimensions (5.1.1) in which the geometry, capacity and power output of the vessels is listed. This is combined with the operational profile data in section 4.1.2 to allow for a load distribution analysis for these vessels in section 5.2

5.1.1. Vessel Dimensions

These four vessels have varying main dimensions, carrying/lifting capacities and powertrain setups. The main information on each vessel is provided in table 5.1. This information will be used in later sections for the creation of the load profile and a general arrangement.

Dimension	Symbol	Vessel A	Vessel B	Vessel C	Vessel D	Unit
Length	L	220	201.6	154	137	m
Breadth	B	102	88.4	106	81	m
Minimum Draft	T_{min}	12	11.9	11	11.28	m
Maximum Draft	T_{max}	32	31.6	25	26.4	m
Depth	D	49.5	49.5	42	39	m
Crane Capacity	C_{cap}	2x10,000	2x7,100	2,721 + 3,628	2x1,800	t
Transit Speed	v_{tr}	10	7	5	8	kts
Thrusters	T	8x5.5	6x5.5	7x3.5	6x3.8	MW
Powertrain	P_E	12 x 8	6x4.9, 4x4.5, 2x5.5	N/A	8x3.86	MW
Total Power	P_T	96	58.4	N/A	30.88	MW
Accommodation	N_{per}	400	736	394	618	-

Table 5.1: Semi-submersibles main dimensions and key information

The only missing base information regarding these vessels was the powertrain configuration and total power output capability of Vessel C. This is assumed to be due to the conversion of the powertrain of this vessel in 2001. This was done in order to ensure vessel C could comply with the tier III dynamic positioning requirements.

The main features shared by all four vessels is this tier III dynamic positioning capability as this is a requirement for the heavy lifting operations. This also means that the thrusters for each vessel are azimuth thrusters. All vessels have a transit depth of around 11-12m with maximum depths ranging from 25m up to 32m. These maximum depths are only reached during these heavy lifting operations in which the dynamic positioning is also active. The crew accommodation appears to vary quite heavily from 400 persons up to 736 persons. These main points of information are used to determine the expected power requirements for each operating mode.

5.2. Load Distribution

The load distribution for each vessel is determined through a thorough load profile of each vessel in which the load types are identified. The power demand for each load type is estimated according to the methods in section 4.2. These are then used along with the mission operational profile to simulate a load profile graph. From these simulations, the ranges of the hybrid split are determined as well as the average total power consumption that can be used for weight estimation and dimensioning in section 5.4.

5.2.1. Load Profile

The load profile starts with a look at the load types as well as the expected power demand for each consumer for each vessel in each operating mode (5.2.2). This is followed by a visual representation of the load profile simulations in the form of a time vs power graph (5.2.3). From this information, the original powertrain can be analysed and adapted to a hybrid powertrain for each vessel (5.2.4).

5.2.2. Load Types

The loads per operational mode were determined using the method described in subsection 4.1.2 as well as the data provided for each vessel summarized in table 5.1. Taking information from the power requirements of an existing semi-submersible crane vessel, the 'Sleipnir', the power ranges could be extrapolated to each of the four vessels based on the information of each vessel. These estimated power requirements were split over the three main consumers of the vessel, the thrusters, cranes and hotel load. These estimated power ranges are displayed for each consumer and each vessel in tables 5.2, 5.3, 5.4.

Hotel Load				
Operating Mode	Vessel A	Vessel B	Vessel C	Vessel D
Idle Mode	4-5 MW	6-7 MW	4-5 MW	5-6 MW
Sailing Mode	6-7 MW	9-10 MW	6-7 MW	8-9 MW
Working Mode	1-4 MW	1-6 MW	1-4 MW	1-5 MW

Table 5.2: Hotel load range estimates for each vessel

The idle and sailing modes are considered to be constant loads for each vessel and the values are of course highest for Vessel D and the Vessel B. This is to be expected as these vessels have a significantly higher crew accommodation capacity compared to Vessel A and Vessel C. The hotel load is more varied in working mode on each vessel depending on the tasks of the crew.

Thrusters				
Operating Mode	Vessel A	Vessel B	Vessel C	Vessel D
Idle Mode	0.15-0.3 MW	0.15-0.3 MW	0.15-0.3 MW	0.15-0.3 MW
Sailing Mode	29-31 MW	22-23 MW	16-17 MW	15-16 MW
Working Mode	5-22 MW	4-16 MW	3-12 MW	2-12 MW

Table 5.3: Thruster load range estimates for each vessel

The thruster loads are highest in sailing mode as is to be expected. This is the case for each vessel and as expected, the vessel with the highest thruster power, Vessel A, also has the highest power requirement. The thruster load in sailing condition is generally considered to be constant as well as the thruster load in idle. The idle thruster load is dependent on the sea state however, as DP is generally not required in idle mode, the power requirement is quite low. This is not the case for the working mode as the thruster load is much more dynamic, a base positioning DP load is required accompanied by extra DP load depending on crane operations. This explains the larger range for the thruster load in working mode as it varies from base load to maximum load.

Cranes				
Operating Mode	Vessel A	Vessel B	Vessel C	Vessel D
Idle Mode	0-3 MW	0-2 MW	0-1 MW	0-1 MW
Sailing Mode	0 MW	0 MW	0 MW	0 MW
Working Mode	2-40 MW	2-15 MW	1-4 MW	1-3 MW

Table 5.4: Crane load range estimates for each vessel

The crane load is obviously equal to zero when in sailing mode as the cranes are not used in this mode. They are used at generally lower capacities in idle mode for cargo transfer. The main use of the cranes is in the working mode when the heavy lifting operations begin. These can lead to peaks of up to 40MW for Vessel A and up to 15MW for Vessel B. These peak loads are much lower for Vessel C and Vessel D because of their much lower crane capacities.

5.2.3. Load Profiles

The load profiles are generated for each vessel with the assumption that they are all following the same mission profile described in subsection 4.1.2. Taking an relatively large distance from port to wind farm of around 100 nautical miles and an expected distance between wind turbines of around 5 nautical miles [Nijssen et al., 2016], the sailing profile can be determined depending on the transit speed of each vessel in table 5.1. It is further assumed that each vessel will take 32 hours to complete the installation of a single wind turbine [Lacal-Arántegui et al., 2018]. Using the distribution of time spent in working, sailing and idle mode described in section 4.1, the following load profiles were created. Each vessel was given the same mission time of 12 weeks and the loads were split between each main consumer; cranes, thrusters and hotel load. From this split, a total power profile was created by summing the load requirements of each consumer. The total power consumption for each vessel was determined as the average over the 10000 load profile simulations run.

Vessel A

The load profile estimations for Vessel A is shown in figures 5.2 and 5.3. Figure 5.2 shows a distribution of the main consumers of power; the thrusters, cranes and hotel loads. These are important to determine the variation of the loads as the operating modes change. These are then summed up to create a total power profile in figure 5.3. From this load profile a base and variable load can be determined.

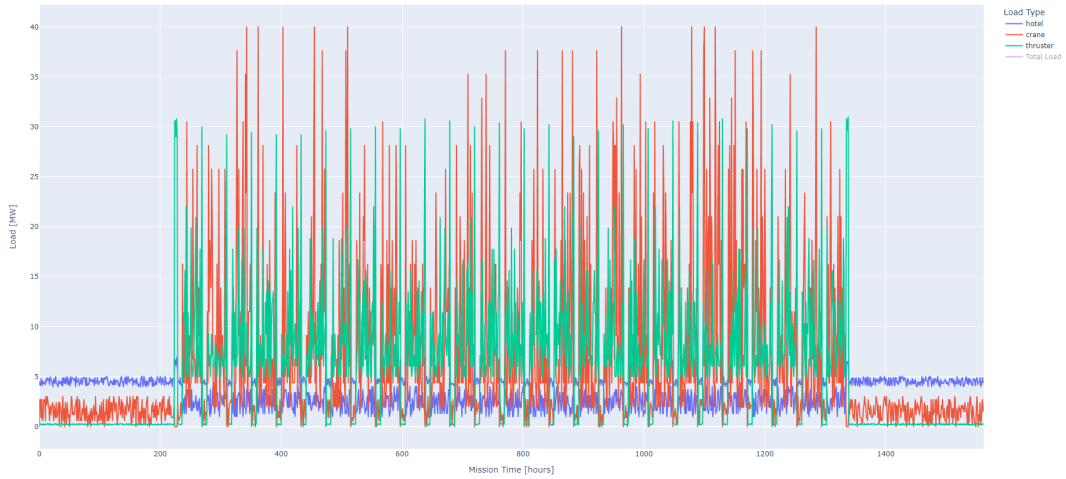

Figure 5.2: The power profile of Vessel A split over the three main consumers of power

The power split over the three consumers shows that the largest variation of power occurs in the working mode as would be expected. The highest peak consumer on Vessel A is the crane at 40MW, however, it does not often reach this peak level over the course of the mission. This is also the case for the thrusters, whose peak load is around 31MW in sailing condition. As expected, the hotel load does not vary significantly over the course of the mission, this will likely be the main proponent of the base load.

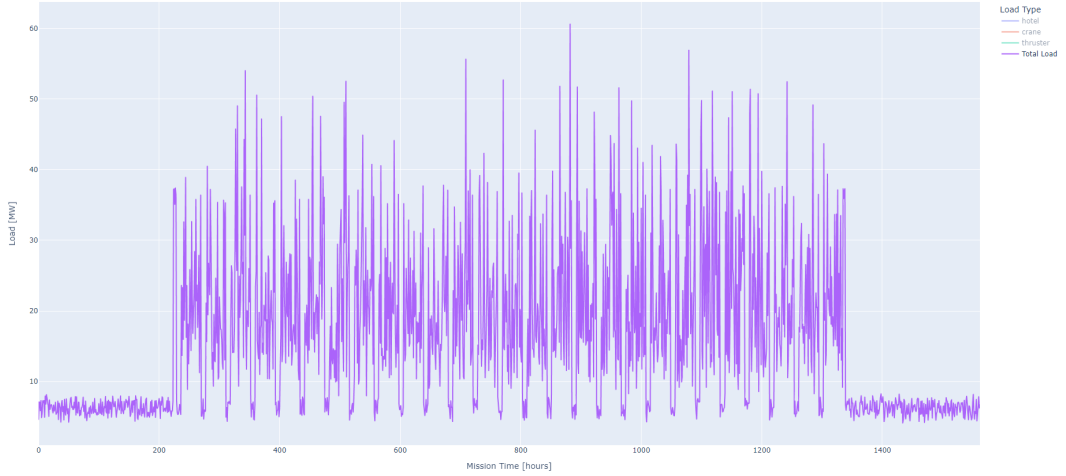

Figure 5.3: The power profile of Vessel A as the total load required

The total power profile shows a much clearer distinction between the base and variable load. The lowest load requirements appear to vary between 5MW and 6MW whilst the loads above the 6MW level are far more dynamic. This suggests that the base load of Vessel A should be set around this 5MW power output with the variable load able to cover the remaining power requirement up to a maximum of 61MW. The total energy required for a full mission is calculated as the area under this power

profile. The average of the total power requirement determined for each simulation results in around 21,000MWh of power required to complete a 12 week turbine installation mission.

Vessel B

The load profile estimations for Vessel B is shown in figures 5.4 and 5.5. Figure 5.4 shows the load distribution split over the main power consumers while figure 5.4 shows the total power requirement over the course of the mission from which the base and variable load can be determined.

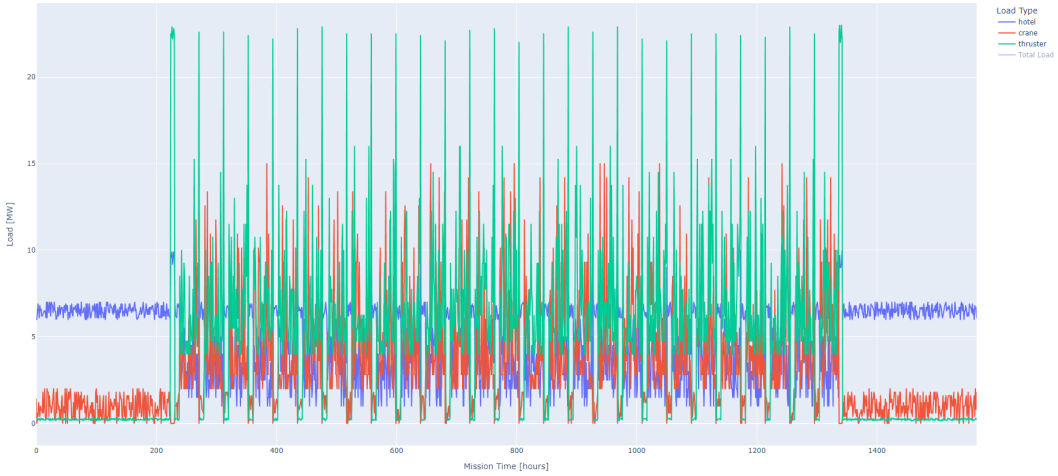

Figure 5.4: The power profile of Vessel B split over the three main consumers of power

The main difference between the power profiles of Vessel A and the Vessel B are the sources of the peak loads. In the case of Vessel A it was the cranes that were the peak consumers while in the case of Vessel B it is the thrusters. The peak thruster loads come from the sailing mode reaching up to 23MW. The hotel loads on the other hand are higher than that of Vessel A, ranging from 6 to 7MW. When comparing to the base hotel load of 1MW in working condition, the variation of hotel load over the course of the mission is much larger.

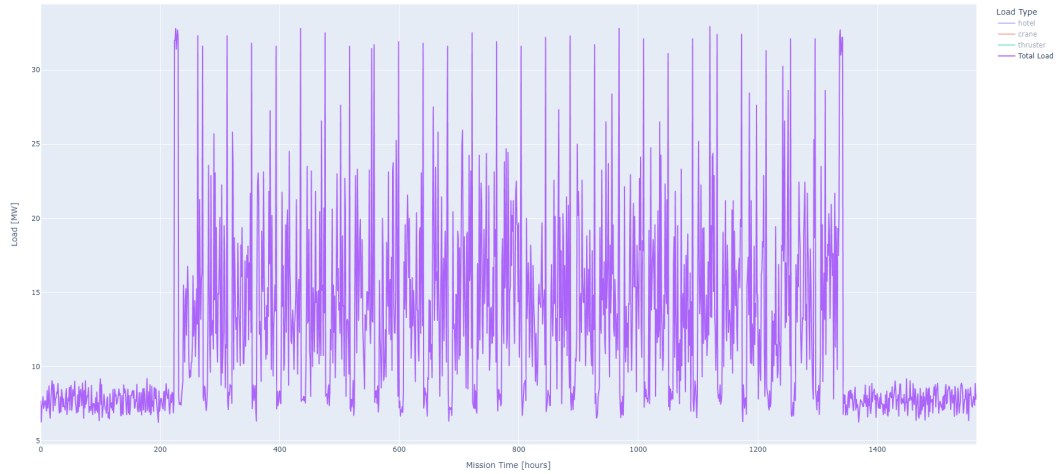

Figure 5.5: The power profile of Vessel B as the total load required

This increased hotel load results in a higher base load for Vessel B as the total power consumption ranges between 7 and 8MW. The loads above 7-8MW are far more dynamic leading to a base load power output of around 7MW with the variable load covering up to the peak load of up to 33MW. Taking the average total power requirement of the 10000 simulations run, the amount of total power needed

for Vessel B to complete a 12 week turbine installation mission ends up being around 19,500MWh.

Vessel C

Figures 5.6 and 5.7 show the load profile estimations created for Vessel C. Figure 5.6 shows the load distribution split over the three main consumers while figure 5.7 shows the sum of these consumers as the total power requirement.

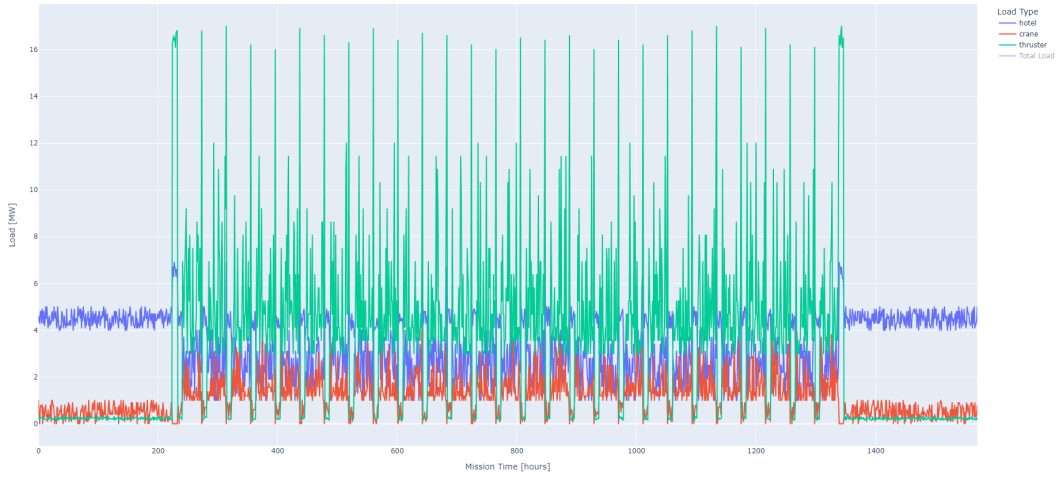

Figure 5.6: The power profile of Vessel C split over the three main consumers of power

Same as with Vessel B, the thruster load in sailing mode are the peak consumers at around 17MW. This is to be expected as the crane capacity is far lower than Vessel A. The hotel load of Vessel C is similar to that of Vessel A with a range of 4-5MW. This hotel load does not vary as much over the course of the mission as opposed to Vessel B. A key difference is the change in crane loads, the peak being much lower at around 4MW will likely reduce the power requirement of the vessel as whole.

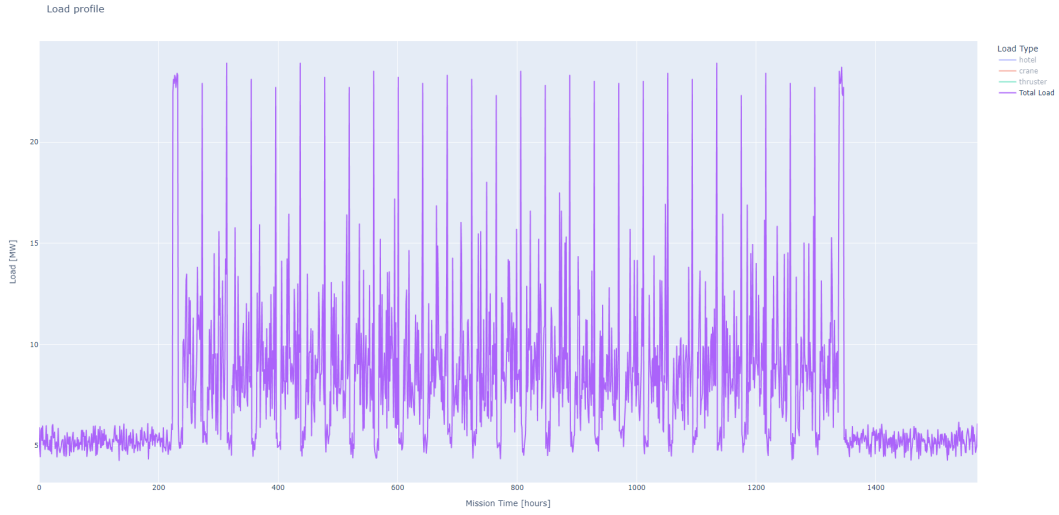

Figure 5.7: The power profile of Vessel C as the total load required

The total power distribution of Vessel C has the same shape as Vessel A and Vessel B with the main discern-able difference being the much lower peak loads. The lowest power requirements in idle mode are around 5-6MW with loads above 6MW being far more dynamic. This suggests a base load power output of around 5MW with the variable load to cover the remaining power up to the peak of around 24MW. The average of all simulated total power requirements of Vessel C for a 12 week wind

turbine installation mission is around 12,500.

Vessel D

The load profile estimations of Vessel D are displayed in figures 5.8 and 5.9, with figure 5.8 showing the distribution of power over the three main consumers and figure 5.9 showing the total power requirement.

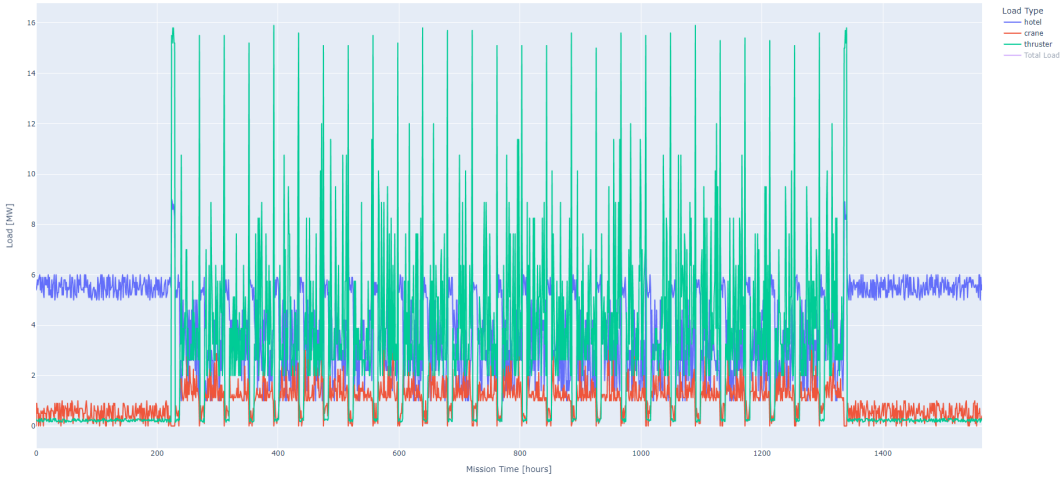

Figure 5.8: The power profile of Vessel D split over the three main consumers of power

The power consumption of Vessel D is very similar to that of Vessel C in the fact that the thruster load in sailing mode is the peak consumer. This is also coupled with the fact that the crane load is far lower than Vessel A and Vessel B, as is also the case with Vessel C. The hotel load is higher at 5-6MW staying relatively steady over the course of a mission. The peak thruster load is lower than that of Vessel C capping out at 16MW.

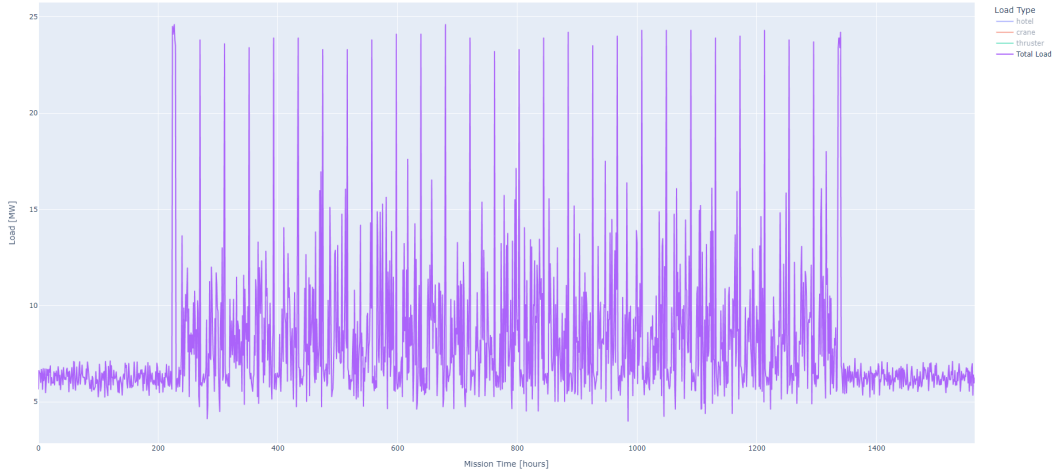

Figure 5.9: The power profile of Vessel D as the total load required

The total power consumption of Vessel D is also very similar to that of Vessel C. The main difference is the determination of the base load. In the case of Vessel D, the lowest required power is in the range of 5.5-7MW meaning a base load of around 6MW would be optimal. The dynamic load above 6MW would be covered by the variable load provider up to the peak load of 24.5MW. The average total power requirement determined for Vessel D over all simulations is similar to Vessel C's at around 12,000MWh.

5.2.4. Powertrain

The load profiles show what is required from the powertrains in order to complete a mission. To reduce redesign necessity the hybrid powertrain designs aim to not be drastically different from the original powertrains. The original powertrain setup is analysed for each vessel to determine what is required for the hybrid powertrain in terms of design and power demand.

Original Powertrains

Information regarding the original powertrains of each of the four vessels can be determined or estimated. For some vessels, the powertrain schematics are made available (Vessel A and Vessel B) and for others it can be inferred from the information that is available (Vessel C and Vessel D).

Vessel A

Vessel A has the most complex existing powertrain setup of the four vessels investigated. This is due to the fact that it is already operating in a hybrid configuration. Vessel A is an LNG and MGO hybrid as shown in the schematic in figure 5.10.

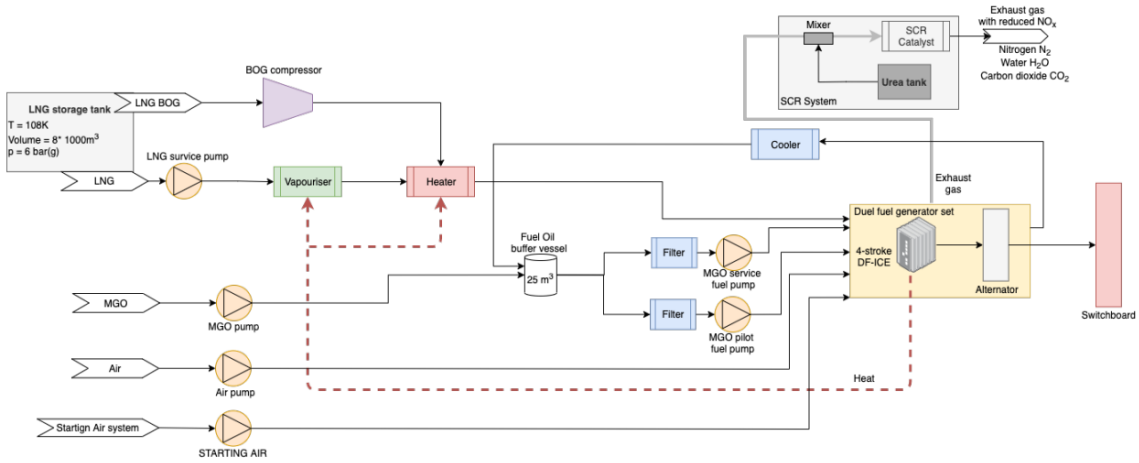

Figure 5.10: A schematic overview of the existing Vessel A powertrain, [Hagen, 2021]

This schematic shows a setup with both MGO and LNG tanks connected to 12 dual fuel generator sets (MAN 8L51/60DF) rated at 8000kW, [Hagen, 2021]. These generator sets convert this energy to mechanical energy which is promptly converted to electrical energy through 12 General Electric 9129kVA 60Hz AC synchronous alternators, [Hagen, 2021]. This electrical energy is then transferred throughout the vessel to the consumers through the switchboards. As was shown in figure 4.7, there is a switchboard for each of the four engine rooms in Vessel A. Each engine room is capable of supplying power with either MGO or LNG as a fuel source. Dual fuel engines will not be applicable for an iron powder hybrid configuration meaning an adapted powertrain setup is required without deviating too far from the existing one.

Vessel B

Vessel B is very similar to Vessel A in that it also contains 12 generator sets. That are directly connected to alternators converting the mechanical energy straight into electrical energy. This energy is then also distributed throughout the vessel using the switchboards in the engine rooms. Vessel B has three engine rooms compared to the four in Vessel A. In contrast to Vessel A, Vessel B is not driven by a hybrid setup and is fully fueled by marine diesel fuels. The engine types and ratings are varied as the originally fitted engines from 1985 are accompanied by newer engines installed on Vessel B in 2007 and 2010 respectively [Lyu, 2016]. These engines are detailed in table 5.5 and can be found in the schematic diagram of Vessel B's powertrain in 4.8.

Information	Engines 1-6	Engines 7-8	Engines 9-12
Type	MAK 8M552	Sulzer 8ZAL40S	Sulzer 6ZAL40S
Manufacturer	Ube Industries Ltd.	Wärtsilä	Wärtsilä
Rated Power	4898 kW	6000 kW	4500 kW
Year Installed	1985	2010	2007

Table 5.5: Overview of engines installed on Vessel B, [Lyu, 2016]

Vessel C

As stated earlier, the powertrain for Vessel C is not readily available however some information about Vessel C's powertrain upgrade is known. As Vessel C is based of an existing vessel similar to vessels A and B, it is likely that it will contain a powertrain similar to that of those two vessels. The powertrain upgrade of Vessel C included an additional 6 azimuth thrusters accompanied by six individual diesel engines and generators [Reed, 1998]. The original vessel contained only one engine room but the powertrain upgrade increases the total to 7 meaning that each generator set was fitted with into its own engine room [Reed, 1998]. Furthermore, three sets of two engine rooms were connected through cross-link buses in order to allow two thrusters to be powered by one engine in more ideal DP conditions [Reed, 1998]. This will mean that the rated power of these added engines is likely to be around 7000kW as each azimuth thruster is rated at 3500kW.

Vessel D

While a detailed schematic of the powertrain configuration of Vessel D is not available. There is more information regarding the likely engine setup when comparing to similar vessels owned by OOS International. The OOS Zeelandia, a similar vessel to Vessel D, is powered by 12 dual fuel engines in hybrid MDO and LNG configuration similar to Vessel A ["Huge Semisub Crane Vessel gets AIP", 2019]. These engines are split between six engine rooms on the OOS Zeelandia ["Huge Semisub Crane Vessel gets AIP", 2019]. Comparing this to the 8 generator sets rated at 3860kW aboard Vessel D, it is likely that Vessel D's generator sets are split between four engine rooms. It is also further assumed that the setup is similar to the other vessels in that the power from the generator sets is distributed to the consumers similarly to Vessel A and Vessel B.

5.2.5. Hybrid Powertrain

With the base and variable loads determined. The hybrid powertrain can be configured. In order to minimize alterations to the existing powertrain configurations of each vessel, the choice was made to have all vessels be fitted with a variant of an MDO and iron powder hybrid setup. A visual overview of the hybrid configuration can be found in figure 4.9. This configuration would mean that each vessel contains four total engine rooms. Three of the four engine rooms would be fitted with diesel generator sets to provide mainly the variable load required for each vessel. The final engine room would be fitted with the iron powder setup including the UST adapted to iron powder combustion as well as a electrical motor for mechanical to electrical energy conversion. In order to maintain the high level of redundancy required for semi-submersible crane vessels, two adapted UST setups will be placed in the final engine room to ensure the base load can always be delivered.

5.3. Load Split

Through further analysis of the range of load profile simulations of each vessel, the general split between iron powder and MDO power can be shown in the form of a percentage range of the total power requirement of the vessel. These values are shown in table 5.6 for all four vessels.

	Base Load % of Total Demand	Variable Load % of Total Demand
Vessel A	18 - 45	55 - 82
Vessel B	31 - 63	37 - 69
Vessel C	41 - 67	33 - 59
Vessel D	45 - 73	27 - 55

Table 5.6: Range of percentage total power demand covered by base and variable load

As is expected, the larger crane and thruster demands for Vessel A and Vessel B result in a relatively higher variable load meaning the ratio of the base load contribution to total power and variable load contribution to total power skews toward the variable load. The smaller vessels, Vessel C and Vessel D, have a far lower crane capacity resulting in the variable load being mainly dominated by the thruster load only, this decreases the total variable load and means more of the total power demand can be covered by the base load. For the dimensioning of the engine room and bunker storage components, the average of the load distribution is used. As this is based off of previously made estimations, this value serves largely as an indicator for the general total power consumption. This does not take into account the low efficiency points of each generator set due to redundancy requirements and intermittent loading. These points will be further discussed in section 4.3 when determining the amount of bunker required.

5.4. Dimensions and Weights

The dimensions and weights of the powertrain components as well as of the ship structural elements are all taken either from existing dimensioning methods or from regression analyses of similar existing components. The precise method of dimensioning for each component is outlined in section 4.

5.4.1. Iron Powder Components

The dimensioning of the iron powder setup is split over the main components required for iron powder combustion. There are many other small but important components required in the iron powder engine room, however, these ones that are handled are the key components that determine the volume and mass requirement of the iron powder engine room and bunker storage. As stated in section 5.2.4, the iron powder engine room will be equipped with two UST setups for redundancy purposes.

Turbines

The UST configuration is largely distinguished by its three turbines through which the super-heated and further reheated steam pass through. These turbine dimensions are mainly based off of the total power rating of the UST system being installed. From the load profiles in section 5.2.3, three different power ratings were determined for the four vessels. Vessel A and Vessel C would be fitted with a 5MW setup, Vessel B with a 7MW setup and Vessel D with a 6MW setup to cover the base load of these vessels. This means that the turbine dimensions and weights will differ for each vessel. The main dimensions, volumes and mass estimations based off of the methodology described in section 4.3 are found in tables 5.7, 5.8 and 5.9 for each power rating.

Power Rating: 5MW				
	Length [m]	Max Diameter [m]	Volume [m^3]	Mass [t]
High Pressure	3.45	2.04	11.3	61.6
Intermediate Pressure	3.95	2.07	13.3	72.4
Low Pressure	5.00	2.11	17.4	100

Table 5.7: Main dimensions for the UST turbines at a power rating of 5MW

Power Rating: 6MW				
	Length [m]	Max Diameter [m]	Volume [m^3]	Mass [t]
High Pressure	3.48	2.12	12.3	71.7
Intermediate Pressure	3.86	2.14	13.9	81.0
Low Pressure	5.01	2.21	19.2	117

Table 5.8: Main dimensions for the UST turbines at a power rating of 6MW

Power Rating: 7MW				
	Length [m]	Max Diameter [m]	Volume [m3]	Mass [t]
High Pressure	3.93	2.27	15.9	93.3
Intermediate Pressure	4.35	2.28	17.8	106
Low Pressure	4.12	2.16	15.1	94.2

Table 5.9: Main dimensions for the UST turbines at a power rating of 7MW

Boilers

The boilers are estimated using a general estimation technique described in section 4.3. This means that while it will not be an exact measure of the actual boiler of a UST configuration, it can serve as an accurate indicator of the volume and mass required for such a boiler. This boiler design incorporates both the combustion chamber as well as the heat exchangers and is as previously described, vertical and cylindrical. The main boiler dimensions, volume and mass are listed in table 5.10 for each power rating.

Power Rating	Height [m]	Max Diameter [m]	Volume [m^3]	Mass [t]
5MW	6.51	1.57	15.9	27.3
6MW	6.51	1.72	17.8	32.9
7MW	6.51	1.86	15.1	38.61263

Table 5.10: Main dimensions for the UST boilers

Filters

The filtering system is made up of the cyclone and bag house filter. These filters are also dependent on the power rating of the UST setup as this dictates both the size of the filters and the pressure drop. The cyclone filters are designed to ensure that two filters will incur an acceptable allowable pressure drop for efficient particle filtration. These cyclone filter main dimensions, volume and mass are listed in table 5.11.

Power Rating	Height [m]	Max Diameter [m]	Volume [m^3]	Mass [t]
5MW	8.8	2.2	33.5	1
6MW	9.6	2.4	43.4	1.2
7MW	10.4	2.6	55.2	1.4

Table 5.11: Main dimensions for the cyclone filters

The bag house filter are designed to be for one filter module to be able to accommodate the expected pressure drop. The dimensions, volume and mass of the bag house filter are listed in figure 5.12.

Power Rating	Height [m]	Cross-sectional Area [m^2]	Volume [m^3]	Mass [t]
5MW	5	12.9	64.4	2
6MW	6	15.4	92.5	3
7MW	7	18.0	126	4

Table 5.12: Main dimensions for the bag house filters

The significant volume required for these filters means that they will need to be placed outside the engine room. To minimise the distance for the outlet mass flow to travel, the filters will be placed as near to the engine rooms as possible. While the volume requirements for these filters certainly requires attention, the mass requirements are deemed to be negligible compared to the other components. Therefore, the filter masses will not be taken into consideration for the stability calculations in section 5.5.

Engine Room

As stated earlier, one of the four engine rooms on each vessel will be fitted with the iron powder setup. This engine room will contain the turbines, boiler and the electrical motor. The dimensions of the engine room are therefore determined by the dimensions of the turbines, boiler and electrical motor combined. A minimum additional margin 10% of length, breadth and height is added for other components as well as to give space for engineers. The length, breadth, height and the total mass of each engine room is listed in table 5.13.

	Length [m]	Breadth [m]	Height [m]	Total Mass [t]
Vessel A	14	6	7	572
Vessel B	16	10	7	734
Vessel C	14	6	7	572
Vessel D	15	9	7	662

Table 5.13: Main dimensions for each iron powder engine room

The breadth and total mass are double the amount needed for one UST setup. Semi-submersible crane vessels have strict redundancy regulations which as one failure in an engine room must not lead to a total powertrain failure. In that regard, the UST engine room is fitted with two setups, the second setup in this case serves purely as a reserve in case of a failure in one. This setup is also chosen due to the more complex nature of this UST setup compared to the conventional diesel generator setup in other engine rooms, a failure may require a specialist for repair. In this case, one iron powder setup can continue to provide the base load while the other waits for repair keeping the total power output of the powertrain optimal.

With the power output and estimated mass of each iron powder setup known, the power to weight ratio can be easily calculated. This power to weight ratio of the iron powder setup is then compared to that of other energy sources to provide a comparison and some context as to the size of the engine setup. Table 5.14 displays the power to weight ratio of each iron powder setup alongside that of a typical engine types in kW/kg.

	5MW Setup	6MW Setup	7MW Setup	Wärtsilä 80MW	GE 30MW	Mazda 184kW
kW/kg ratio	0.0175	0.0181	0.0191	0.03	1.31	1.5

Table 5.14: Comparison of power-to-weight ratios

This comparison indicates two things, the iron powder setup has a relatively low power-to-weight ratio and the power-to-weight ratio seems to increase with power rating. The three iron powder setups have a power-to-weight ratio of between 0.017 and 0.019 kW/kg it seems. This is just over half the power-to-weight ratio of the Wärtsilä RTA96-C 14-cylinder two-stroke diesel engine used on the Emma Maersk container ship, [“The world’s most powerful engine enters service”, n.d.]. When compared to a GE LM2500+ marine turboshaft used on certain cruise ships and the Mazda 13B-MSP Renesis engine used in the Mazda sports cars, the difference in power-to-weight ratio becomes even larger with the iron powder setup estimated at around 10% of the power-to-weight ratio of these engines, [“LM2500+ Marine Gas Turbine”, n.d.]. Steam cycles have historically been known to have low power-to-weight ratios so this does not come as a complete surprise considering the UST cycle is also a steam cycle. What is interesting to note is the increase in power to weight ratio as the engine rating increases. This would mean that in order to optimise the power-to-weight ratio as much as possible one would have to choose the absolute maximum power rating available for this engine type.

Silos

The design of the silos done according to the method described in section 4.3 is dependent mainly on the dimensions of the vessels. These silos will be placed in the pillars of the main structures of each vessel and each vessel has different sized pillars. The height of the pillars are the main factor in determining the dimensions. The number of silos is taken as the amount of silos needed to carry the required bunker including the bunker margin plus the additional 4 empty silos required for initial oxide deposit. The total number of silos must be an even number to allow for even distribution among the pillars on each side of the vessel. The main dimensions and volume of one silo as well as the amount of silos required and total iron powder bunker mass for each vessel are listed in table 5.15.

Vessel	Total Height [m]	Diameter [m]	Volume [m^3]	Number of Silos [-]	Total mass [t]
Vessel A	21.6	3.93	232	34	16600
Vessel B	21.5	3.91	229	46	23200
Vessel C	20.7	3.76	204	38	16600
Vessel D	18	3.27	134	66	19900

Table 5.15: Main dimensions for the silos on each vessel

The impact of the mass requirements will be determined in section 5.5 but the volume requirements are likely to be met as the silos do not take up more space than is available in the silos. This is also taking into account the percentage of available space per silo based on the cross-section in figure 5.11 from a similar semi-submersible vessel, the 'Safe Boreas'. Here, an estimate of 75% of the cross-sectional area is assumed to be available for silo placement to keep 25% open for piping, wiring and other openings.

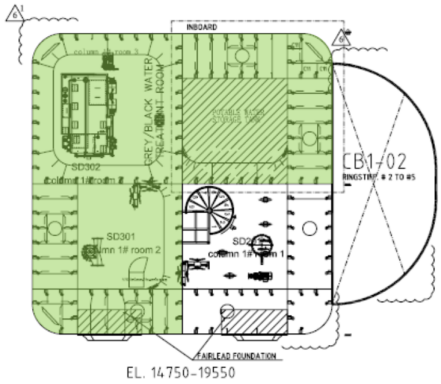

Figure 5.11: A cross-section of a the 'Safe Boreas's pillar, [MacGregor et al., 2019]

5.4.2. Diesel Generator Components

The diesel generator components consist of the generator sets fitted in the engine room and the bunker tanks fitted in the pillars.

Generator Sets

The diesel generator components are available commercially for all kinds of power ratings and practical applications. The diesel generators configurations chosen for each vessel comprise of two parts, mechanical energy generation in the generators and electrical energy conversion in the electrical motor. The generator sets available at Wärtsilä cover all the power ratings required while also combining both the generator and the motor. The main dimensions and mass for each generator set chosen based on the method described in section 4.3 are listed in the table below.

Vessel	Power Rating [MW]	Length [m]	Breadth [m]	Height [m]	Mass [t]
Vessel A	9.37	12.9	3.59	4.3	154.5
Vessel B	7.37	11.2	3.06	3.97	121
Vessel C	3.84	10.4	2.69	3.98	76
Vessel D	5.67	10.2	3.59	4.15	109

Table 5.16: Main dimensions for the diesel generator sets on each vessel

MDO Bunker

The bunker level is determined based off of the specific fuel consumption of the chosen generator sets. The bunker will be placed in the remaining available area in the pillars. The total MDO bunker level required for each vessel as well as its mass are listed in table 5.17.

Vessel	Bunker Mass [t]	Bunker Volume [m3]
Vessel A	5030	5650
Vessel B	2610	2930
Vessel C	2140	2400
Vessel D	1930	2170

Table 5.17: Required weight and volume of the MDO bunker on each vessel

Engine Room Generator Sets

The diesel generator engine rooms are determined by the size and number of generator sets assigned to each vessel. Three of the four engine rooms to be placed on the vessels will be fitted with diesel generators. As with the iron powder engine room, a margin of at least 10% extra length, breadth and height are added for the remaining smaller components as well as room for engineers. The length, breadth, height and total mass of each engine room is listed in table 5.18.

	Length [m]	Breadth [m]	Height [m]	Total Mass [t]
Vessel A	13.5	15	5	616
Vessel B	12	10	5	363
Vessel C	11	9	5	228
Vessel D	11	10.5	5	327

Table 5.18: Main dimensions for each diesel powered engine room

The mass and breadth of Vessel A are multiplied by four as this is the amount of engines to be fitted in one engine room. The mass and breadth of the remaining vessels is multiplied by three as these engine rooms are fitted with one less generator set each.

5.4.3. Ship Structural Elements

The ship structural elements contains the remaining significant elements of the vessel who have a significant mass and therefore significant impact on the ship stability calculations. These include the crane, ballast, thrusters and structural weight of the vessel. Using the methodology described in section 4.3, the total mass of each of these elements are listed in table 5.19 per vessel.

Vessel	Crane Mass [t]	Ballast Mass [t]	Thruster Mass [t]	Ship Structure Mass [t]
Vessel A	6850	113000	512	83500
Vessel B	5980	120000	384	66100
Vessel C	5160	30000	329	44100
Vessel D	2240	21000	282	31100

Table 5.19: Mass estimations of key ship elements

These values alongside the other estimated masses for each engine room will be used to calculate

an initial static stability to evaluate the feasibility of a hybrid iron powder configuration and to visualise how this would best fit. This evaluation is done in section 5.5.

5.5. Feasibility

The feasibility of an iron powder hybrid configuration on a semi-submersible vessel can be measured in many ways depending on the resources at your disposal. In this case, due to a limited amount of information about these vessels and their dynamic seakeeping behaviour, the choice was made to keep to a base feasibility determination. This means that the main static stability criteria will be evaluated such as the draft, transverse stability and longitudinal stability. Calculations will be made for each of these categories and the results will be compared to either the original powertrain setup of the vessel or the Det Norkse Veritas (DNV) classification bureau stability requirements for semi-submersible crane vessels [*Part 5: Ship Types, Chapter 10: Vessels for special operations*, 2021].

5.5.1. Draft

The hybrid iron powder configuration on a semi-submersible crane vessel will have a significant impact on the mass of the vessel. This is mainly due to a substantial increase in bunker mass. The original bunker fuel of marine diesel fuel has a density of around 0.9 tons per cubic meter, this is compared to a density of 2.45 tons per cubic meter. This, alongside a larger required volume, results in a much higher bunker mass for the same energy production level. This can have a significant impact on the semi-submersible design through its changing the vessel's draft. Its draft is of course a semi-submersible crane vessel's key feature in that it should be able to increase and decrease its draft according to its operating mode. A significant change in the total mass of the bunker will increase the draft of the vessel. By comparing the hybrid bunker mass level with a marine diesel fuel only mass level, the methodology described in section 4.3 can be used to determine the change in draft due to the increased bunker mass. The resulting draft increase is listed in table 5.20 for each vessel.

Vessel	Increase in Bunker Mass [t]	Increase in Draft [m]
Vessel A	15200	1.16
Vessel B	21200	2.22
Vessel C	15200	6.02
Vessel D	18300	8.06

Table 5.20: Draft increase due to increased bunker mass

The results are quite varied for each vessel as could be expected. This change in draft depends on both the mass increase as well as the ship's waterline area. The draft change was measured at minimum or transit draft as this is where the change in draft has the most impact. The maximum draft level can be much more easily maintained by adjusting the level of ballast. This is not the case for transit draft as there is no ballast to adjust. Of the four vessels, the only vessel indicating that the increased bunker will not necessarily require a redesign of the pillars and pontoons is Vessel A. The draft increase on Vessel C and Vessel D are mainly due to their small waterline area over the all their pillars especially when compared to Vessel B and Vessel A. The substantial draft increase on these two vessels points to a need for a pontoon and pillar redesign if it is to accommodate the expected iron powder bunker level. While, the increase in draft is not as severe as for Vessel C and Vessel D, Vessel B will likely also require a redesign of the vessel to a lesser extent. This is due to the draft now being above the pontoon height as shown in figures 5.12a and 5.12b.

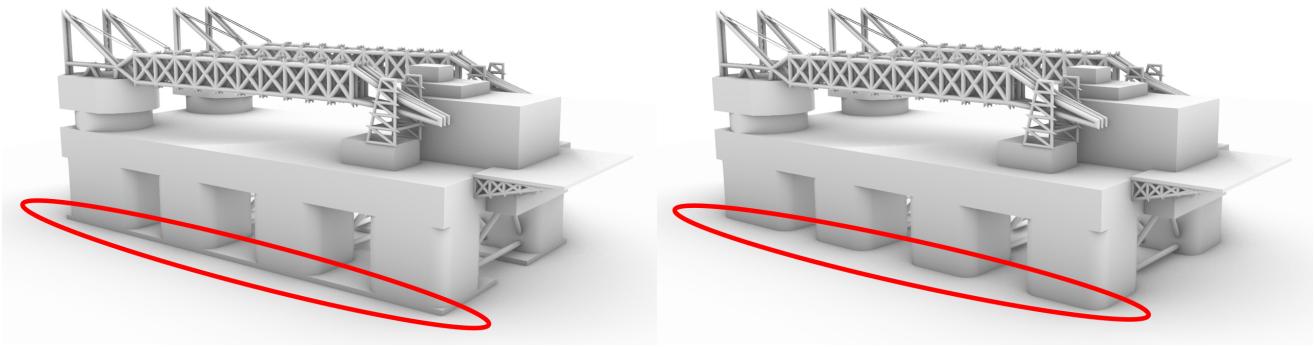

(a) 3D Render of Vessel B at regular transit draft

(b) 3D Render of Vessel B at increased transit draft due to bunker

As is shown in red circles on the figures, the draft is now at the level of the pillars, this means that the draft has increased to a point where the waterline area has changed. This means that the transit stability of the vessel is changed and may no longer be at an acceptable level. This increased draft would also mean that the surface area of the vessel under the waterline has increased. This increase in the surface area under the waterline leads to an increase in resistance of the vessel while in transit which would lead to more power being required for the original transit speed. These are also serious design changes that would have to be considered for not only Vessel B but Vessel C and Vessel D as well. The draft increase of just over 1 meter for Vessel A will likely require a few design considerations but nowhere near the level of the other three vessels. This is because this draft increase will only have a minimal impact on the power required for transit as the surface area under the waterline is only increased slightly. Furthermore, the waterline area at this increased draft will not change significantly, if at all as the draft level stays well below the height of the pontoons. This means that the hybrid iron powder configuration could still be technically feasible on Vessel A without extreme vessel redesign requirements.

5.5.2. Stability

The stability calculations are made for each vessel using the geometry of the vessel and the estimated engine, bunker and ship element masses calculated in section 5.4. These calculations will not provide fully accurate stability values due to these assumptions, however, can be used as a good indication of whether certain stability concerns are warranted with a hybrid iron powder configuration.

Transverse Stability

The transverse stability of semi-submersibles is an interesting and crucial factor for determining stability. Crane operations require a high level of transverse stability due to the added moments created by the crane movements. These crane movements need to be as stable as possible and to minimise the impact of the sea state on the vessel's movements, the crane operations are performed at the maximum draft of the vessels. This draft decrease the response amplitude operators (RAO) of the vessel which means that wave motions will have less impact on the vessel's motion. Another key advantage of these SSCVs is that they are multi-hulled vessels. Two pontoons connected to the deckbox by pillars over a generally wide breadth ensures that these vessels have a high initial transverse stability.

Most vessels experience an increase in GM as the draft of the vessel increases due to the increasing BM value. This BM value is dependent on both the water-plane area and the volume of the submerged section of the vessel. In the case of these semi-submersible crane vessels, an increase in draft from transit to working draft means a decrease in water-plane area as the water-plane moves from the pontoons to the pillars. Coupled with this, the significant increase in volume of the submerged section leads to a serious decrease in the BM value. This change in BM is far greater than the resulting decrease in KB value therefore resulting in an overall decrease in GM as the draft increases. Therefore, the stability calculation is done at maximum draft at maximum load to evaluate stability at its least stable point. If the minimum GM value at this point is satisfied, it can be assumed that the minimum GM value will be satisfied for any other draft as well. This will result in much higher GM values at

lower drafts, for many vessels, a higher GM results in higher accelerations which can also become a problem. Through talks with experts at Heerema Engineering Solutions (HES), it was determined that due to the substantially larger size of the semi-submersible crane vessels, these accelerations due to a high GM are not as high as for smaller vessels and therefore not considered a critical point of concern.

Using the methodology described in subsection 4.4.2, the meta-center height can be calculated for each vessel which is a determining factor for static transverse stability. Due to the limited information available for these vessels, only a base static transverse stability calculation can be made from which any reasonable conclusions can be drawn. Table 5.21 lists the KB, KG, BM and GM values for each vessel in a fully loaded condition at the maximum draft.

Vessel	KB [m]	KG [m]	BM [m]	GM [m]
Vessel A	11.4	35.7	28	3.62
Vessel B	12.2	30.9	25.1	6.35
Vessel C	9.05	30.8	26.8	5.11
Vessel D	7.61	26.7	19.6	0.52

Table 5.21: Transverse stability values for each vessel

The KB was determined through the 3D renders made of each vessel's geometry, the KG was determined at described in subsection 4.4.2 and the mass estimations of all major onboard components. The BM calculation from subsection 4.4.2 was made for each vessel according the the geometry of the pillars and pontoons. The GM (meta-center height) was then determined from these values. According to the classification rules by DNV [*Part 5: Ship Types, Chapter 10: Vessels for special operations*, 2021], the minimum allowed GM of 0.3m at maximum operating draft has been met by all four vessels. Vessels A, B and C even have a wide margin of safety above the minimum required GM value. This indicates that it may be possible for the iron powder hybrid configuration to be installed without negatively impacting the transverse static stability of the vessel. It must be taken into account that these GM values are determined based off of rough estimations and may in fact not reflect reality. There are certain extra mass elements aboard the vessel that may not be as large as the ones considered but may add up alter the estimated KG value. This is why the margin of a few meters regarding the GM values of Vessels A, B and C are more promising than the 0.2m margin for Vessel D. If these estimations were to be altered and the GM were to lower, the chances of Vessels A, B and C still fulfilling the initial transverse stability criteria are far higher than that of Vessel D.

Continuing on with the assumption that the GM values determined are in fact accurate enough indicators of the vessel's transverse stability, the GZ-curve can be modeled next. According to the classification rules by DNV [*Part 5: Ship Types, Chapter 10: Vessels for special operations*, 2021], the positive range of the GZ-curve at maximum draft must be minimum 15 degrees. The GZ-curve can be accurately modeled as described in subsection 4.4.2 up to 15 degrees so only a GZ-curve of up to 15 degrees (0.131 radians) are displayed in figures 5.13a, 5.13b, 5.14a, and 5.14b, [Rawson and Tupper, 2001b].

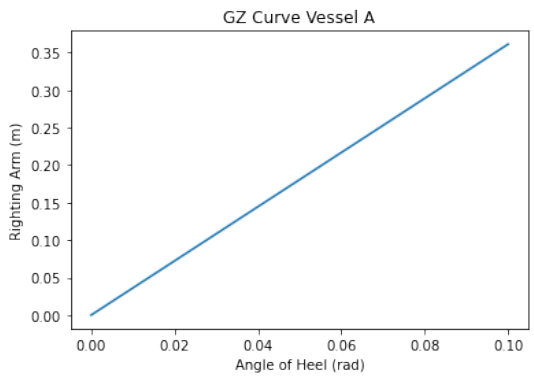

(a) An estimated GZ-curve for the first 15 degrees, Vessel A

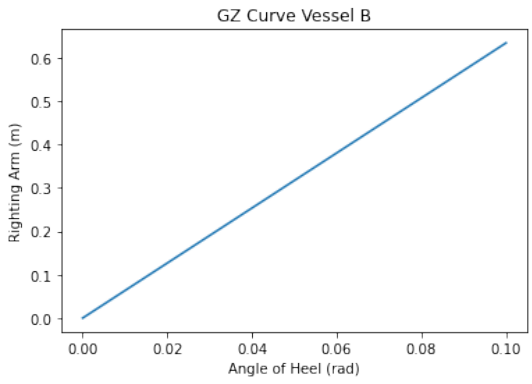

(b) An estimated GZ-curve for the first 15 degrees, Vessel B

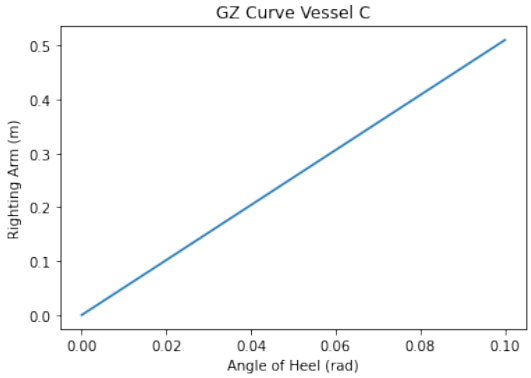

(a) An estimated GZ-curve for the first 15 degrees, Vessel C

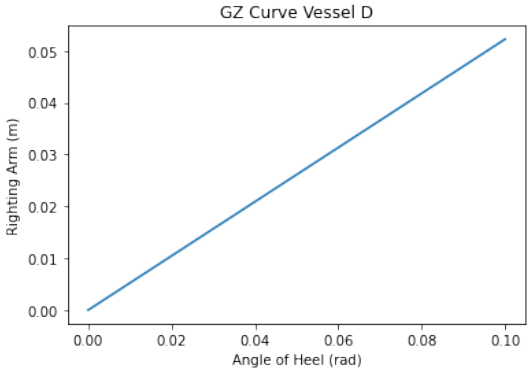

(b) An estimated GZ-curve for the first 15 degrees, Vessel D

Once again, from the figures it is clear that the positive range of the GZ-curve is likely to be larger than the first 15 degrees in accordance with the DNV classification rules. This being the case, another DNV rule [*Part 5: Ship Types, Chapter 10: Vessels for special operations*, 2021] describes the requirement of a minimum height of 0.1m within this range. While Vessel A, B and C's righting arms all reach values above 0.1m in this 15 degree range, Vessel D's GZ-curve is far below this limit reaching a righting arm height of only around 0.05m at 15 degrees. This means that Vessel D does not comply with the DNV classification rules with an iron powder hybrid configuration in this case. The final GZ-curve requirement from DNV [*Part 5: Ship Types, Chapter 10: Vessels for special operations*, 2021] is that the maximum righting arm of the vessel must not occur at an angle of heel of 7 degrees or below. This is not the case for any of the vessels as the maximum righting arm seen on these figures is at 15 degrees with a high probability of it being even at an even higher angle of heel.

The lack of margin above the minimum GM, a GZ-curve that does not satisfy the DNV classification rules and a far to severe increase in draft result in the conclusion that Vessel D cannot be equipped with a hybrid iron powder configuration without serious changes in vessel design. This means that Vessel D will not require a longitudinal stability determinations or general arrangement layout as it can be assumed that no general arrangement of the components will result in the feasible implementation of the iron powder hybrid setup on Vessel D.

Longitudinal Stability

The longitudinal stability of each vessel is largely determined by the trimming moment created by the vessel. The trimming moment is dependent on the longitudinal centers of gravity of each component/element placed on the vessel. Each vessel has its own longitudinal centre of buoyancy and its own structural longitudinal centre of gravity. These elements cannot be altered same as the longitudinal centres of gravity of the cranes, thrusters and ballast. The trimming moment is minimised by keeping the total longitudinal centre of gravity of each vessel within one meter of the longitudinal centre of buoyancy of each vessel. The longitudinal centres of gravity of the engine rooms and bunker tanks/silos have the largest impact on the longitudinal centre of gravity of the vessel. Table 5.22 shows the needed longitudinal centres of gravity of the engine rooms, fuel bunker and iron powder bunker to ensure this minimal trimming moment.

Vessel	LCG Engine Rooms [m]	LCG MFO [m]	LCG Iron Powder [m]
Vessel A	75	156	90
Vessel B	70	163	80
Vessel C	50	100	60

Table 5.22: Longitudinal centres of gravity for each element that can be placed for each vessel

With the placement of the engine rooms, MFO tanks and iron powder silos in accordance with the above longitudinal centres of gravity, the longitudinal difference between the centre of gravity of the vessels and centre of buoyancy of the vessels will remain within 1m. This results in a low trimming

moment which can be easily managed through distribution of ballast. These conditions alongside the vertical component placement conditions determined for the transverse stability can be used to create a general arrangement for Vessels A, B and C in subsection 4.4.

5.5.3. General Arrangement

A perspective view of the general arrangement of Vessels A, B and C are shown in figures 5.15, 5.16 and 5.17. These general arrangements contain all the main components used for the powertrain as well as the key elements of these semi-submersible crane vessels such as the cranes and the ballast. These components are placed in such a way that the vessel can maintain both transverse and longitudinal stability.

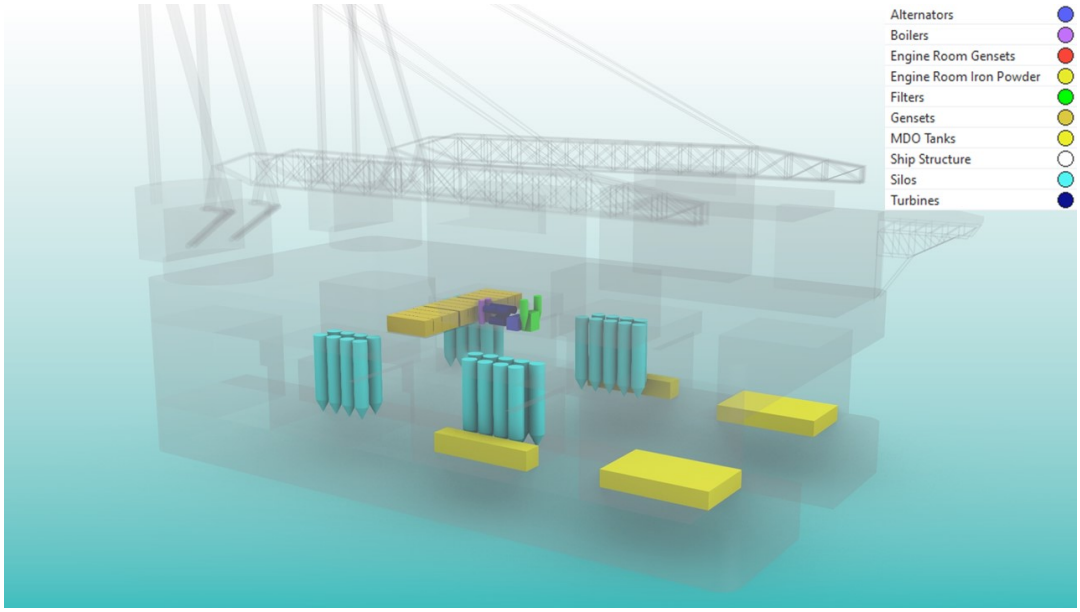

Figure 5.15: Perspective view of Vessel A's hybrid general arrangement

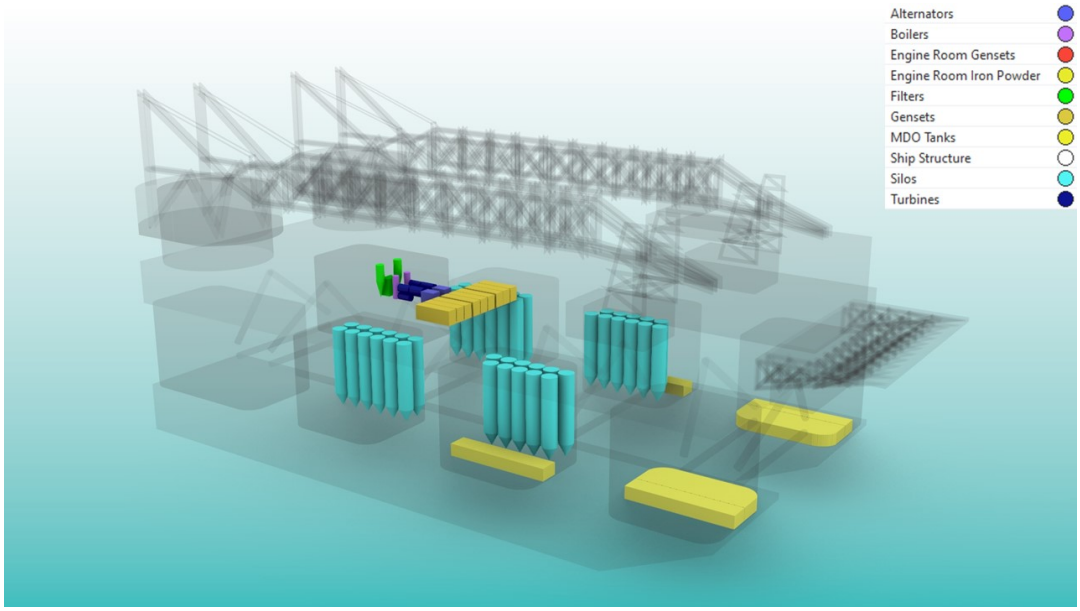

Figure 5.16: Perspective view of Vessel B's hybrid general arrangement

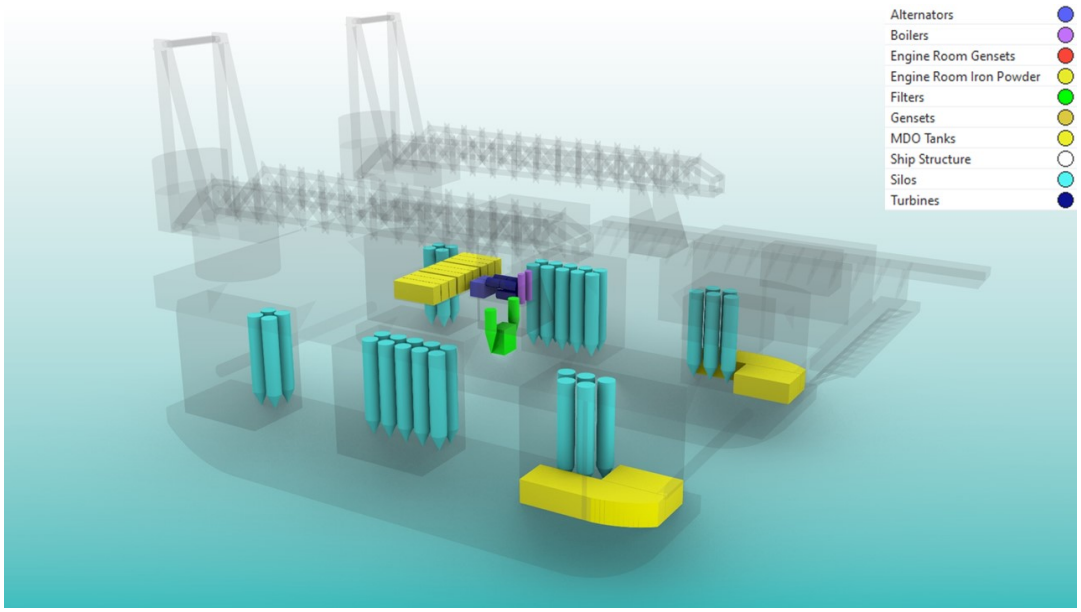

Figure 5.17: Perspective view of Vessel C's hybrid general arrangement

These general arrangements show a compact and centralized unit of engine rooms similar to the layout seen in figure 4.18. The silos and bunker tanks are placed as close to the centreline of the vessel as possible to minimise their impact on the bending force on the deckbox. Each pillar is left with sufficient room for passageways, wiring and piping. The general arrangement shows only the components required for energy production however, it is assumed that the remaining volume of the deckbox and the structures is sufficient for distribution systems, hotel accommodations, pump systems and other components that are generally present on semi-submersible crane vessels.

In order to provide a clearer overview of the component placement over all axes, a front, top and side view of each vessel is presented. Here, the key differences and similarities in component placement and the reason therefore are discussed.

Vessel A

Figures 5.18a, 5.18b and 5.19 show the front, top and side views of Vessel A respectively. The general arrangement of Vessel A shows the silo's placed in two central pillars with 9 silos placed in the forward pillars and 9 placed in the pillars pillars behind. The engine rooms are placed quite centrally and the bunker tanks are placed at the bottom of the front two pillars. The filters are not placed within the iron powder engine room but can be fitted in the deckbox, near the engine rooms. The placement of the engine rooms near the middle of the vessel reduced the transport distance required for the iron powder as well as for the MDO. The size of the deckbox makes the placement of the engine rooms easier compared to the limitations of the bunker tanks and especially the silos.

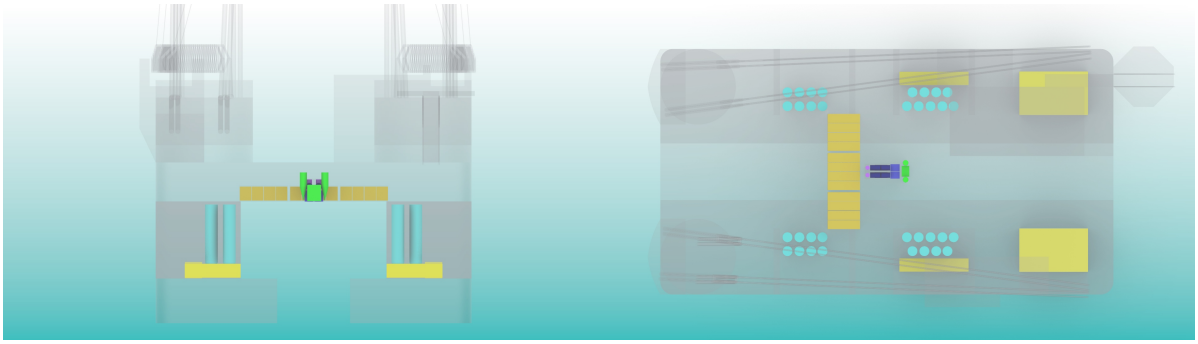

(a) Front view of Vessel A's general arrangement

(b) Top view of Vessel A's general arrangement

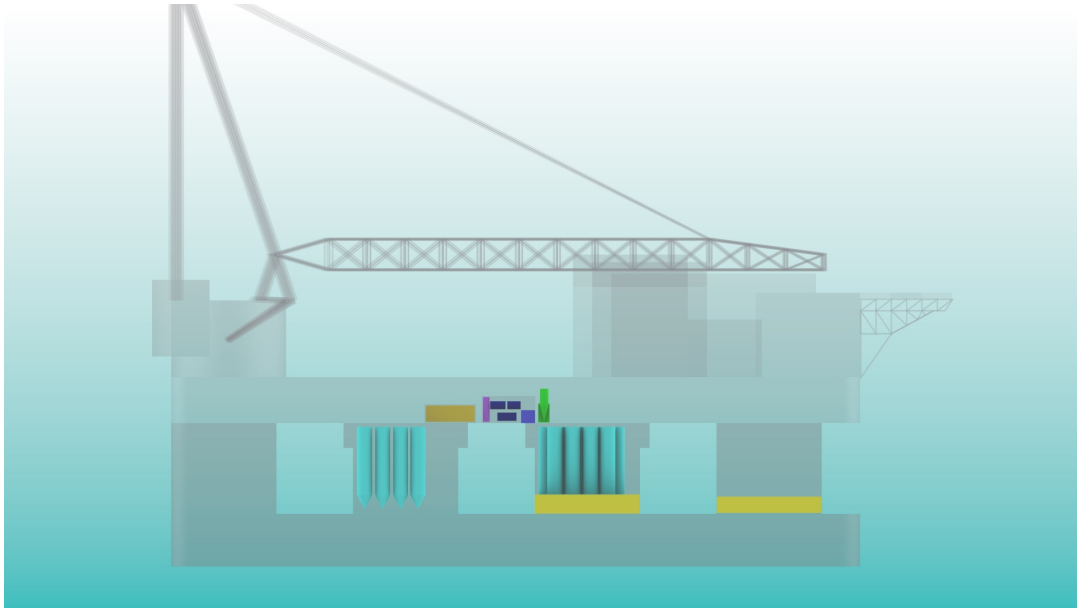

Figure 5.19: Side view of Vessel A's general arrangement

Vessel B

Figures 5.20a, 5.20b and 5.21 show the front, top and side views of Vessel B respectively. Vessel B's general arrangement is very similar to that of Vessel A. Vessel B is fitted with more iron powder silos but these are also distributed over the central pillars of the vessel. The forward pillars are fitted with 11 silos each and the pillars behind are fitted with 12 each. The engine rooms are placed relatively centrally in the deckbox as was the case for Vessel A. This has the same added benefit of lower transport distances from the bunker tanks to the engines. The filters on Vessel B are also able to be placed within the deckbox and are located near the iron powder engine room.

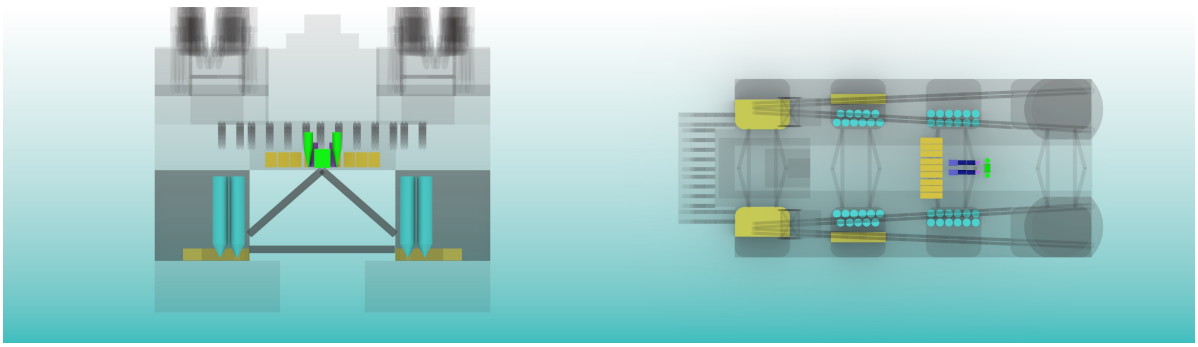

(a) Front view of Vessel B's general arrangement

(b) Top view of Vessel B's general arrangement

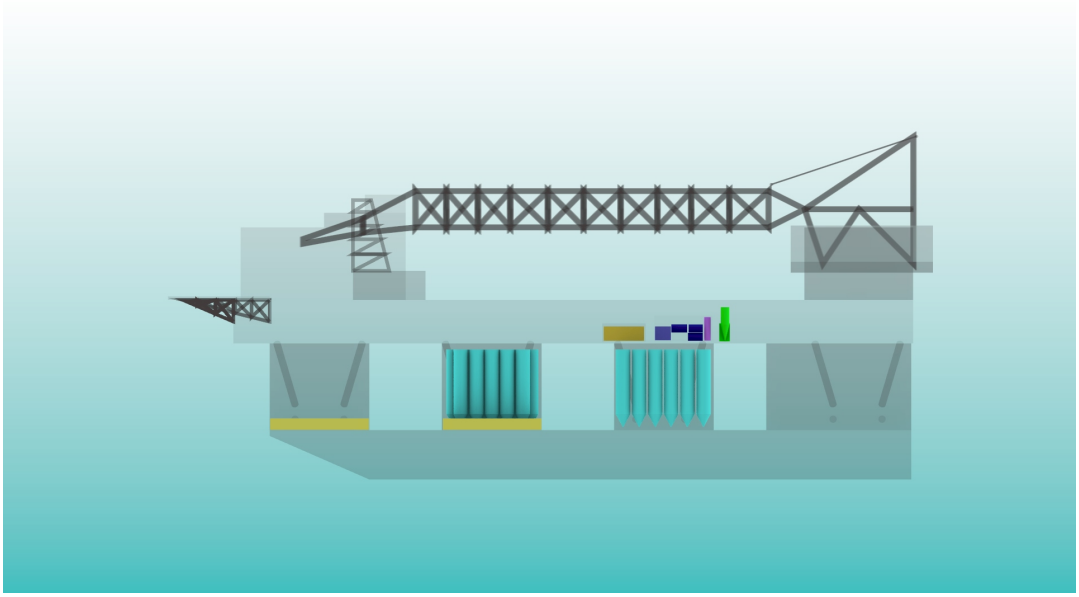

Figure 5.21: Side view of Vessel B's general arrangement

Vessel C

Figures 5.22a, 5.22b and 5.23 show the front, top and side views of Vessel C respectively. The general arrangement of Vessel C is slightly divergent from Vessels A and B. The engine rooms are still placed quite centrally in the deckbox of the vessel. The height of Vessel C's deckbox is however too small to fit the filter system completely. These are therefore placed to one side inside a small superstructure used for crane boom placement. This means that the filter system can still be covered fully and is not too far from the engine rooms. The silo placement is also different as Vessel C has only six pillars compared to the eight pillars on Vessels A and B. The silos are distributed over all six pillars with the main bulk of silos based in the central pillar. Four silos are placed in each aft pillar and five silos are placed in each front pillar. The front pillars are also fitted with the bunker tanks.

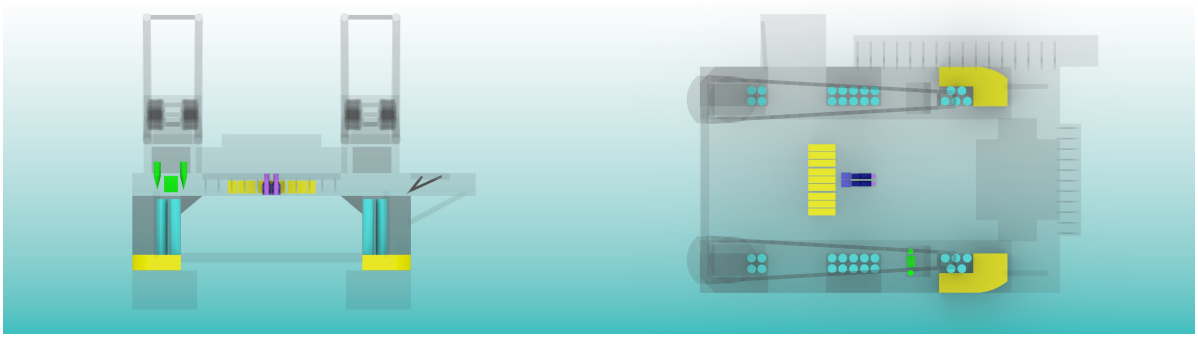

(a) Front view of Vessel C's general arrangement

(b) Top view of Vessel C's general arrangement

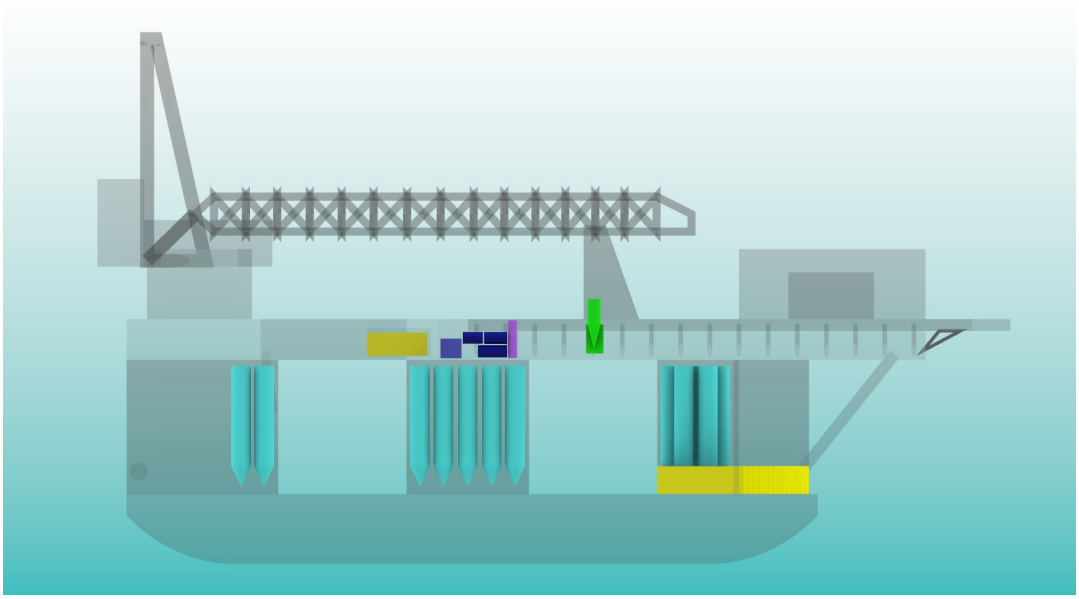

Figure 5.23: Side view of Vessel C's general arrangement

5.6. Emissions

The environmental impact of installing a hybrid iron powder powertrain on these existing semi-submersible crane vessels can be determined through an emissions comparison. This determines whether the capital costs of the hybrid setup and ship redesign costs are worth it. The distribution of base vs variable power varies significantly for each vessel and is in this case taken as a range of output values as opposed to a singular value. This is due to the high variance in the variable load as it is simulated using probabilities of peak loads occurring.

5.6.1. Pollutants

Marine diesel fuel combustion releases a multitude of different pollutants as a byproduct. The main pollutants are of course carbon dioxide (CO_2) and nitrous oxides (NO_x), however, carbon monoxide (CO), hydrocarbons (HC) and particulate matter (PM) are also abundant [Ma et al., 2023]. The only emissions output information available for iron powder combustion is the CO_2 output and the NO_x output and therefore only these pollutants will be compared. The output values of each pollutant for either power source is taken from section 4.5

5.6.2. Original vs Hybrid

The original emission output of Vessels A, B and C can be estimated through the assumption that the full power requirement of each vessel were supplied by diesel generator sets. By comparing the total output of both CO_2 and NO_x for the hybrid and full diesel generator setup, the difference in emission can be estimated over the course of one mission which can then be extrapolated to a difference in emission over the course of a year. Using the methodology described in section 4.5, table 5.23 shows the ratio of kg CO_2 output over the total kWh energy supplied for both the hybrid and original setup. The values for the hybrid setup are varied over a range between the maximum and minimum output values due to its dependence on the ratio of base load vs variable load. This range of base load vs variable load ratios can be found in table 5.23.

CO_2 Output Range Comparison					
Vessel	Hybrid Output [kg/kWh]		Original Output [kg/kWh]	Difference [kg/kWh]	
	Min	Max	Expected	Min	Max
Vessel A	0.33	0.45	0.59	0.14	0.26
Vessel B	0.31	0.38	0.58	0.2	0.27
Vessel C	0.3	0.33	0.54	0.21	0.24

Table 5.23: CO2 output comparison for the hybrid configuration vs the original configuration

The results show that CO_2 output can be reduced by over 50% in the best case scenario while the maximum output for the hybrid results in around a 25% reduction in CO_2 output. While this is quite a significant reduction it must be noted that these reductions are highly dependent on what the mission type is as well as the external factors like sea state. The variable load is dependent on these factors and it in turn dictates the percentage of power output delivered by the generator sets as opposed to the iron powder setup. Table 5.24 shows the NO_x output comparison as displayed for the CO_2.

NO_x Output Range Comparison					
Vessel	Hybrid Output [kg/kWh]		Original Output [kg/kWh]	Difference [kg/kWh]	
	Min	Max	Expected	Min	Max
Vessel A	0.0014	0.0017	0.002	0.0003	0.0006
Vessel B	0.001	0.0013	0.002	0.0007	0.001
Vessel C	0.0009	0.0012	0.002	0.0008	0.0011

Table 5.24: NOx output comparison for the hybrid configuration vs the original configuration

As with the CO_2 emissions, the NO_x emission results show a significant decrease in NO_x output. This output reduction ranges from around 15% to over 50% depending on the vessel. This is once again highly dependent on the operations of each vessel. A trend that can be seen is that the smaller vessel, Vessel C, with a lower crane and thruster power demand is seeing more emissions reductions compared to the larger vessels, Vessels A and B.

What can be concluded is that the hybrid configuration is certain to reduce the emission of both CO_2 and NO_x, however, the degree to which it can reduce emissions depends on the power profile of the vessel and more specifically on the variable load. The irregular nature of the peak loads can only be simulated using probabilities based off of existing data however this does not guarantee that this is the case for each mission and each vessel. If we take the CO_2 and NO_x output in hybrid configuration and compare it to the original configuration of each vessel, the total kg output of each pollutant is listed in table 5.25.

	CO_2 Total Output Comparison		NO_x Total Output Comparison	
Vessel	Hybrid Output [t]	Original Output [t]	Hybrid Output [t]	Original Output [t]
Vessel A	44100	66900	175	226
Vessel B	27900	46800	93	162
Vessel C	18300	31500	61	116

Table 5.25: Total CO2 and NOx output comparison for single year of 3 missions.

This comparison is based off of the assumption that three 12 week missions will be completed in a year to leave over 10 weeks for non-mission transit and potential maintenance and repair. The total CO_2 reduction is significant reaching around 20,000 tons of CO_2 a year for each vessel. The total NO_x reduction is not as large as the total output values are far lower than the CO_2 output. A reduction of around 50 tons of NO_x yearly can still be achieved which is in the case of Vessel C is around half of its total expected NO_x output.

Whether these expected emissions reductions are enough to warrant a hefty redesign of a semi-submersible vessel is difficult to decide. However, there is clear improvement in the total emissions output which makes this hybrid alternative worth considering at the bare minimum. A further analysis of the emissions compared to feasibility will be discussed in chapter 7.

6

Validation

Research validation is a crucial component when deciding on whether the results of a method can be trusted or not. Validation is referred to as the justification of knowledge claims by Pedersen et al., 2000. Most scientific research is based in mathematical models and simulation with certain inputs that result in certain outputs. These scientific research methods are often based around logical induction or deduction when it comes to validation. In short, either the answers are wrong or they are right. With most mathematical models in scientific research, this form of validation works extremely well. However, when it comes to design research, the formal, rigorous and quantitative validation methods become far more difficult to apply. Pedersen et al., 2000 explored this validation conundrum with the key question "How does one validate design research in general, and design methods in particular?". Being that the focus of this thesis centers around the design process of a semi-submersible crane vessel, these validation ideas appear to be far more applicable to the validation of the method described in chapter 4. Pedersen et al., 2000 describe the two opposing validation viewpoints as the 'Logical empiricist validation' and the 'Relativist validation' ideas. The 'Logical empiricist validation' is a rigid and algorithmic process stating that the new knowledge obtained is either true or false. While this approach is ideal for closed problems such as mathematical expressions or algorithms, its focus is more on the accuracy of the results rather than the practical use. For a research design method, the 'Logical empiricist validation' is not easily applicable. Therefore, the choice is made to go with a 'Relativist validation' process explained further in section 6.1.

6.1. Relativist Validation

The 'Relativist validation' process is not as rigid and objective as the 'Logical empiricist validation' process. Pedersen et al., 2000 states that 'Relativist validation' is "seen more as a gradual process of building confidence in the usefulness of the new knowledge (with respect to a purpose)". A key indicator that this validation method is more optimal for the method described in chapter 4 is its appropriateness for open problems and association with heuristics and most importantly non-precise representations. The design method described in chapter 4 has been described multiple times in the case study problems as likely not being entirely accurate in its actual results but serving more as a solid indicator or reference. 'Relativist validation' accepts the nature of engineering design research in its involvement of both objective and subjective elements without there being one single correct answer. The adoption of this validation process leads to a validation strategy in Pedersen et al., 2000 that is based around the following statement.

> 'We define scientific knowledge within the field of engineering design as socially justifiable belief according to the Relativistic School of Epistemology. We do so due to the open nature of design method synthesis, where new knowledge is associated with heuristics and non-precise representations, thus knowledge validation becomes a process of building confidence in its usefulness with respect to a purpose.'

In the case of the method used for this thesis, the purpose can be best described as the research objective.

> ”Analyse and evaluate the feasibility of an iron powder powertrain on a specific type of service vessel with specific focus on the vessel design as well as the powertrain configuration and components.”

This purpose is not to provide an exact correct answer for an iron powder powertrain installation on any semi-submersible crane vessel but instead to determine whether a conclusion can be made as to whether this idea is feasible from a vessel design perspective. The method in chapter 4 is validated with respect to this stated purpose through means of a ’Validation square’ created by Pedersen et al., 2000.

6.2. Validation Square

The ’Validation square’ is a process described in figure 6.1 that provides a framework for validating internal consistency of the method and the external relevance for specific instances. This is done to generate a level of confidence in its usefulness with respect to the stated purpose.

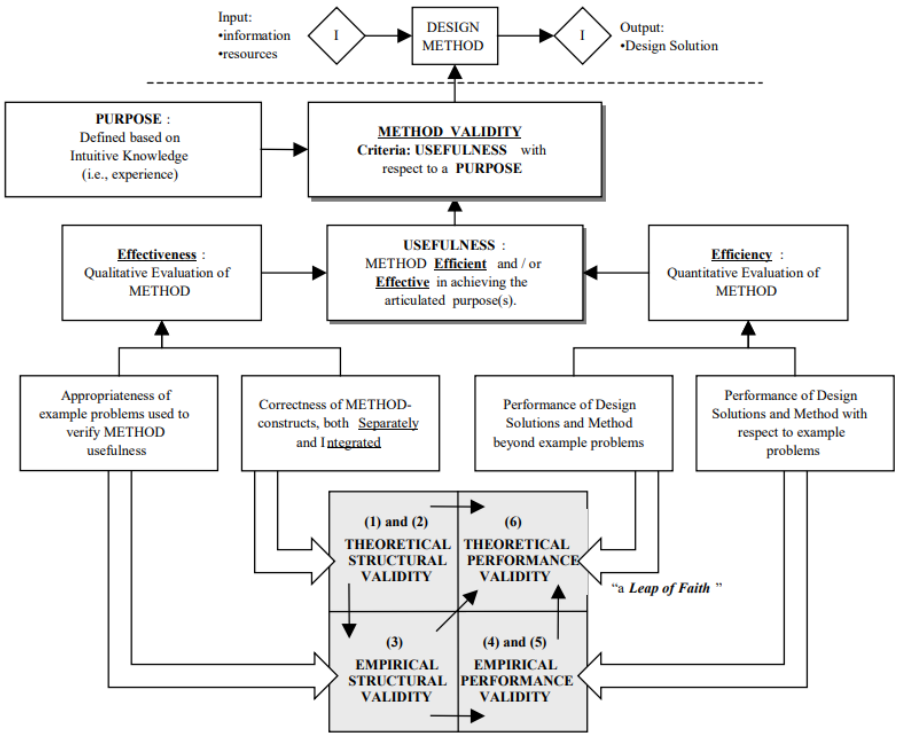

Figure 6.1: A schematic overview of the ’Validation square’, [Pedersen et al., 2000]

The bottom of the figure shows the gray box in which the validation square is described. This process consists of six total parts. The first three parts discuss the effectiveness of the method in looking at ’Construct Validity’ (1), ’Method Consistency’ (2) and ’Example Problems’ (3). The other three parts discuss the efficiency of the method in looking at the ’Usefulness for some example problems’ (4), ’Usefulness linked to applying method’ (5) and ’Usefulness beyond example problems’ (6). Each part will be discussed in the context of the method in chapter 4.

6.2.1. Construct Validity

This first step of the validation process focuses on the literature used for the constructs in the method. By looking at the authors, publishers and number of references associated with the construct, a general acceptance towards this construct can be developed. Figure 6.2 shows the list of constructs on one side alongside their relation to a condensed visualisation of the method. Of the key sources mentioned, the most heavily used sources are ’Hagen, 2021’ and ’de Kwant, 2021’. These sources are both master theses from former Delft University of Technology students. This means that these reports are

published by the University making them acceptable sources for use in this master thesis. Certain sources like 'Hagen, 2021' and 'Vessel Brochures, 2023' are sources used for multiple constructs. This is because these sources are much more closely linked to this particular method than most other sources used. As seen in figure 6.2 these constructs are all connected in a linear flow in which each previous construct is referenced by the following construct. While the flow chart shows only a few key sources of literature for each construct, most constructs are built off of a significant amount of literature. The 'weight and dimensions' construct is associated with a large number of references based around iron powder component and diesel generator component dimensioning.

6.2.2. Method Consistency

The method consistency is best validated using an information flow chart of the method according to Pedersen et al., 2000. This flow chart presents both the constructs used in the method and their ordering as well as the sources of information used to create each construct. Figure 6.2 shows this flow chart from top to bottom.

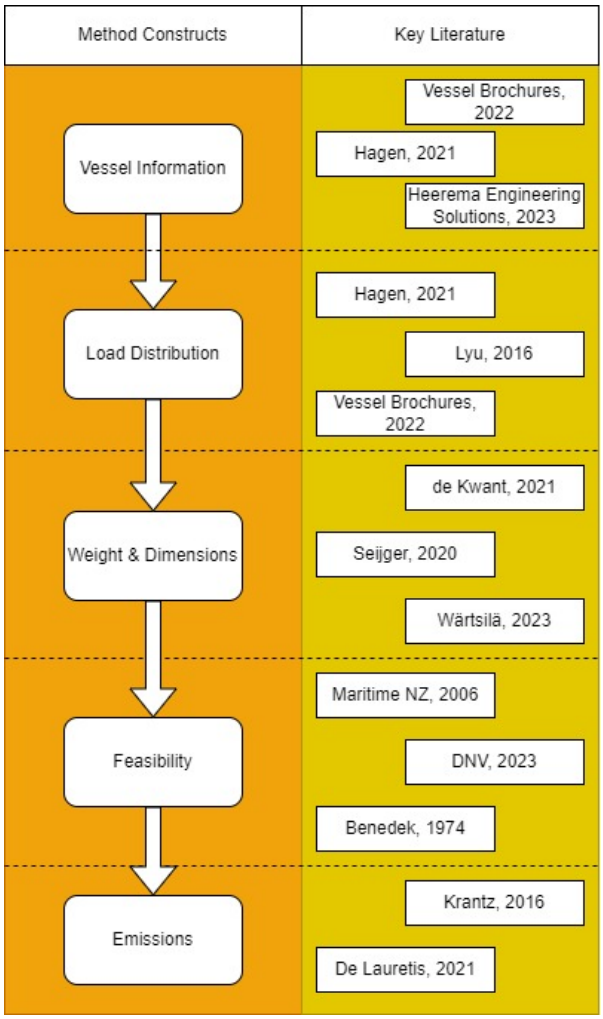

Figure 6.2: Flow chart showing the different constructs of the method and their key sources

The constructs and key sources used for those constructs are split by the dotted lines. This flow chart shows a constant influx of inputs for each construct. The first construct is of course based solely off of the information found from sources. Each following source is based off of information from both the previous construct as well as new literature sources. This means that the output of the final construct will be dependent on the input of any of the previous constructs. While it is true that certain estimations are made in the constructs, these are combined with information garnered from trusted sources and therefore can be assumed to be adequate for use in the following construct.

6.2.3. Example Problems

Acceptance of the example problems used in the method is done in stages. The example problems used in this method are four semi-submersible crane vessels, the Sleipnir, Thialf, Balder and Gretha. These are put through the constructs shown in the flow chart in figure 6.2. These constructs are built using information about semi-submersible type vessels. The constructs regarding vessel dimensions, operating profile, load distribution, weight estimation and feasibility are all generated with semi-submersible crane vessels in mind. Each construct is tailored specifically around the requirements, limitations and functions of these vessels. The largely generalised constructs of 'weight & dimensions' and 'emissions' are viable for any structure with these particular components that produce any level of emissions, including semi-submersible crane vessels. This means that the example problems, the four semi-submersible crane vessels, are not only similar to the problems for which the constructs are generally accepted, but also for the exact problems the method is intended for. Inputting the information from these example problems results in data from each construct that can all be combined to formulate a coherent conclusion.

6.2.4. Usefulness for representative example problems

The usefulness of the method for the example problems, in this case the four chosen semi-submersible vessels, can be confirmed for each vessel. Each of the four vessels fits within the specifications and the intentions of the method constructs. Putting these four vessels through the method constructs results in an analysis and evaluation pertaining to the feasibility of an iron powder powertrain on a semi-submersible vessel. This means that the method fulfills its purpose. This is because the nature of this purpose is not to determine the exact correct setup but to suggest whether there is potential for a fitting setup that is technically feasible. While this model does not give a detailed or fully accurate design profile for the semi-submersible in the hybrid setup, it does provide enough insights into the disadvantages and possibilities that lie with this hybrid setup. This is further confirmed in the conclusion and discussion in chapter 7.

6.2.5. Usefulness linked to applying method

In order to link the usefulness of the example problem results with the method, each construct within the method is run individually. The results from these constructs individually compared to their results as a whole determine whether the entire method is the reason for these results. If we take only the 'vessel information' for each of the four semi-submersibles we have accurate information but no way of determining feasibility resulting in the purpose of the method not being met. This is the same for the 'load distribution' and 'weight & dimensioning' constructs when run individually. Even more crucial for these constructs, they require information obtained in the 'vessel information' construct in order to provide any meaningful results. The 'feasibility' construct does provide results that relate to the purpose of the method, however they are also dependent on the data gathered in the previous constructs. The 'emissions' construct provides results that adds extra substance to the main results pertaining to the purpose of the method. Of the constructs described, only the 'emissions' construct could conceivably be removed and the purpose of the method still be achieved. However, the resulting conclusion is improved significantly with the information obtained in the 'emissions' construct. The method described in this thesis is certainly not as refined as existing design methods such as the ship design spiral, [Vossen et al., 2013].

There are, however, comparisons to be found between this established design process and the process described in chapter 4. Both start off with key vessel information such as the dimensions, operating profile then move to loads and powering options before a weight estimation is made and stability calculations are made. Disregarding the level of detail found in the design spiral and the fact it is designed for more conventional vessels, it can be seen as quite similar in its step-by-step process to the one described in this thesis. From these comparisons, the usefulness of the applied method can be linked to the usefulness of the results obtained from the example problems.

6.2.6. Usefulness beyond example problems

To argue the usefulness beyond just the example problems discussed, the conclusions from the previous five parts are combined to claim generality. It is confirmed in the first part (6.2.1) that the individual constructs have acceptable literature backing when looking at the purpose of the method as a whole. It is also confirmed in the second part (6.2.2) that placement of these constructs in the method is con-

sistent. Furthermore, the third part (6.2.3) confirms that these constructs are only being applied within their accepted ranges, providing only information that it is deemed to be able to adequately provide. The fourth part (6.2.4) the usefulness of the method is demonstrated for the chosen example problems. Finally, the fifth part (6.2.5) confirms the link between the usefulness achieved from this method to the method itself. With all of these parts deemed to be satisfied by the method described in chapter 4, one can in fact claim generality for this particular method as an effective and efficient method of analysing and evaluating the technical feasibility of an iron powder powertrain on a particular service vessel.

6.3. Validation of Validation Square

The validation of this framework for validation must be done as well in order for the resulting conclusions to have any real meaning. This validation of the validation method is done by validating its internal consistency and external relevance. While it seems like a circular argumentation to validate a validation framework, this is a case similar to that of validating mathematical methods with mathematical expressions. The validity is determine for each part of the square shown in figure 6.3 known in this case as constructs of the method.

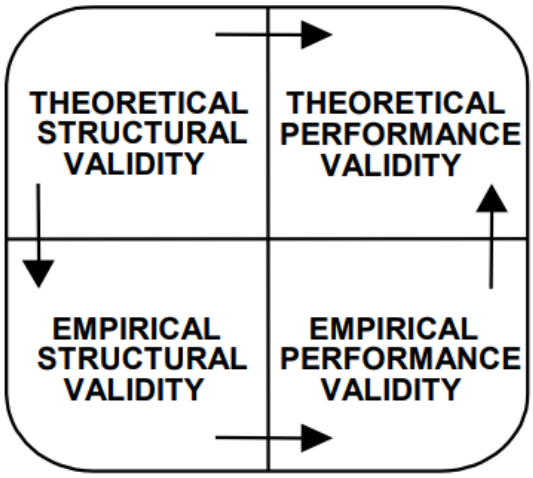

Figure 6.3: Simplified validation square, [Pedersen et al., 2000]

Each box; the Theoretical Structural Validity, Empirical Structural Validity, Empirical Performance Validity and Theoretical Performance Validity are all put through this validation process to prove its validity. This validation process covered in Pedersen et al., 2000 states that the 'Validation Square' is deemed valid for validating new knowledge associated with heuristics and non-precise representations.

7

Conclusion & Discussion

The results of the literature review, method and case study are discussed and reviewed in section 7.1 while the overall scope and limitations of the entire research process are discussed in section 7.2.

7.1. Conclusion

The conclusion looks to determine whether the initial research objective; ”Analyse and evaluate the feasibility of an iron powder powertrain on a specific type of service vessel with specific focus on the vessel design as well as the powertrain configuration and components” has been achieved. This answer is obtained by attempting to answer the research sub-questions stated in chapter 1 that make up the contents of this research objective. By going through and answering these sub-question, the final conclusion from this research can be decided.

7.1.1. Research Questions

The first research sub-question; ”What is the current state-of-the-art of energy generation using iron powder? What are the most significant physical components?” refers to the conclusions drawn in chapter 2. Here the current state-of-the-art is decided by the choice for the optimal on-board iron powder powertrain setup. This also highlights the key components of ’storage’, ’transport’, ’combustion’ and ’energy conversion’. This chapter of research concludes that the storage is currently best done using vertical silo structures while the powder transport is ideally performed by a pneumatic two-phase conveyor. Furthermore, the combustion of iron powder was determined to be possible only using an external combustion system while the energy conversion process is most practically done using an improved Rankine steam cycle known as the ultra steam turbine (UST) cycle developed by Mitsubishi. These components make up the state-of-the-art of iron powder energy generation at this current level of technological development and will likely be subject to change as the development of these systems continues to grow.

The second research sub-question; ”What types of service vessels are best suited for iron powder powertrain installation? What are key features and operational profiles of these vessels?” refers to the vessel made in chapter 3. This chapter outlines a two-step filtering process of a wide array of service vessel types by evaluating their potential for an iron powder powertrain setup. The first filter eliminated certain service vessel types due to size, range and functional constraints. The few remaining vessel types were put through the second filter by diving deeper into their operating profiles and estimated power requirements. Through this filtering process, the optimal vessel type was chosen to be the semi-submersible crane vessel. This was largely due to the vessel’s size and geometry which provided a good opportunity for the iron powder silo placement as well as having a larger deadweight capacity needed for the expected increase in bunker mass.

The third research sub-question; ”What are the key challenges faced by installing an iron powder powertrain on a marine service vessel? What are potential solutions to these challenges?” refers to the conclusions drawn in both chapters 2 and 3. The information regarding the iron powder powertrain

showed some limitations in terms of output possibilities. The output of the iron powder setup, in particular the combustion and energy conversion, is best suited for a constant energy output and does not respond well to dynamic or part loading. The operating profiles of a large majority of the service vessels shows a highly dynamic load profile in which the output required over the course of a mission can vary significantly over irregular intervals. This ended up becoming the main challenge for the installation of an iron powder powertrain on a service vessel. The problem was addressed with the decision to implement a hybrid power generation setup on the chosen optimal service vessel type. This would allow the iron powder setup to perform at its optimal state, providing the base load of the vessel. Meanwhile a secondary source, in this case diesel generator sets, would be able to provide the dynamic loads that are required.

The fourth research sub-question; ”How can models and simulations be used to analyse and compare different variations of the iron powder powertrain aboard a service vessel?” refers to chapter 4 and 5. Chapter 4 outlines the model designed for this particular purpose of testing and comparing feasibility as stated in the research objective. This model, while not being able to provide fully precise results, does give a strong indication as to the base feasibility of installing this hybrid iron powder setup on the chosen service vessel type. By running a case study in chapter 5 of four uniquely dimensioned semi-submersible crane vessels through this model, a base feasibility determination can be made for each vessel by estimating the static stability impacts as well as the estimated emission decrease. This case study of multiple vessels allows for a comparison to be made between the different vessels to provide more context to the results.

The fifth research sub-question; ”What techniques of validation and verification can be used to back up the results from this model?” refers to chapter 6. in which the model is validated using the ’Validation square’. This validation method is applied to the method described in chapter 4 in order to ensure that the results from the case study can be trusted for the purpose for which they will be used. Applying this validation study to the method proves that the method is decidedly sufficient for the purposes of the research, namely; providing a base level feasibility assessment of iron powder power generation aboard a service vessel.

The sixth research sub-question; ”What can be concluded from these models and simulations of the powertrain and the vessel design regarding iron powder implementation on service vessels?” refers mainly to the results of chapter 5. This relates also directly to the main research objective in that an analysis and evaluation is obtained for each vessel in the case study. This final conclusion of the results of this research can be divided into three main categories, the Volume & Mass Analysis, the Stability Analysis and the Emissions Analysis.

Volume & Mass

The impact of the hybrid setup on the volume and mass of the vessel is quite significant in determining the feasibility of the setup. The volume requirement of the hybrid setup is substantially higher than that of the original setup. The iron powder filtering systems will require additional deckbox volume or a separate housing structure on the deck as these components are added to the powertrain with the iron powder components. While the placement of the iron powder filtering systems requires attention in regards to design, the main cause of the volume increase is the bunker silos placed in the pillars. The placement of the silos in the pillars does allow enough volume for other systems such as passageways, pumps and ballast tanks. This increase in volume, while significant, does not pose as large a threat to the feasibility of the setup as it would on other vessels. The total volume of the pontoons, pillars and deckbox is significantly larger than that of any of the other service vessels researched in chapter 3. This means that the impact of the increased volume taken up by the hybrid setup is less severe when considering the total available volume of the vessel. The rearranging of certain other systems to accommodate the iron powder components is therefore considerably easier on a semi-submersible crane vessel than on other conventional vessels. In this regard, it can also be concluded that the larger vessels, vessel A and B, will be impacted less by the hybrid setup when it comes to volume than the smaller vessels C and D.

The impact of the mass increase that comes with the hybrid setup is a far more serious concern than

that of the volume increase. The mass of the UST engine room, especially when fitted with two setups for redundancy purposes, is a few hundred tons larger than that of the three diesel generator engine rooms for all four case study vessels except for vessel A. In the case of vessel A, the mass of the UST engine room is only slightly lower than the combined mass of the other three engine rooms. This is a significant increase in machinery mass largely due to the use of three turbines per UST setup. While this mass increase is something that must be taken into account, the scale of this mass increase is far smaller than the scale of the bunker mass increase. As is the case with the volume, the mass of the bunker silos are the main source of the mass increase caused by the iron powder hybrid setup. For the particular mission profile of a wind turbine installation performed over the course of 12 weeks, the estimated increase in bunker mass ranges from 15,000 tons to around 21,000 tons. The impact of this mass increase on the draft of the vessel is concerning. The draft increase results in an increased underwater area of the vessel which in turn increases the resistance of the vessel. This would mean that more power is required for the same thrust level to be reached. The estimated draft increase for the larger vessels is around 1-2m with a far larger draft increase for the smaller vessels at around 6-8m. The larger vessels may get off with requiring only minor redesign considerations as the draft increase is around or below the height of the pontoons. This is not the case for the smaller vessels as the draft increase results in a transit draft at a height around halfway up the pillars. At this point, the impact on the resistance, power and stability of the vessel are so extreme that serious changes to the design are required. These redesign considerations can be approached in multiple ways. The first approach focuses on the vessel dimensions to see if they can be altered in order to compensate for this increase in mass. This is best done by increasing the breadth of the pontoons of the vessel as this increases the water-plane area and therefore also ability of the vessel to remain buoyant at a higher mass load. This increase in breadth also has a positive impact on the vessel's transverse stability as it increases the BM value of the vessel. The second approach aims to see if the mission profile can be adapted regards the time between bunkering operations. If this time between bunkering operations is reduced, less bunker will be required within the storage silos which results in a lowered mass. The third approach looks at the distribution of the hybrid split. In this case the hybrid split, as shown in the load profile graphs in section 5.2.3, can be altered to decrease the percentage of total power distribution delivered by the iron powder setup. This would reduce the total power required from the iron powder setup and therefore also the level of bunker mass. The second and third approaches result either in a reduction of time spent in operation of the vessel or a reduction in emissions output of the vessel, meaning the first approach of altering the geometry of the vessel is the most ideal solution. The mass concerns are mainly important when looking at the transit state of the vessel. In this state, the vessel is at minimum draft with minimal ballast in the tanks. Any state of draft of the vessel other than transit, the mass increase of the hybrid setup can be compensated by the amount of ballast taken aboard. In this case, the iron powder bunker acts as a sort of ballast meaning less water ballast is required.

Stability

The static stability of each case study vessel has been determined and evaluated against the classification rules stated by the DNV [*Part 5: Ship Types, Chapter 10: Vessels for special operations*, 2021]. According to the calculations made in section 5.5, the initial requirement of a metacentre height (GM) of 0.3m was met by all four vessels. However, when looking at the righting arms of each vessel, vessel D did not meet the requirement of 0.1m righting arm in the first 15 degrees of roll. This resulted in the overall conclusion that vessel D would not be suitable for an iron powder hybrid setup. This lack of transverse stability coupled with the increased draft mentioned in subsection 7.1.1 mean that it is likely that a full redesign of the vessel is required in order for the hybrid iron powder setup to reach a base feasibility level. The other three vessels achieved a sufficient GM as well as a sufficient righting arm in the first 15 degrees of roll meaning they are capable of achieving a base feasibility level with a hybrid iron powder setup. The level of GM for vessels A to C ranges from 3m to around 6m. For a standard vessel, these GMs are considered quite high and can result in serious accelerations aboard the vessel. From discussions with experts at HES it was confirmed that this does not apply to vessels of the size of these semi-submersible crane levels and that the impacts of an increased GM has a far smaller impact on the accelerations to the point that this is not considered a serious issue. The estimation of the GM as well as the righting arm is impacted by the three potential approaches to minimise draft

increase. The first approach will increase the BM of the vessel resulting in a higher GM. The second and third approach will decrease the KG of the vessel also increasing the GM. The longitudinal stability of the vessel is not as significantly affected by the hybrid setup as the trim can be minimised by correct placement of the engine rooms and bunker silos/tanks along the length of the vessel. Furthermore, ballast can be used to accurately control the level of trim quite easily as the length of these vessels ranges from 130m to 220m. Overall, it can be concluded that vessels A, B and C all comply with the static stability requirements for semi-submersible crane vessels while vessel D does not. This leads to the conclusion that vessel D cannot reach a base level feasibility with an iron powder setup without massive redesign considerations.

Emissions
The emissions comparison results serve as a counterpoint against the volume, mass and stability concerns. The reduction of both CO_2 and NO_x emissions for the vessels that satisfy stability requirements (Vessels A-C) are quite significant. Depending on the level of base load compared to variable load over the course of the mission the output of CO_2 can decrease by 25% up to around 50%. Taking into consideration the current estimated output of CO_2 for a diesel generator set, this can lead to total reductions of around 20,000 tons of CO_2 per year. While the absolute value difference in NO_x output is not as large, it is still proportionately significant as around 20% up to 30% of the total output yearly can be decreased according to the estimates made. The reduction in emissions, especially with regards to the CO_2 output, show that despite the concerns with regards to feasibility, the benefits can also be abundant. The emissions reduction can lead to many monetary and physical benefits as the regulations regarding vessel emissions grow stronger.

7.1.2. Feasibility Evaluation

Based upon the results gathered to achieve the research objective to ”Analyse and evaluate the feasibility of an iron powder powertrain on a specific type of service vessel with specific focus on the vessel design as well as the powertrain configuration and components”, certain feasibility evaluations can be made. Firstly, it was determined that there is an optimal iron powder setup that can feasibly be placed aboard a marine service vessel. Furthermore, it was determined that a semi-submersible crane vessel would be the most optimal vessel on which to place this iron powder setup. From this literature level research, the importance of implementing a hybrid setup was made clear. Through application of a model and simulation of said model on a case study of a set of semi-submersible crane vessels, the level of base feasibility can be determined for each vessel as shown in table 7.1. In this table, the impact of the hybrid setup on the draft, stability and emissions of each vessel is compared. In the case of the draft, ’1’ indicates the lowest increase in vessel draft due to the increased mass while in the case of the stability ’1’ indicates the highest level of metacentre height and initial righting arm. In case of the emissions, ’1’ indicates the largest estimated decrease in CO_2 and NO_x emissions.

Vessel	Draft	Stability	Emissions
Vessel A	1	3	2
Vessel B	2	1	1
Vessel C	3	2	3
Vessel D	4	4	N/A

Table 7.1: Short comparison table ranking the feasibility of each case study vessel

Vessel A claims the second highest feasibility level as it is least affected by the mass increase in terms of both draft and stability while still seeing significant emissions reductions. Vessel B has highest feasibility with only a minor concern regarding draft increase and satisfying the initial stability estimations whilst having an estimated highest emissions decrease. Vessel C is still considered base level feasible despite its issues with increased draft as its initial stability levels are more than sufficient. Vessel D is considered not feasible at a base level due to its lack of stability coupled with a high draft increase at a higher mass making an emissions comparison unnecessary. This leads to the main conclusion that the larger semi-submersible vessels are generally considered to be more feasible

candidates for iron powder hybrid powertrain installation, as they are generally shaped to provide a larger water-plane area and equipped with a far larger deadweight carrying capacity.

7.2. Discussion

The discussion of this research is split into three main categories, namely; the scope, the limitations and future research recommendations. These will attempt to mention and outline the topics that have either been intentionally left out of this report or have been unable to be properly analysed. These topics then serve as potential follow up studies that can be done in possible future studies.

7.2.1. Scope

This research topic covers a wide variety of areas that have to be either placed within or outside the scope of the research. Unfortunately, not all areas of research can be placed within the scope due to time constraints. As the main concerns regarding iron powder implementation on marine vessels lies largely in the technical feasibility study, it was this area that was focused on most. This does leave out a significant factor that is always considered when looking at the feasibility of a sustainable energy source; the economic aspect. There was not sufficient time to conduct a proper cost estimation for the vessels. This would have provided interesting context to the technical feasibility, as the initial costs of the setup can be compared to conventional energy sources as well as the yearly bunker costs. This is especially interesting considering the iron powder cycle and the possibility of becoming a fully cyclical energy source, meaning only one initial bunker cost is made for the lifetime of the powertrain. Redesign costs and port infrastructure costs can also be considered in this economic feasibility analysis to provide a full picture of the potential of iron powder as an energy source.

The vessel scope also sets a limit on what technical components will be analysed and evaluated in the research. While all the on-board components are mentioned, the on-shore components are left out. These are crucial for determining key operations in the energy generation cycle such as the bunkering and reduction of the iron oxide. An analysis of these components would provide an even clearer picture of the iron powder setup as a whole. The reduction facility possibilities include a look at a potential mobile reduction facility that can be transported to the working area of the vessel or even look at the possibility of placing a reduction facility within the vessel itself. Bunker operations research could look at the different storage options both on land and aboard the vessel to see whether silos can be lifted out of the vessel through hatches or whether the transport system is required.

7.2.2. Limitations

This research was done as an in-house project meaning that there was no continuous contact with companies within this particular field during the course of the research. This meant that the information provided about certain iron powder powertrain components and the semi-submersible crane vessels was generally quite limited. The key information used as the main inputs of the method in chapter 4 were taken from official vessel brochures and reports that highlight the operating profile of select semi-submersible crane vessels. This information was then taken and extrapolated as carefully as possible to be applied to a wider range of semi-submersible crane vessels with the knowledge that the results would not be a complete reflection of reality. While these results were considered sufficient for evaluating a base level of feasibility for each vessel, more base information would allow for a more in depth analysis of the impact of a hybrid iron powder setup. This includes a look at the impact of crane operations on the stability with a hybrid setup as well as a potential damage stability simulation to provide a more rigorous analysis of the stability of the vessel. More information regarding the performance and output of the existing semi-submersible crane vessels would contextualise the emissions results outside simply the estimated original setup for each vessel. With continuous contact with experts in these fields, it is likely that even more measures of feasibility can be considered to go beyond simply a base level feasibility.

7.2.3. Future Research

Looking at the scope, limitations as well as the fact that this particular area of research is developing at a considerable rate; a list is given below of potential future research topics to improve upon the existing iron powder + vessel research.

1. Economic feasibility study of iron powder setup on a semi-submersible crane vessel
2. Full iron powder cycle analysis; including reduction process, on land storage, and bunkering
3. Detailed intact stability study of semi-submersible vessel with iron powder; dynamic loads, crane motions
4. Damage stability study of semi-submersible vessel with iron powder
5. Developing technologies for new optimal iron powder powertrain setup; combustion process, transportation, storage, energy conversion

8

Personal Reflection

This page covers the entire research process in the lead up to this thesis report submission. What got me personally interested in this area of research was the fact that I had never heard of iron powder being used as a source of energy. When Austin Kana mentioned that one of his master students was working on the application of iron powder systems on a short-sea shipping vessel, this piqued my interest. I decided I would try to further this area of research despite the knowledge that specific research into maritime applications of iron powder were extremely limited. Through a few discussions with some experts in the iron powder field at TU Eindhoven, I was able to find a specific area to focus to my research on. I would start looking at the possibilities of iron powder systems on service vessels.

The literature review would be an attempt to narrow this research area to a specific iron powder setup and a specific type of service vessel. While it was occasionally difficult to find enough information, especially regarding iron powder systems, an eventual optimal setup and optimal vessel choice was made. This research process took longer than expected due to a busy summer with a lot of longer breaks between researching and writing. With the new study year starting, I was able to pick up the pace of the literature review report and submit in order to start my own research.

My own research would look at testing the feasibility of an iron powder setup on a semi-submersible crane vessel, the chosen optimal service vessel type. A general method was clear, however, with a lack of concrete information regarding these types of vessels, the reliability of the method's results were in considerable doubt. Thankfully, some discussions with experts at Heerema Engineering Solutions helped to ease these concerns. Using the method and applying it to some case study models proved more time consuming than expected with multiple steps being applied to four vessel designs. Especially the calculations and simulations in python ended up being the most difficult part of the research process. The most enjoyable part was the replicating of the semi-submersible designs on the 3D modelling software Rhinoceros. This would prove helpful both in providing a visual overview of the general arrangement but also in using the geometry and dimensions of the vessel designs in stability calculations. The overall results ended up being far more positive than I was expecting, which was a relief. Only one of the four vessels was deemed completely infeasible while some were far less severely impacted by the increased mass of the hybrid setup. Overall, the research process has helped increase my knowledge of metal powders as fuel sources as well as increase my knowledge of construction vessels, mainly the semi-submersible crane vessels. These are both incredibly interesting fields that can be combined surprisingly well.

Erik Scherpenhuijsen Rom
4422104

Appendix A: Service Vessels

The first filter of the service vessel selection done in the literature review starts with a wide range of service vessel types. These vessel types are mentioned and outlined in this appendix. Based upon the information regarding each vessel, certain vessels would be eliminated due to their attributes not fitting the potential installation of an iron powder energy generation setup. The vessels mentioned in this section are all of the vessels listed in table 3.1, split into the four aforementioned categories of vessel; transport vessels, support vessels, construction vessels and specialty vessels.

A.1. Transport Vessels

(a) Walk to Work Vessel [“Damen SOV 7017/ SOV 8417 Walk to Work Vessel”, n.d.]

(b) Platform Support Vessel [“MMA Valour”, 2013]

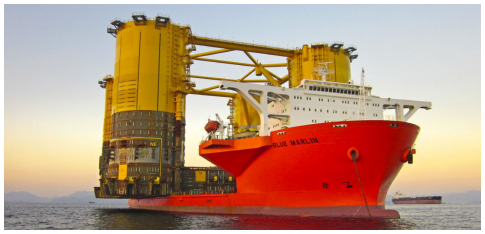

(c) Heavy Lifting Cargo Vessel [Bajic, 2019]

(d) Daughter Craft/Crew Transfer Vessel [“Norsafe Daughter Craft”, n.d.]

Walk to Work Vessel

Walk to Work vessels (figure A.1a) are designed specifically for the maintenance of offshore wind farms [Bronkhorst, 2021]. These vessels are purpose built to transport technicians to wind turbines as quickly and efficiently as possible. The defining feature onboard is a motion-compensated crane and gangway. These vessels also include large accommodation areas and large deck space for components

and equipment to be stored. DAMEN and Royal Wagenborg are some of the world leaders in design and construction of these walk to work vessels with their vessels being the state-of-the-art regarding systems onboard and functionality. These vessels tend to be 80-90m in length with a maximum speed of 13-15 knots. Along with the motion-compensated gangway there is a deck crane onboard as well for transport of equipment. These vessels are also equipped with dynamic positioning systems onboard with both aft and bow thrusters [Bronkhorst, 2021]. The size of the vessel makes them interesting for a potential iron powder powertrain with the main point of concern being the range of the vessel. For maintenance at wind farms nearer to the coast, an iron powder powertrain may be feasible.

Platform Support Vessel

Platform support vessels (figure A.1b) are similar to walk to work vessels in the fact that they serve to provide maintenance support for offshore structures. Whereas the walk to work vessel is specially designed for offshore wind farms, the platform support vessel is designed for all offshore platforms. The key objective of the platform support vessel is the transport of equipment and supplies as opposed to people. These vessels are designed for large deck space and high storage capacity in the form of both dry and wet cargo [Bronkhorst, 2021]. Along with a waste disposal system the platform support vessel also has the capability for dynamic positioning. MMA Offshore is a company with a large variety of offshore vessels including platform support vessels. The overall length of these vessel types tends to be around 75-95m. The design speed varies from 10-15 knots and same as the walk to work vessel, these vessels are equipped with deck cranes for ease of cargo transport [Bronkhorst, 2021]. These vessels are very comparable to the walk to work vessels and within a certain range off of the coast would be a potential target for iron powder powertrain implementation.

Heavy Lifting Cargo Vessel

Heavy lifting cargo vessels (figure A.1c), also known as heavy lift vessels, are designed for transport of entire offshore structures rather than supplies. These vessels provide a massive deck space for the offshore structure to be placed on. These vessels are often fit with a crane many factors larger and stronger than that of a walk to work or platform support vessel. The Boskalis offshore transport fleet includes two heavy lifting cargo vessels. The overall length of these vessels is around 200-250m with a maximum speed of around 10-13 knots. These heavy lift vessels are also equipped with dynamic positioning systems. The size of this vessel would make it feasible to install an iron powder powertrain keeping in mind any power scaling challenges. Increased size and tonnage as compared to the walk to work and platform support vessel allow for a larger range when installed with an iron powder powertrain.

Daughter Craft/Crew Transport Vessel

Daughter craft (or Crew Transport Vessel) (figure A.1d) have a similar function to that of the walk to work vessel with the key difference being range and size. Daughter craft/Crew Transport vessels provide access to wind turbines at a wind farm and operate from a service operation vessel or a fixed offshore hub [Brans, 2021]. Its limited size means it has a lower capacity and range however it does have a much higher design speed. The vessel is also equipped with a dynamic positioning system however it does have more trouble with seakeeping at higher sea states [Brans, 2021]. The length of these vessels is often around 10-15m with a speed of 30-50 knots. The size of this vessel is too limiting for an iron powder powertrain to be installed.

A.2. Support Vessels

Tugboat

Tugboats (figure A.2a), also known as tugs, are some of the most common support vessels providing maneuverability to larger vessels by pushing or pulling it. These vessels have a high bollard pull allowing it to create a large thrust level with little to no speed. These vessels have a length around

20-35m with a design speed around 10-15 knots. Similar to the daughter craft, the limited size and volume of the vessel makes it near impossible for iron powder powertrain implementation.

Anchor Handling Tug Supplier

Anchor handling tug suppliers (figure A.2b) are vessels designed for the same purpose as tugs but at a much larger scale. These vessels reach a bollard pull up to 2-3x that of a regular tug. They are designed to assist large floating offshore structures through towing or handling of mooring lines [Bronkhorst, 2021]. These vessels are also partly equipped for supply operations with enough storage capacity available onboard. Dynamic positioning systems are also installed along with a crane for potential cargo transport [Bronkhorst, 2021]. The length overall of these vessels is around 70-90m with a speed of 13-18 knots. The size of this type of vessel can be compared to that of a walk to work vessel or a platform support vessel making it potentially suitable for iron powder powertrain installation. The main concern becomes the range and mission duration of the vessel alongside the heavy load differences when in bollard pull or other tugging mode.

(a) Tugboat [“Tugboat Sparky”, n.d.]

(b) Anchor Handling Tug Supplier [“MMA Monarch”, n.d.]

A.3. Construction Vessels

(a) Offshore Subsea Construction Vessel [“Siem Offshore Secures Work for Its Subsea Construction Vessel”, 2019]

(b) Semi-submersible Crane Vessel [“Heerema Sign with Sembcorp for Sofia OWF HVDC Offshore Converter Platform”, 2021]

(c) Jack-Up Vessel [“NG-20000X Self-propelled jack-up”, n.d.]

Offshore Subsea Construction Vessel

Offshore subsea construction vessels (figure A.3a) are used for both construction and maintenance. The key features of the vessel are an onboard crane, a remotely operated vehicle (ROV) and moon-pool for deployment as well as a helicopter pad for ease of transport [Bronkhorst, 2021]. Furthermore, these vessels have large open deck areas for construction and maintenance equipment and are equipped with dynamic positioning systems as well. The length of these varies from 90m to 120m generally. The speed is generally around 13-14 knots. This makes the offshore subsea construction vessel a comparable size to the walk to work, and anchor handling tug supplier vessels. Similar to these other two vessels, the range will play a key role in determining whether an iron powder powertrain would be realistic for this vessel type with larger ranges making implementation more difficult.

Semi-submersible Vessel

Semi-submersible vessels (figure A.3b) distinguish themselves through their ability to submerge partly while performing heavy lifting, transport or drilling operations [van Lynden, 2021]. Heavy lift and drilling semi-submersibles are generally large, barge-like, vessels that do not conform to the common ship hull form. The transport semi-submersibles do have a more commonly recognisable mono-hull form. Three different semi-submersible vessels include the heavy lift crane vessel *Sleipnir*, the heavy lift transport vessel *GPO Grace* and the *Noble Developer*. These have a range of length between 100-250m and are all equipped with cranes. The transit speed is near 10 knots for these vessel types vessels and all are equipped with dynamic positioning systems. The size and requirement for ballast weight make iron powder powertrains potentially suitable to this type of vessel.

Jack-up Vessel

Jack-up vessels (figure A.3c) are used for installation and heavy maintenance of offshore structures such as wind turbines and oil/gas platforms. Their main distinguishing feature is their ability to lift their hull out of the water through the use of four pillars (legs) that are placed on the sea floor [van Lynden, 2021]. There are are self-propelling jack-up vessels and there are non-propelled jack-up vessels available. Three different jack-up vessels (*Pacific Orca*, *Vole au vent* and *Aeolus*) have been looked into to provide a overview of the general main dimensions and characteristics of these types of vessels [van Lynden, 2021]. The length of these vessels comes in at around 140-180m with a speed of around 10-13 knots [van Lynden, 2021]. These vessels all have one heavy lifting crane on deck and a dynamic positioning system installed. For both the self-propelling and non-propelled jack-up vessels, the iron powder powertrain is potentially suitable depending on scaling as with the semi-submersible crane vessel.

A.4. Specialty Vessels

(a) Pipe-Laying Vessel [“Solitaire”, n.d.]

(b) Regional Class Research Vessel [“R/V Roger Revelle”, n.d.]

(c) Split Barge Vessel [“Splijthopper”, n.d.]

Pipe-laying Vessel

Pipe-laying vessels (figure A.4a) are vessels designed for the specific purpose of laying pipes down onto the seafloor [Aguilar Tejero, 2019]. Most pipe-laying vessels can also perform similar tasks such as installing risers or subsea structures. Allseas is one of the world leaders when it comes to pipe-laying vessels with a fleet of 8 pipe-laying vessels. The vessels *Solitaire*, *Audacia* and *Lorelay* are taken for further investigation [“Solitaire”, n.d.]. The length of these vessels can range from 220m to around 400m depending on the pipe-laying tasks it is designed for. Transit speed ranges between 13-16 knots with dynamic positioning systems installed on all of the recent pipe-laying vessels [Aguilar Tejero, 2019]. The size of the vessel makes it suitable for iron powder powertrain installation with range becoming an important factor to consider. The primary issue with the pipe-laying vessel regarding iron powder powerplant implementation is the fact that a majority of the hull is used for pipe-welding in an open area. This makes the placement of an iron powder powertrain too difficult in its current state.

Research Vessel

Research vessels (figure A.4b) are designed for any ocean related research. There are five classes of research vessel: global, ocean, regional, coastal and local [Betzler et al., 2019]. The local and coastal research vessels are too small to be considered for iron powder powertrains while the large range of the global and ocean class compared to their size make it an unlikely suitor for iron powder powertrains. The regional class have a range more suitable for iron powder fuels. The regional research vessels Magnus Heinason in the Faroe Islands and RV Celtic Voyager are examples of regional research vessels. These vessels have a length of around 30-70m with a larger hotel capacity needed for research equipment onboard. Mission duration is often no longer than a fortnight making it a possible candidate for iron powder powertrain installation [Betzler et al., 2019].

Dredger

Dredgers (figure A.4c) are ships designed to move ocean sediment from one location to another through pumps. There are two types of dredger vessels; the conventional trailing suction hopper dredger and the conventional split barge. The trailing suction hopper dredger is a vessel that does both the pumping of sediment in one area as well as the offloading of sediment in another [Curzi et al., 2021]. The conventional split barge is designed specifically for offloading. For ease of possible iron powder implementation, the focus will be on split barges. Jan de Nul is a world leader in dredging with a fleet of 17 split barges, three of which have been further looked into. These split barges have a length of around 100m with a speed of 12-13 knots [“Splijthopper”, n.d.]. The key feature of the split barge is its ability to split its hull open in two in order to release the collected sediment in its hull to the seafloor. The simple functionality and generally large size make it interesting for iron powder but it is held back by a large bulk storage capacity which decreases the opportunity for iron powder powertrain placement.

B

Appendix B: Turbine Dimensions

This appendix will serve as a description of the method used to dimension the turbines in the UST engine room. As stated in section 4.3, this turbine estimation is taken largely from the method used by de Kwant, 2021 in which the turbine must be operating at a specific flow coefficient (ϕ) and stage loading coefficient (ψ). Figures B.1a and B.1b, there is an optimal total-to-total turbine efficiency (η_{tt}) that can be reached when the flow coefficient and stage loading coefficient reach 0.5 and 1 respectively.

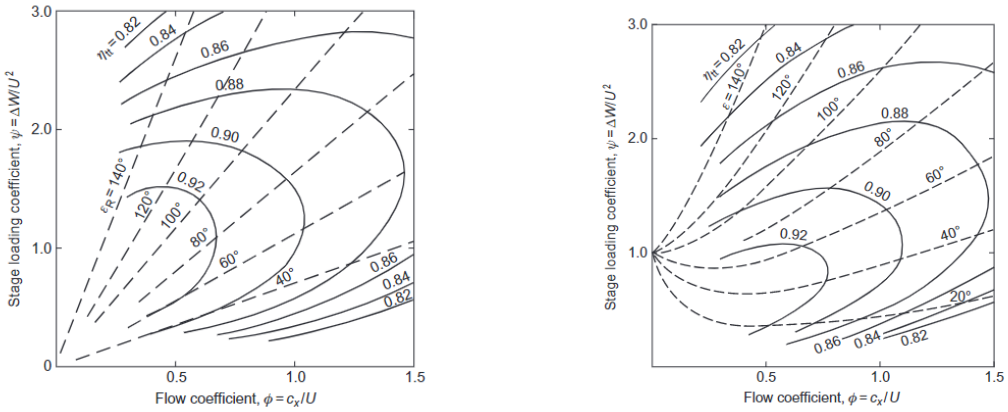

(a) Relation between ϕ, ψ, η_{tt} and ϵ for an impulse stage, Dixon and Hall, 2014

(b) Relation between ϕ, ψ, η_{tt} and ϵ for a reaction stage, Dixon and Hall, 2014

The main formulas used for the estimation are equations B.1 and B.2, [Dixon and Hall, 2014].

$$\phi = \frac{c_x}{U} = \frac{\dot{m}}{A_{mean} * \rho * U} \tag{B.1}$$

$$\psi = \frac{\Delta W}{U^2} = \frac{W}{n_{stages} * \dot{m} * U^2} \tag{B.2}$$

In equation B.1 the variable c_x represents the axial speed of the working fluid through the turbine and U represents the mean blade speed. The variable c_x can be redefined using the mass flow of the working fluid ($\dot{m}$), the mean cross-sectional area of the annulus between stages (A_{mean}) and the the density of the working fluid (ρ). In equation B.2 the variable ΔW represents represents the specific work output per stage. This specific work output per stage can be redefined as the specific output of the whole turbine (W) divided by the number of stages in the turbine (n_{stages}). The turbine power W, mass flow of the working fluid $\dot{m}$ and inlet/outlet conditions of the working fluid can be determine from the base loads determined for each vessel and the UST cycle data points in table 2.3 respectively.

An initial estimation of the turbine speed and mean blade speed are made. It is best to use a high

starting estimation for both values (12000 RPM turbine speed and 600 m/s mean blade speed) as these values would result in less turbine stages. Based on these starting values, the shaft diameter mean blade radius of the first stage is calculated using equations B.3 and B.4.

$$D_{shaft} = \frac{W}{S_s * n_{turbine}} \tag{B.3}$$

$$r_{mean,inlet} = \frac{2 * \pi * U_{inlet}}{60 * n_{turbine}} \tag{B.4}$$

In equation B.3, S_s stands for the shear strength of the turbine, which is estimated to be around 34.5MPa according to *Ignition of Metals in High Pressure Oxygen*, 1985. The variable $n_{turbine}$ stands for the turbine speed in rpm. In equation B.4, U_{inlet} stands for the mean blade speed. With these two variables estimated, the tip diameter of the blades at the inlet can be estimated using equation B.5.

$$D_{tip,inlet} = 2\sqrt{2 * r_{mean,inlet}^2 - (\frac{D_{shaft}}{2})^2} \tag{B.5}$$

This tip diameter is used to calculate the inlet annulus area as shown in equation B.6. Using the data in 2.3, the specific volume of steam at the inlet and outlet can be determined which are used to calculate the required annulus area of the final stage as shown in equation B.7.

$$A_{inlet} = (D_{tip,inlet}^2 - D_{shaft}^2) * 0.25 * \pi \tag{B.6}$$

$$A_{outlet} = A_{inlet} * \frac{v_{outlet}}{v_{inlet}} \tag{B.7}$$

With the outlet annulus area calculated, the tip diameter at the outlet can be determined using formula B.8. From this, a mean tip diameter of the turbine can be simply calculated. From here the mean turbine diameter is estimated using equation B.9.

$$D_{tip,outlet} = \sqrt{4 * \frac{A_{outlet}}{\pi} + D_{shaft}^2} \tag{B.8}$$

$$D_{mean} = 2 * \sqrt{\frac{\frac{D_{tip,mean}}{2}^2 + \frac{D_{shaft}}{2}^2}{2}} \tag{B.9}$$

This mean turbine diameter can then be used to determine the actual mean blade speed of the turbine using equation B.10. By taking the optimal stage loading coefficient ψ value of 1, the number of stages n_{stages} can be deduced from formula B.11.

$$U = \frac{120 * n_{turbine}}{2 * \pi * D_{mean}} \tag{B.10}$$

$$n_{stages} = \frac{W}{\dot{m} * \psi * U^2} \tag{B.11}$$

In equation B.11, $\dot{m}$ is the mass-flow of the turbine which is calculated using values in table 2.3. Finally, the mean annulus area of the turbine can be simply calculated using equation B.12.

$$A_{mean} = \frac{A_{inlet} + A_{outlet}}{2} \tag{B.12}$$

With these variables calculated, equations B.2 and B.1 can be filled in to determine the flow and stage loading coefficients. If they are not at the desired values of 0.5 and 1 respectively, the initial speed of the turbine is decreased until both coefficients are sufficiently close (within 0.05).
Once the optimal turbine speed and mean blade speed have been determine per turbine, another final check is done to determine whether the centrifugal force of the rotating blades is within the requirements. Assuming the blades are made of a nickel alloy, the maximum ratio of centrifugal stress over

material density is 35,000 m^2/s^2. The calculation of this stress is done using the equation B.13 taken from *Ignition of Metals in High Pressure Oxygen*, 1985.

$$\frac{\sigma_c}{\rho} = \frac{K * U^2}{2} * (1 - (\frac{D_{shaft}/2}{D_{tip}/2})^2) \tag{B.13}$$

If all requirements are met, the diameter measurements made for each turbine stage can be used to determine the dimensions of the turbine and the turbine casing. Using these diameter measurements, the total volume of the turbine can be estimated which, when multiplied by the density of the alloy used, give an estimation of the weight of each turbine.

Using the tip diameter at the inlet and outlet, as well as the number of stages, the diameter at each stage of the turbine can be calculated using equation B.14.

$$D_{tip,i} = D_{tip,inlet} + \frac{D_{tip,outlet} - D_{tip,inlet}}{n_{stages} - 1}(i - 1) \tag{B.14}$$

With the tip diameter of each stage given, the blade height, axial chord and axial length of each stage of the turbine is estimated in equations B.15, B.16, and B.17 respectively. Here it is assumed that the axial chord of each stage is equal to be a factor 0.125 of the blade height. The axial length is assumed to be a factor 1.2 larger than the blade height.

$$H_i = \frac{(D_{tip,i} - D_{shaft})}{2} \tag{B.15}$$

$$b_i = 0.125 * H_i \tag{B.16}$$

$$a_i = 1.2 * H_i \tag{B.17}$$

Using the schematic displayed in figure B.2 taken from de Kwant, 2021, the total length of the rotor is calculated as the sum of the chords and lengths of each stage of the turbine. The casing of this turbine is assumed to have a diameter of a factor 1.4 larger than the rotor diameter. With these dimensions, the total volume of each turbine component can be estimated. By assuming that the casing is made of cast iron with a density of 8 t/m^3, the blades are made of alloyed steel with a density of 7.85 t/m^3 and the rotor shaft is made of medium carbon steel with a density of 7.85 t/m^3, the total mass of each component can be calculated and summed up to equal the total mass of a turbine. This process is completed for each of the three turbines in a UST setup.

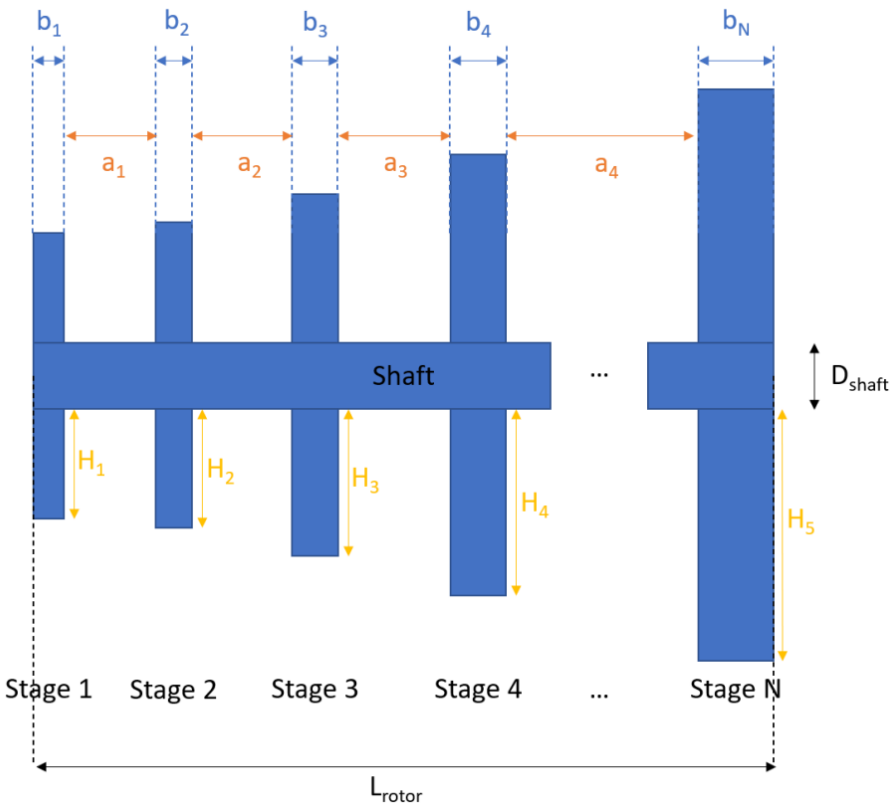

Figure B.2: Schematic overview of turbine dimensions

C

Appendix C: Boiler Dimensions

The boiler design referred to in section 4.3 aims at creating an estimation for a boiler design that incorporates a combustion chamber suitable for iron powder combustion as well as a heat exchanger setup that transfers the heat from the heated air-oxide mixture to the working fluid. The design of this cylindrical boiler starts with determining the mass flow throughout the boiler. From here the combustion chamber and heat exchanger components can be estimated along with a total weight estimate.

C.1. Mass Flow

The diameter of the boiler is determined by the mass flow of the air mixture. There are three minimum mass flow rates that need to be maintained in order for the boiler operate at a high efficiency. These are the hot air flow to ensure adequate heat transfer, air consumption rate to maintain combustion and the minimum mass flow of air to suspend oxide particles in the gas flow. These three mass flow values can be estimated using the equations C.1, C.2 or C.3. In equation C.1, Q_{wf} is equal to the heat level of the working fluid while η_{boiler} is the assumed boiler efficiency, in this case 95%. The values of $h_{hot,in}$ and $h_{hot,out}$ are the specific enthalpy of hot air at either the entrance or exit of the heat exchanger.

$$\dot{m}_{hot,1} = \frac{Q_{wf}}{\eta_{boiler}} * \frac{1}{h_{hot,in} - h_{hot,out}} \tag{C.1}$$

$$\dot{m}_{hot,2} = \dot{m}_{iron} * \lambda * \frac{3 * M_{oxygen}}{4 * M_{iron}} \tag{C.2}$$

$$\dot{m}_{hot,3} = \frac{1}{6} * m_{oxide} \tag{C.3}$$

Taking the lowest of these required mass flow rates ensures that the other two mass flow rate requirements are met. From this chosen mass flow rate ($\dot{m}$), the maximum diameter of the boiler (A_{max}) can be determined through equation C.4, taken from de Kwant, 2021. Here V_{convey} represents the minimal velocity at which the iron particles must be transported to prevent oxides from falling, [Mills, 2016].

$$A_{max} = \frac{\dot{Q}_{hot}}{V_{convey}}, \quad where \;\; \dot{Q}_{hot} = \frac{\dot{m}_{hot}}{\rho_{hot}} \tag{C.4}$$

This maximum diameter can be decreased to increase the flow of hot air above the critical conveying velocity. This does increase the pressure drop resulting in a higher boiler height required. In this case, the lack of volumetric constraints for this particular area of the vessel allowed for the maximum allowable diameter to be used as the inner boiler diameter.

C.2. Combustion Chamber

The combustion chamber is located in the bottom of the total boiler design and is assumed to have the same diameter as the rest of the boiler. The height of the combustion chamber can be determined using equation C.6. This combustion chamber height is dependent on the speed of the iron powder particles entering the chamber which is dependent on the airflow speed. This airflow speed is determined using equation C.5. With the airflow speed and thus particle speed determined, the assumed combustion time of 0.1 seconds can be combined to calculate the height of the combustion flame. This height is added on top of another clearance of 0.9m which is suggested by Garg, 1989.

$$V_{airflow} = \frac{\dot{Q}_{hot}}{A_{boiler}} \tag{C.5}$$

$$H_{cc} = H_{flame} + H_{clearance} \tag{C.6}$$

In equation C.5, $\dot{Q}_{hot}$ represents the volumetric hot air flow through the combustion chamber and A_{boiler} the boiler area determined earlier.

C.3. Heat Exchanger

The heat exchanger is designed in a square tube layout as opposed to the more conventional cylindrical design. This is because the square tube layout will likely be more resistant to the abrasive nature of the iron oxide particles travelling through them. The small diameter of these heat exchanger tubes results in a compact design with a high pressure drop. The external tube diameter is assumed to be around 25.4mm as this is typical for most industrial heat exchangers, [de Kwant, 2021] The tube thickness must meet the pressure requirements while also being as small as possible. Using a safety factor of 1.4, an assumed working fluid pressure and tube yield stress, the tube thickness is calculated using equation C.7.

$$t_{tubes} = 1.4 * \frac{p_{wf} * d_o}{2 * \sigma_{y,tubes}} \tag{C.7}$$

By calculating the heat transfer coefficient and overall heat transfer admittance of the heat exchanger, the required heat exchanger area can be determined. The heat transfer coefficient of the heat exchanger can be determined by using equation C.8

$$\frac{1}{U} = \frac{1}{h_h + h_{rad}} + \frac{1}{h_c} + \frac{t_{tubes}}{k_{tubes}} \tag{C.8}$$

Here the thermal conductivity of the tubes, k_{tubes}, is assumed to be that of copper. Using the Donohue method further described in de Kwant, 2021, the radiative heat transfer coefficients and convective heat transfer coefficients h_h and h_c can be determined. The radiative and convective heat transfer coefficient on the tube side of the heat exchanger, h_h, can be determined using the Siedler-Tate relation described in de Kwant, 2021. The radiative heat transfer coefficient, h_{rad} can be calculated using equation C.9. In this equation, σ is the Stephen-Boltzmann constant, the emissivity ϵ of the oxide particles is 0.505 and T_{hot} and T_{tubes} are the average temperatures of the hot airflow and the tubes respectively.

$$h_{rad} = \sigma * \epsilon * (T_{hot}^4 - T_{tubes}^4) \tag{C.9}$$

With the heat transfer coefficient, U, determined for the heat exchangers, the overall heat transfer admittance can be calculated using the heat admittance equation C.10.

$$Z = U * A_{he} \tag{C.10}$$

Here, the overall heat admittance, Z, must be determined in order to get an estimated heat exchanger required area of A_{he}. The overall heat admittance can be found by looking at two temperature differences, the difference in temperature of the working fluid before and after the heat exchanger and the difference in temperature of of the hot air mixture after combution and after leaving the heat exchanger. These are represented by equations C.11 and C.12 respectively.

$$\Delta\theta_c = \frac{F}{F_c} * \Delta\theta_0 * (1 - e^{-\frac{Z}{F}}) \tag{C.11}$$

$$\Delta\theta_h = \frac{F}{F_h} * \Delta\theta_0 * (1 - e^{-\frac{Z}{F}}) \tag{C.12}$$

Here the fluid strength of the working fluid and the hot air mixture, F_c and F_h, are calculated as the product of their mass flow and their specific energy. The initial temperature difference between the two fluids entering the heat exchanger, $\Delta\theta_0$ is taken as the difference between the temperature of the hot air mixture just after combustion and the temperature of the working fluid before being pumped into the heat exchanger. These allow equations C.11 and C.12 to be combined to determine the overall heat transfer admittance Z which can then be used in equation C.10 to determine the required heat exchanger area A_{he}. The length of the tubes is calculated using this heat exchanger area along with the number of tubes, N_{tubes} and tube diameter, d_o as shown in equation C.14. The number of tubes is estimated using equation C.13 in which P_t is the pitch of the tube layout, D_{shell} is the boiler diameter and C_1 is a constant equal to 1 for a square tube layout.

$$1.25 * d_o * N_{tubes} = \frac{0.7854 * D_{shell}^2}{C_1 * P_t^2} \tag{C.13}$$

$$L_{tubes} = \frac{A_{he}}{N_{tubes} * \pi * d_o} \tag{C.14}$$

The height of the heat exchanger is dependent on the length of the tubes is these are placed vertical as shown in figure 4.11. This height is calculated using equation C.15 in which N is the number of heat exchangers required for the particular setup.

$$H_{he} = \sum_{i=1}^{N} L_{tubes,i} + 0.5N \tag{C.15}$$

C.4. Overall Dimensions and Weight

The overall dimensions of the boiler are determined by the outer diameter of the boiler. In order to maintain a sufficient level of thermal isolation, the wall thickness of the boiler should be around 0.4m, [de Kwant, 2021]. This means that the outer diameter of the boiler can be calculated using equation C.16 where the inner diameter is taken from the inner boiler area A_{boiler}. The height of the boiler is simply the sum of the combustion chamber height and the heat exchanger height.

$$D_{outer} = 0.8 + D_{inner} \tag{C.16}$$

With all component dimensions known, the volume of each component can be calculated. The boiler is assumed to be made of steel with a density of 8.05 t/m^3. Only the tubes are assumed to be made of copper with a density of 8.96 t/m^3. The weight of the boiler is then taken as the sum of of the major components in equation C.17 multiplied by a factor 1.1 in order to account for smaller component weights.

$$W_{boiler} = 1.1 * (W_{cc} + W_{endplates} + W_{tubes} + W_{shell} + W_{ts}) \tag{C.17}$$

In this equation, W_{cc} stands for the combustion chamber weight, W_{tubes} stands for the total tube weight and W_{shell} stands for the weight of the shell of the boiler. $W_{endplates}$ is the weight of the top and bottom plate of the boiler which are assumed to be the same thickness as the the combustion chamber shell thickness. W_{ts} is the weight of the tube sheets which is determined from the total cross-sectional area of the tubes.

Bibliography

Aguilar Tejero, F. (2019). *Feasibility study of solitaire's aftship retrofit*.

Air pollution control methodologies. (n.d.). Retrieved October 16, 2022, from https://ecerinmcduffie.wixsite.com/website/air-pollution-control

Bajic, A. (2019). Pirates destroy boskalis vessel blue marlin. Retrieved October 16, 2022, from https://www.projectcargojournal.com/shipping/2019/05/07/pirates-destroy-boskalis-vessel-blue-marlin/?gdpr=deny

Balakrishnan, B., & Balakrishnan, D. (2017). Design and analysis of boiler pressure vessels based on ibr codes. *IOP Conference Series: Materials Science and Engineering*, *197*, 012045. https://doi.org/10.1088/1757-899X/197/1/012045

Banen, B. (2015). *Concept design optimization: Applied on a new semi-submersible heavy transport vessel in the dockwise s-class market*.

Barge stability guidelines. (2006). https://www.maritimenz.govt.nz/content/commercial/safety/vessel-stability/documents/barge-stability-guidelines.pdf

Bashir, K. (2015). *Design and fabrication of cyclone separator* (Doctoral dissertation). https://doi.org/10.13140/RG.2.2.20727.83368

Bergthorson, J. (2018). Recyclable metal fuels for clean and compact zero-carbon power. https://doi.org/10.1016/j.pecs.2018.05.001

Besarati, S., & Goswami, D. (2017). Supercritical co2 and other advanced power cycles for concentrating solar thermal systems. https://doi.org/10.1016/B978-0-08-100516-3.00008-3

Betzler, C., Carapuco, M., Cattrijsse, A., Coren, F., Danobeitia, J., Day, C., Fitzgerald, A., Florescu, S., Ignacio Diaz, J., Klages, M., Koning, E., Lefort, O., Magnifico, G., Mikelborg, O., & Naudts, L. (2019). *European research vessels: Current status and foreseeable evolution*. https://doi.org/10.5281/zenodo.3477893

Biran, A., & López-Pulido, R. (2014). Chapter 7 - weight and trim calculations (A. Biran & R. López-Pulido, Eds.; Second Edition), 171–187. https://doi.org/https://doi.org/10.1016/B978-0-08-098287-8.00007-4

Brans, S. (2021). *Applying a needs analysis to promote daughter craft for year-round access to far-offshore wind turbines*.

Bronkhorst, P. (2021). *Enhancing offshore service vessel concept design by involving seakeeping*.

Brouwers, J., & Van Kemenade, E. (2012). Condensed rotational separation to upgrade sour gas.

Cavallo, C. (n.d.). All about drag conveyors - types, design, and uses. Retrieved October 16, 2022, from https://www.thomasnet.com/articles/materials-handling/all-about-drag-conveyors/

Ck cyclone collectors. (n.d.). https://www.kice.com/product-specs/cyclone-receivers/

The complete platform supply vessel. (n.d.). Retrieved October 16, 2022, from https://www.damen.com/catalogue/offshore/platform-supply-vessels?view=models&model=Platform-Supply-Vessel-4000-CD

Cooper, C., & Alley, F. (2011). *Air pollution control: A design approach*. Waveland Press. https://books.google.nl/books?id=Xfi7bwAACAAJ

Curzi, F., van Ingen, F., Geleijnse, J., & Kingma, P. (2021). *Emission free maintenance dredging in a harbour environment*.

Damen sov 7017/ sov 8417 walk to work vessel. (n.d.). Retrieved October 16, 2022, from https://products.damen.com/nn-no/ranges/walk-to-work-vessel/w2w-7017

de Kwant, J. (2021). *Design implication and performance assessment of iron fuelled ships*.

Diaz, H., & Guedes Soares, C. (2020). Review of the current status, technology and future trends of offshore wind farms. 10.1016/j.oceaneng.2020.107381

The difference between horizontal and vertical silos. (2019). Retrieved October 16, 2022, from https://batchcrete.net.au/the-difference-between-horizontal-and-vertical-silos/

Dilute phase pneumatic conveying. (n.d.). Retrieved October 16, 2022, from https://www.air-tec.it/en-au/pneumatic-conveying-technology

Dincer, I., & Zamfirescu, C. (2018). Environmental dimensions of energy. https://doi.org/10.1016/B978-0-12-809597-3.00103-6

Dirven, L., Deen, N., & Golombok, M. (2018). Dense energy carrier assessment of four combustible metal powders. https://doi.org/10.1016/j.seta.2018.09.003

Dixon, S., & Hall, C. (2014). Chapter 4 - axial-flow turbines: Mean-line analysis and design (S. Dixon & C. Hall, Eds.; Seventh Edition), 119–167. https://doi.org/https://doi.org/10.1016/B978-0-12-415954-9.00004-8

Doorduin, W., Witlox, L., Lageweg, M., & van Brakel, R. (2016). *The use of electric motors for the propulsion of seagoing vessels.* Rotterdam Mainport University of Applied Sciences - RMU.

Drag conveyor professionals. (n.d.). Retrieved October 16, 2022, from https://screwconveyor.com/product-solutions/drag-conveyors/

Emep/eea air pollutant emission inventory guidebook 2019 - update dec. 2021. (2021). https://www.eea.europa.eu/publications/emep-eea-guidebook-2019

Garg, A. (1989). Better burner specifications. *Hydrocarbon Processing*, *68*.

Geertsma, R., Negenborn, R., Visser, K., & Hopman, H. (2017). Design and control of hybrid power and propulsion systems for smart ships: A review of developments. *Applied Energy*, *194*, 30–54. https://doi.org/10.1016/j.apenergy.2017.02.060

Ghimire, P., Karimi, S., Mehdi, Z., Nagalingam, K., & Pedersen, E. (2022). Model-based efficiency and emissions evaluation of a marine hybrid power system with load profile. https://pscc.epfl.ch/rms/modules/request.php?module=oc_program&action=view.php&id=2090&file=1/2090.pdf

Gualeni, P., Flore, G., Maggioncalda, M., & Marsano, G. (2019). Life cycle performance assessment tool development and application with a focus on maintenance aspects. https://doi.org/10.3390/jmse7080280

Guegan, A., Vik, B., Georgopolou, C., Husdal, L., Koukoulopoulos, L., de Jongh, M., Miyazaki, M., Macedo, P., Torben, S., Calvignac, J., Hassani, V., & le Diagon, V. (2020). *Holistic optimisation of ship design and operation for life cycle*.

Hagen, G. (2021). *Hydrogen powered propulsion for an offshore crane vessel*.

HeavyLiftPFI. (2021). Swan takes on mega module. Retrieved October 16, 2022, from https://www.heavyliftpfi.com/sectors/swan-takes-on-mega-module/10251.article

Heerema sign with sembcorp for sofia owf hvdc offshore converter platform. (2021). Retrieved October 16, 2022, from https://www.heavyliftnews.com/heerema-sign-with-sembcorp-for-sofia-owf-hvdc-offshore-converter-platform/

Horizontal silos eurosilo. (n.d.). Retrieved October 16, 2022, from https://www.sami.info/en/product/horizontal-silos/

Huang, D., Tran, T., & Yang, B. (2013). Investigation on the reaction of iron powder mixture as a portable heat source for thermoelectric power generators. https://doi.org/10.1007/s10973-013-3619-9

Huge semisub crane vessel gets aip. (2019). https://www.oedigital.com/news/466616-huge-semisub-crane-vessel-gets-aip

Huisman. (2018). *Installationof 2 x 10000mt huisman tmc for heerema sleipnir*. Youtube. https://www.youtube.com/watch?v=IPQGXe4q4J0&t=105s

Ignition of metals in high pressure oxygen. (1985). North American Space Agency. oai:casi.ntrs.nasa.gov:19850018563

Imo's work to cut ghg emissions from ships. (n.d.). *International Maritime Organization*. https://www.imo.org/en/MediaCentre/HotTopics/Pages/Cutting-GHG-emissions.aspx

Karakurt, A., & Gunes, U. (2016). Performance analysis of a steam turbine power plant at part load conditions. https://doi.org/10.18186/thermal.298611

Kawasaki receives order from kobe steel for two coal plant ash handling systems. (2016). Retrieved October 16, 2022, from https://global.kawasaki.com/en/corp/newsroom/news/detail/?f=20160411_2354

Klebanoff, L., Madsen, R., Conard, C., Caughlan, S., Leach, T., & Applegate Jr., T. (2020). *Feasibility study of replacing the r/v robert gordon sproul with a hybrid vessel employing zero-emission propulsion technology*. https://energy.sandia.gov/programs/sustainable-transportation/hydrogen/fuel-cells/maritime-applications/

L-drive azimuthing thrusters bottom mounted. (n.d.). https://www.thrustmaster.net/azimuth-thrusters/thru-hull-l-drive-azimuth-thrusters/#techspecs

Lacal-Arántegui, R., Yusta, J. M., & Domínguez-Navarro, J. A. (2018). Offshore wind installation: Analysing the evidence behind improvements in installation time. *Renewable and Sustainable Energy Reviews*, *92*, 133–145. https://doi.org/https://doi.org/10.1016/j.rser.2018.04.044

Lanzerstorfer, C., & Hinterberger, M. (2017). Influence of the moisture content on the flowability of fine-grained iron ore concentrate. *International Journal of Chemical and Molecular Engineering*, *11*(3), 265–268. https://publications.waset.org/vol/123

Linstad, H., Eskeland, G., & Rialland, A. (2017). Batteries in offshore support vessels - pollution, climate impact and economics. http://dx.doi.org/10.1016/j.trd.2016.11.023

Lm2500+ marine gas turbine. (n.d.). *www.ge.com/marine*. https://www.geaerospace.com/sites/default/files/datasheet-lm2500plus.pdf

Lyu, Z. (2016). *Concept design of hybrid crane vessel*.

Ma, Z., Du, T., Duan, S., Qu, H., Wang, K., Xing, H., Zou, Y., & Sun, P. (2023). Analysis of exhaust pollutants from four-stroke marine diesel engines based on bench tests. *Journal of Marine Science and Engineering*, *11*, 413. https://doi.org/10.3390/jmse11020413

MacGregor, J., Mayekar, S., & Watson, D. (2019). Semi-submersible design – a new generation of offshore accommodation vessels. *Ocean Engineering*, *172*, 759–787. https://doi.org/https://doi.org/10.1016/j.oceaneng.2018.11.053

Maritime shipping. (n.d.). *International Council on Clean Transportation*. https://theicct.org/sector/maritime-shipping/

McCoy, T. J. (2002). Trends in ship electric propulsion. *IEEE Power Engineering Society Summer Meeting, 1*, 343–346 vol.1.

Mills, D. (2016). Chapter 12 - conveying capability (D. Mills, Ed.; Third Edition), 273–288. https://doi.org/https://doi.org/10.1016/B978-0-08-100649-8.00012-3

Mma monarch. (n.d.). Retrieved October 16, 2022, from https://www.mmaoffshore.com/vessel-fleet/mma-monarch

Mma valour. (2013). Retrieved October 16, 2022, from https://www.mmaoffshore.com/vessel-fleet/mma-valour

Mohajeri, M. J., van den Bos, M. J., van Rhee, C., & Schott, D. L. (2020). Bulk properties variability and interdependency determination for cohesive iron ore. *Powder Technology*, *367*, 539–557. https://doi.org/https://doi.org/10.1016/j.powtec.2020.04.018

Monitoring, reporting and verification of co2 ... - european parliament. (n.d.). *www.europarl.eurpa.eu*. https://www.europarl.europa.eu/RegData/etudes/BRIE/2019/642224/EPRS_BRI(2019)642224_EN.pdf

Nakhaei, M., Lu, B., Tian, Y., Wang, W., Dam-Johansen, K., & Wu, H. (2020). Cfd modeling of gas-solid cyclone separators at ambient and elevated temperatures. *Processes*, *8*, 228. https://doi.org/10.3390/pr8020228

Ng-20000x self-propelled jack-up. (n.d.). Retrieved October 16, 2022, from https://www.nov.com/products/ng-20000x-self-propelled-jack-up

Nijssen, R., Lahuerta, F., Wandji, W., Natarajan, A., Ibsen, L., Scholle, N., Radulovic, L., Kohlmeier, M., Foglia, A., Shirzaden, R., Kuhn, M., Tiedemann, S., Fischer, T., & Kaufer, D. (2016). *Deliverable d4.1.5 – innovations on component level for coming 20mw turbines*. INNWIND EU. http://www.innwind.eu/publications/deliverable-reports

Nomoto, H. (2022). Development in materials for ultra supercritical and advanced ultra-supercritical steam turbines. https://doi.org/10.1016/B978-0-12-824359-6.00004-4

Norsafe daughter craft. (n.d.). Retrieved October 16, 2022, from http://www.scanpacificmarine.com/daughter-craft

Papanikolaou, A. (2021). *A holistic approach to ship design: Volume 2: Application case studies*. Springer International Publishing. https://books.google.nl/books?id=O1w0EAAAQBAJ

Part 5: Ship types, chapter 10: Vessels for special operations. (2021). DNV Rules for Classification. https://standards.dnv.com/explorer/document/DD751DE556864C6DA3C4F24616EF6CB2/26

Pedersen, K., Emblemsvag, J., Bailey, R., Allen, J., & Mistree, F. (2000). Validating design methods and research: The validation square. 10.1115/detc2000/dtm-14579

Pneumatic conveying: Process technology. (n.d.). Retrieved October 16, 2022, from https://www.dinnissen.eu/machine/pneumatic-conveying

Product brochure: Cranes. (n.d.). https://www.huismanequipment.com/documenten/brochures/brochure_cranes_web.pdf

Product detail information. (n.d.). Retrieved October 16, 2022, from https://www.mhi.com/products/ship/turbine_ust.html

R/v roger revelle. (n.d.). Retrieved October 16, 2022, from https://scripps.ucsd.edu/ships/revelle

Rawson, K., & Tupper, E. (2001a). 3 - flotation and trim (K. Rawson & E. Tupper, Eds.; Fifth Edition), 52–90. https://doi.org/https://doi.org/10.1016/B978-075065398-5/50006-6

Rawson, K., & Tupper, E. (2001b). 4 - stability (K. Rawson & E. Tupper, Eds.; Fifth Edition), 91–144. https://doi.org/https://doi.org/10.1016/B978-075065398-5/50007-8

Reducing emissions from the shipping sector. (n.d.). *Climate Action*. https://climate.ec.europa.eu/eu-action/transport-emissions/reducing-emissions-shipping-sector_en

Reed, J. (1998). *Balder vessel upgrading for 6,500-ft deep king project*. https://www.offshore-mag.com/rigs-vessels/article/16756196/balder-vessel-upgrading-for-6500ft-deep-king-project

Ricci, D., Bassetti, F., & Savastano, S. (2018). Beneficial effects of dry bottom ash extraction and recycling in modern pcf power plants. https://doi.org/10.1016/j.fuel.2017.10.088

Safe boreas. (n.d.). https://www.prosafe.com/wp-content/uploads/2019/09/Spec-Sheet-Safe-Boreas.pdf

Satpathi, K., Balijepalli, V., & Ukil, A. (2017). Modeling and real-time scheduling of dc platform supply vessel for fuel efficient operation. https://doi.org/10.1109/TTE.2017.2744180

Schulze, D., Schwedes, J., & Carson, J. (2008). Powders and bulk solids: Behavior, characterization, storage and flow. *Powders and Bulk Solids: Behavior, Characterization, Storage and Flow*, 1–511. https://doi.org/10.1007/978-3-540-73768-1

Seijger, V. (2020). *High-efficient heat engines for iron-fired power systems*.

Semi submersible accomodation / crane vessel: O.o.s. gretha. (n.d.). https://www.oosinternational.com/sscv-oos-gretha/

Siem offshore secures work for its subsea construction vessel. (2019). Retrieved October 16, 2022, from https://www.offshore-energy.biz/siem-offshore-secures-work-for-its-subsea-construction-vessel/

Sleipnir hmc equipment. (n.d.). https://www.heerema.com/heerema-marine-contractors/fleet/sleipnir

Solitaire. (n.d.). Retrieved October 16, 2022, from https://allseas.com/equipment/solitaire/

Splijthopper. (n.d.). Retrieved October 16, 2022, from https://www.jandenul.com/nl/vloot/splijthopper

Stempinski, F., Wenzel, S., Luking, J., Martens, L., & Hortamani, M. (2014). *Modelling installation and construction of offshore wind farms*. http://proceedings.asmedigitalcollection.asme.org/

Sustainability report. (2021). Heerema Marine Contractors. https://www.heerema.com/hubfs/Sustainability/Heerema-Sustainability-Report-2021-web-spread.pdf?hsLang=en

Thialf hmc equipment. (n.d.). https://www.heerema.com/heerema-marine-contractors/fleet/thialf

Thialf hmc equipment. (n.d.). https://www.heerema.com/heerema-marine-contractors/fleet/balder

Tugboat sparky. (n.d.). Retrieved October 16, 2022, from https://echandia.se/projects/tugboat-sparky/

Turner, J. H., Viner, A. S., McKenna, J. D., Jenkins, R. E., & Vatavuk, W. M. (1987). Sizing and costing of fabric filters. *JAPCA*, *37*(6), 749–759. https://doi.org/10.1080/08940630.1987.10466261

van Daalen, S. (2015). *A study of a tub crane with an unconventional quadruple hook arrangement*.

van Lynden, C. (2021). *Offshore wind installation vessels: Generating insight about the driving factors behind the future design*.

van Nood, N. (2019). Finding the right balance for the future. *InSide*. https://doi.org/https://issuu.com/gustomsc/docs/gustomsc-inside31-web

van Rooij, N., Seijger, V., & Spee, T. (2019). *Ijzer als brandstof voor schepen*. Maritiem Kennis Centrum.

Vole au vent: Offshore jack-up installation vessel. (n.d.). Retrieved October 16, 2022, from https://www.jandenul.com/sites/default/files/2022-01/Voleauvent28EN29_.pdf

Vossen, C., Kleppe, R., & Hjørungnes, S. (2013). Ship design and system integration.

Wärtsilä generating sets - tailored to optimize performance. (n.d.). https://www.wartsila.com/marine/products/engines-and-generating-sets/generating-sets/wartsila-gensets

The world's most powerful engine enters service. (n.d.). *Wartsila.com*. https://www.wartsila.com/media/news/12-09-2006-the-world's-most-powerful-engine-enters-service

Yoonhan, A., Seong, J., Minseok, K., Seong, K., Seungjoon, B., Jeong, I., & Jae, E. (2015). Review of supercritical co2 power cycle technology and current status of research and development. http://dx.doi.org/10.1016/j.net.2015.06.009